

report

ERMS

Environmental Risk Management System

Program participants: - Agip - Conoco Phillips - Exxon Mobil - Hydro - Petrobras - Shell - Statoil - Total



TOTAL



HYDRO

ConocoPhillips

ExxonMobil





ERMS- and PROOF programmes

Experimental validation of drilling effects in the field



Authors:

Harald Berland, Henrik Rye, Steinar Sanni

Report: AM 2006 / 004



ERMS Report No. 20

SINTEF report no. STF80MK A06225, ISBN 82-14-03770-0

NFR project 153882/ 720

NFR PROOF programme

Harald Berland ²⁾, Henrik Rye ³⁾, Steinar Sanni ¹⁾

**Experimental validation of
drilling effects in the field**

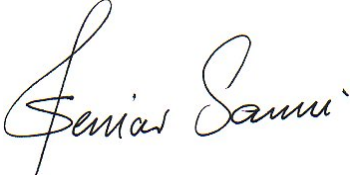

¹⁾ Akvamiljø a/s, ²⁾ IRIS-Marine Environment,
³⁾ SINTEF

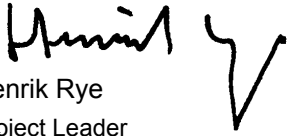

Report AM 2006/004


Project number: 697000
Project titles: NFR Validation ERA and ERMS Field experiment
Client(s): Norwegian Research Council and ERMS consortium (Statoil, Hydro, Total, Eni, ConocoPhillips, ExxonMobil, Shell, Petrobras)
Research program: PROOF-Validation and ERMS
ISBN: 82-8192-015-7

Mekjarvik, 31.08.2006

	 <p>Akvamiljø</p>	 <p>SINTEF</p>
---	--	---

 <p>Steinar Sanni Project Leader Akvamiljø</p>	<p>Sign date 28/08-06</p>	 <p>Jan F. Børseth Project Quality Assurance IRIS</p>	<p>Sign date 28/08-06</p>
---	-------------------------------	---	-------------------------------

 <p>Henrik Rye Project Leader SINTEF</p>	<p>Sign date 25/8-06</p>	 <p>Mark Reed Project Quality Assurance SINTEF</p>	<p>Sign date 25/8-06</p>
---	------------------------------	--	------------------------------



28/08-06

Director
Akvamiljø a/s

Sign date

Contents

Summary	- 1 -
List of symbols	- 3 -
PART A. Layout of field trial and discharges, model validation	- 4 -
A.1. Introduction.....	- 4 -
A.1.1. General.	- 4 -
A.2. Overview of data collection.....	- 5 -
A.2.1. Site selection.....	- 5 -
A.2.2. Data collection overview	- 6 -
A.3. Deployment of cages with blue mussels and sea scallops.	- 12 -
A.4. Ambient data collection	- 15 -
A.4.1 General weather conditions.....	- 15 -
A.4.2. Temperature and salinity.	- 16 -
A.4.3. Ocean currents.....	- 17 -
A.5. Discharge conditions.....	- 19 -
A.5.1 Amounts of discharge.....	- 19 -
A.5.2. Particle size distributions.....	- 21 -
A.6. Numerical modeling of the discharges at the SVAN field.....	- 25 -
A.6.1. About the (revised) DREAM model.....	- 25 -
A.6.2. Comparison between model simulations and measurements.....	- 32 -
A.6.3. Modelling the near field dilution of the discharge.....	- 38 -
A.6.4. Calculations of barite concentrations at cage locations.....	- 40 -
PART B The validation of biological effects in blue mussels and scallops.	- 44 -
B.1. Introduction.....	- 44 -
B.2. Biological material	- 45 -
B.3. Test organisms.....	- 45 -
B.3.1. Storage and transport	- 46 -
B.4. Biological measurements	- 47 -
B.4.1. Fitness parameters.....	- 49 -
B.4.2. Lysosomal membrane stability	- 49 -
B.4.3. Comet assay	- 49 -
B.4.4. Protein (Bradford method).....	- 49 -
B.4.3. Glutathion-S-transferase (GST) activity	- 49 -
B.4.5. Total Oxyradical Scavenging Capacity (TOSC).....	- 50 -
B.4.6. Clearance rate (Algae density estimation).....	- 50 -
B.4.7. Stress on stress (survival time in air)	- 51 -

B.4.8. Proteomics	- 51 -
B.4.9. Body burden of barite	- 51 -
B.5. Results and discussion	- 53 -
B.5.1. Fitness results	- 53 -
B.5.2. Lysosomal membrane stability	- 55 -
B.5.3. Comet assay	- 56 -
B.5.4. GST	- 58 -
B.5.5. TOSC	- 59 -
B.5.6. Clearance rate of exposed mussels and scallops	- 60 -
B.5.7. Stress on stress (survival in air for blue mussels)	- 62 -
B.5.8. Proteomic analysis	- 63 -
B.5.9. Body burden of barite	- 65 -
B.5.10. Evaluation of the simulated exposure regime.	- 67 -
B.6. Conclusion	- 70 -
 PART C Comparison between risk estimates and biomarker response	
in general	- 72 -
C.1. Risk calculations for the cage locations	- 72 -
C.2. Relationship between Risk and Biomarkers	- 81 -
 APPENDIX	
Appendix A. Solutions	- 86 -
Appendix B: Protein list blue mussel	- 87 -
Appendix C. Protein list, scallops.	- 89 -
REFERENCES	- 91 -

Summary

This report consists of three parts:

- **Part A:** Layout of field trial and discharges, model validation
- **Part B:** The validation of biological effects in blue mussels and scallops
- **Part C:** Comparison between risk estimates and biomarker response in general

Part A explains details of a measurement program that took place at the Sleipner field in the North Sea, where drill cuttings and mud were discharged. The measurements were used to compare results from a numerical model (DREAM) to simulate the discharge behaviour in the sea. The model was then used to calculate expected concentration levels at selected sites for measurements of biologic responses (biomarkers) triggered by the discharges.

Part B considers the deployment and analysis of biomarker signals in sea scallops and blue mussels deployed during the discharge period. The use of filterfeeding scallops and blue mussels in an exposure experiment towards drilling wastes revealed biological impacts as physical disturbance affecting energy storing and reproduction (reduced gonad weight), algae filtration and metabolism. The changed conditions for the exposed transplanted animals increased the oxidative stress and revealed significant DNA damages in the assumed highest drilling waste sited blue mussels. A pattern of protein production was found towards depth alone in proteomics measurements and from the membrane stability measurements reduced conditions were found for all mussels, with an enlarged reduced stability for blue mussels at 100 m and in the 20 m exposed zone. The evidence of barite exposure was measured through barium measurements, in the scallops and blue mussels soft tissue and hard shell part.

The experiment setup for the placement of transplanted animals in the North Sea revealed the importance of rating the equipment and again the importance in use duplex systems ensuring that you find some of your gear when returning.

Part C deals with a comparison between environmental risks calculated with the numerical model for the location of the cages (sea scallops and blue mussels) and the biomarker responses. The environmental risks were calculated with the DREAM model, where the discharge component barite was assumed to represent the largest potential impact on the cages. The risk calculations were based on a PEC/PNEC approach where risks for damage are larger than 5 % when the actual concentration (PEC) exceeds the predicted no effects (PNEC) concentration level. The report outlines how a comparison between biomarker signals and risk analysis can be developed further. One of the difficulties encountered is the highly time variable exposure of the cages in the field. This makes a direct comparison between the two methods difficult.

Acknowledgement

A large number of persons and organizations have been involved in this work. Besides researches from SINTEF and IRIS-Akvamiljø, the following organizations have contributed to this work:

Statoil has assisted in providing data on the amounts and the contents of the discharges, as well as making facilities on the drilling rig "*Transocean Searcher*" available to the SINTEF personnel.

Oceaneering assisted in making their ROV equipment available for observations of the underwater plumes and depositions on the sea floor. The ROV type was denoted "*Magnum – Work ROV*", equipped with two cameras and hand manipulators, used by Oceaneering to assist during the drilling operations.

List of symbols

BOP	Blow-Out Preventer
BSD	Biomarker Sensitive Distribution
DREAM	Dose related Risk and Effect Assessment Model
EC50	The concentration where a specific effect is observed for 50% of the test specimen
EIF	Environmental Impact Factor
ERMS	Environment Risk Management System
GST	Glutathion-S-transferase activity
HOCNF	Harmonized Offshore Chemical Notification Format
ICP-MS	Inductively Coupled Plasma Mass Spectrometry
LC50	The concentration which causes lethality for 50% of the test specimen
LOEC	Lowest Observed Effect Concentration
Milli-Q®	Millipore filtration unit; Ultra pure water
NCS	Norwegian Continental Shelf
NOEC	No Observed Effect Concentration
OBM	Oil Based Mud
PAF	Potentially Affected Fraction of species
PAH	Poly-Aromatic Hydrocarbons
PEC	Predicted Environmental Concentration/Change
PNEC	Predicted No Effect Concentration/Change
PLONOR	Pose Little or No Risk to the environment
POW	Partition oil-water coefficient
ROV	Remote Operating Vehicle
POM	Particulated organic material
SBM	Synthetic Based Mud
SELDI-TOF:	Surface Enhanced Laser Desorption Ionization – Time of Flight
SFT	Norwegian State Pollution Control Authority
SPM	Suspended Particle Matter
SSD	Species Sensitive Distributions
Spex® water standard	Standards in ultra pure water
TGD	Technical Guideline Document (EC 1996)
THC	Total HydroCarbons
TOSC	Total oxygen scavenging capacity
WBM	Water Based Mud

PART A.

Layout of field trial and discharges, model validation

A.1. Introduction

A.1.1. General.

The ERMS project (ERMS = *Environmental Risk management System*) is aimed at developing models for prediction of impacts from regular releases to sea caused by the offshore industry. The types of discharges considered are discharges during production (basically produced water releases) and discharges during drilling (basically discharges of drill cuttings and mud). The main purpose of the ERMS project is to develop an EIF (EIF = *Environmental Impact Factor*) for drill cuttings and mud discharges along the same lines as has been developed previously for discharges of produced water.

As a part of the ERMS project, a field experiment was conducted. The purpose of the field trial was to collect field data for comparison with model results. The Sleipner field in the North Sea was selected because a drilling program was planned at the Sleipner Vest Alfa Nord (SVAN) location. This location is about 18 km northwest of the existing Sleipner A and T platforms.

At the same time, IRIS-Akvamiljø has been granted by the Norwegian Research Council (NFR) to carry out a project termed "Validation" over the NFR PROOF Programme. This project is aimed at validation of methods for carrying risk analysis offshore. Because the ERMS project is aimed at developing numerical models for carrying out risk analysis for discharges to sea offshore, it was decided that IRIS-Akvamiljø should join the ERMS project by deploying cages with sea scallops and blue mussels close to the discharge site. Then the methods validated by IRIS-Akvamiljø could be tested on the real field case, by comparing risks deduced from the responses on the biota with the risks calculated by the numerical models developed as a part of the ERMS project.

The present report compares impacts of drilling discharges in the water column only.

A.2. Overview of data collection

A.2.1. Site selection.

The field data were collected at the SVAN field in the North Sea (Figure A.2.1).

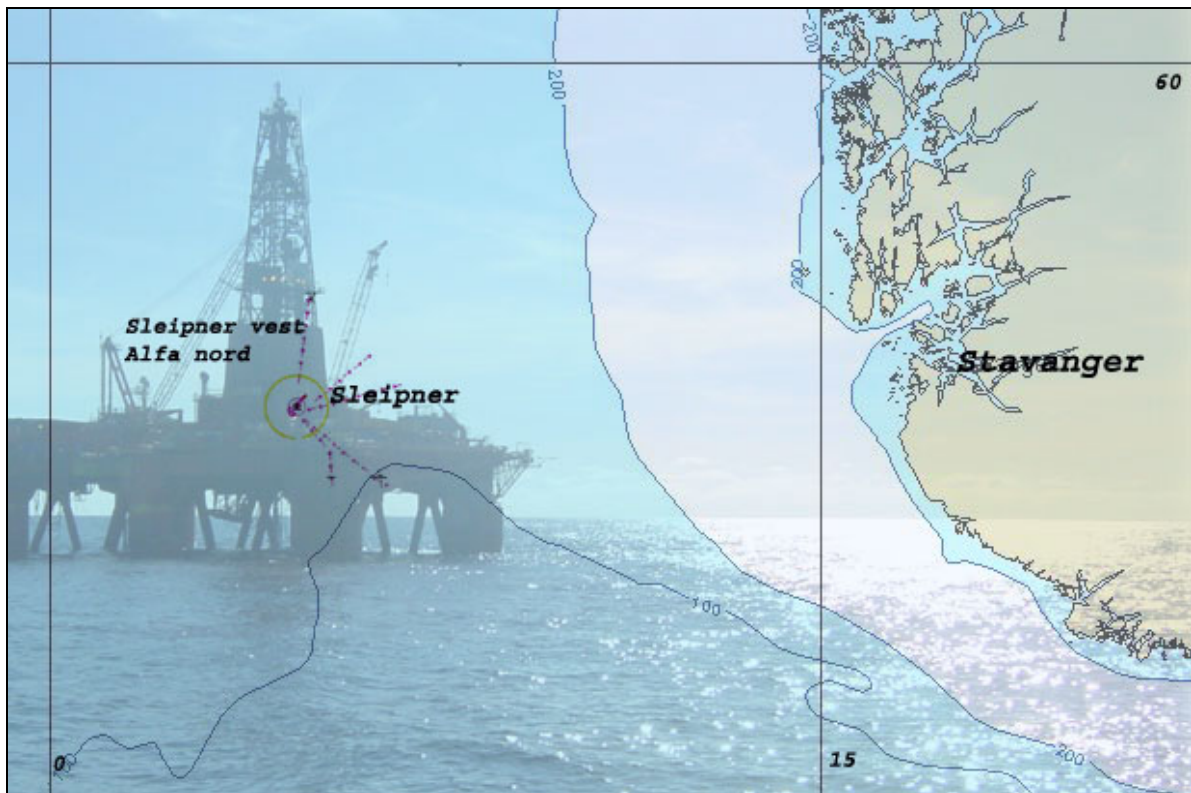


Figure A.2.1. Location site of the drilling rig Transocean Searcher at Sleipner Vest Alfa Nord (SVAN).

Figure A.2.2 shows a lay-out of the location of the SVAN field. The distance from the nearest field is about 17 km towards SE. The prevailing currents are rotating due to the tidal action, with a residual current component directed towards NE (see presentation of ocean current statistics in Figure A.4.3 shown later in the report). The direction of the residual currents in the area is favourable with respect to possible influence from discharges at other fields nearby.

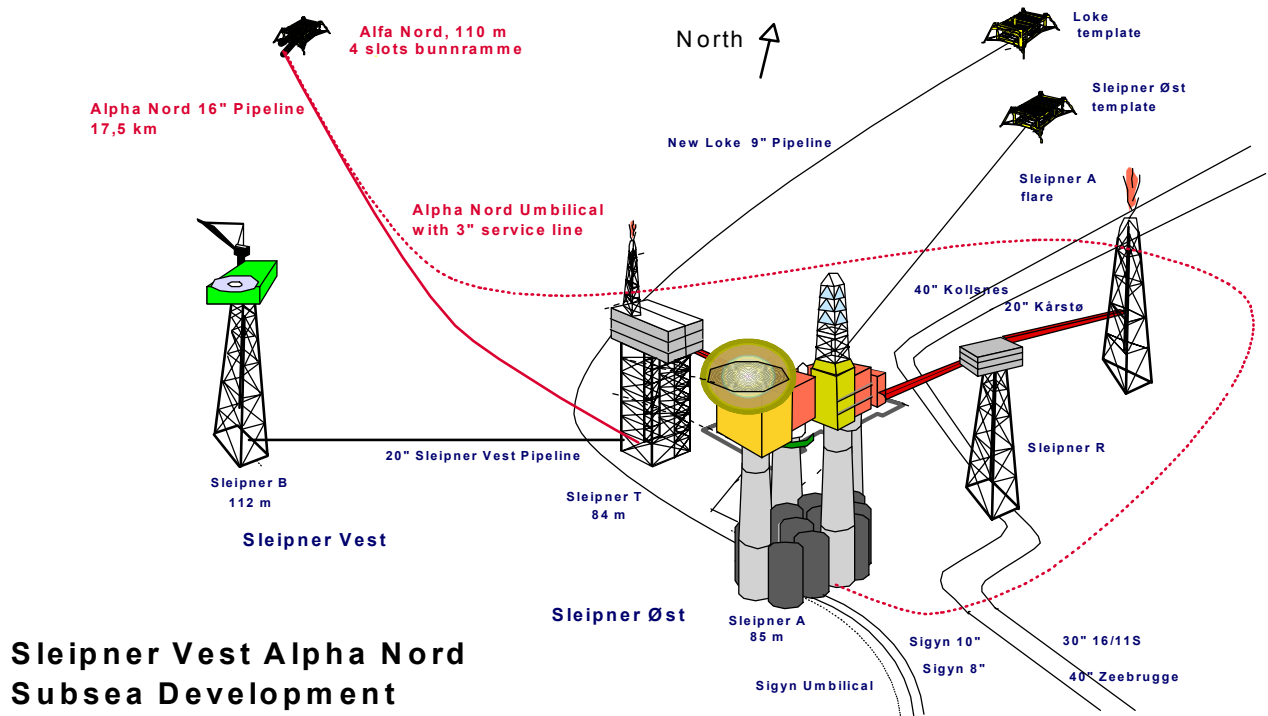


Figure A.2.2. Lay-out of the Sleipner Vest Alfa Nord field. Figure provided by Statoil.

This field trial represented an attempt to carry out measurements on a actual discharge experienced during drilling. The trial was also supplemented with analysis of biomarker responses and with numerical modeling of the discharges. The model applied was the one developed as a part of the ERMS project.

A.2.2. Data collection overview

In this chapter, only a short overview is given. Details on the actual winds, currents and the discharges are given in later chapters.

A lay-out of the field data collection program is shown in Figure A.2.3.

Measurements and drilling at SVAN, overview:

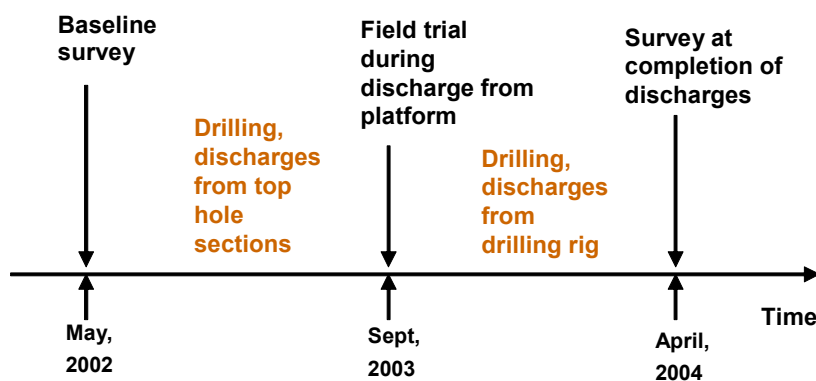


Figure A.2.3. Lay-out of the drilling program on the SVAN field.

A baseline sediment survey was carried out in April 2002, prior to the commencement of the drilling program (RF 2003). After all drilling activities had been completed, a sediment survey was carried out again in April 2004 (Akvaplan-niva, 2006).

The present report deals with the measurement program carried out in 2003, during the drilling operations. The drilling of the top-hole sections (36" and 26") for three of the four wells was carried out in August/September 2003. The debris from these drilling operations was discharged directly onto the sea floor. The content of these discharges was basically cuttings and "spud mud" with barite, bentonite and KCl as the main ingredients. Pictures collected with a ROV showed that these discharges were deployed at the sea floor in thick layers (up to order 1 m thickness in piles) in the vicinity of the drilling site.

The fourth well was not drilled at this time because a decision was not taken about drilling the fourth well. The fourth well was actually drilled later, in the beginning of 2004.

The field cruise was designed such that the actual cruise to the site was carried out when the discharges from the platform started. (The discharges directly at the sea floor from three of the wells were however carried out). This gave the opportunity to sample at the sea floor before the discharges from the platform commenced (9 September 2006). The measurements in the water column were then carried out during discharges from the platform at 9 and 10 September 2003. These discharges were performed from the drilling rig at 5 m depth. Water Based Mud (WBM) was used with cuttings, barite, KCl and the drilling fluid *Glydrill MC* as the main ingredients.

After the completion of the cruise to the site (at 10 September 2003), the drilling of the 17 1/2" and the 12 1/4" sections continued until the beginning of December 2003. Then finally the 4th well was then drilled, including the top-hole sections as well. This took place in February 2004.

All drilling activities were completed at February 17th, 2004. The final surveillance of the bottom sediments was then carried out in April 2004 (Akvaplan-niva 2006).

Figure A.2.4 shows the details of the field activities carried out during the autumn 2003. The actual cruise to the site took place at 5 – 10 September 2003. (SINTEF 2004). Before the discharges started, In addition, currents measurements and cages with blue mussels and sea scallops were deployed. These were deployed at the site before the actual discharges from the platform commenced.

Barite was used as the weighting material for both discharges directly on the sea floor and the discharges from the platform. The amount of barite discharged directly on the sea floor (from 36" and 26" drilling sections) was in total 1064 tons, and the amount of barite discharged from the drilling platform was in total 845 tons.

Field activities, autumn 2003:

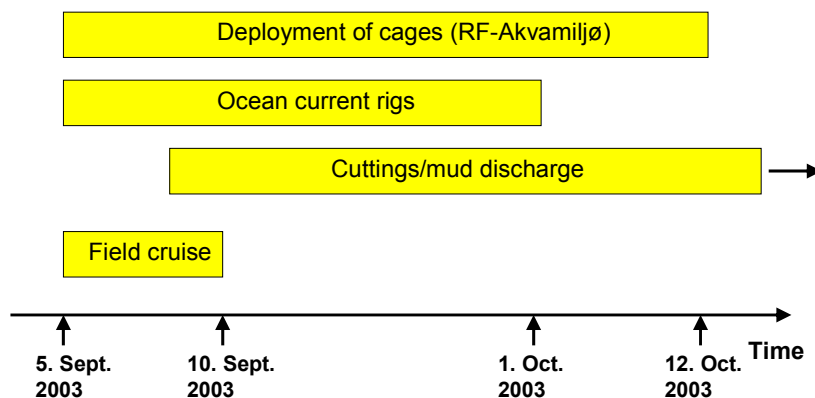


Figure A.2.4. Overview of the measurements carried out at the SVAN field in September/October 2003.

As a part of the field activities, a number of rigs were deployed:

- Three rigs with cages containing blue mussels and sea scallops. Two of the rigs were deployed close to the discharge location, while the third was deployed at a larger distance as a reference station.
- Two rigs with ocean current meters were deployed as well, one rig close to the discharge location and another rig at a larger distance (back-up for the ocean current measurements).

The cages with the blue mussels and sea scallops were deployed by IRIS-Akvamiljø as a part of the NFR FROOF “*Validation*” project. The purpose of this deployment was to study the responses of the blue mussels and the scallops on the discharges into the water column. The cages were retrieved at 12 October 2003.

The ocean currents meters were retrieved at 1 October 2003.

Except from the deployment of the cages and the current meters, the field measurements carried out on the SVAN field in September 2003 involved different activities:

- Baseline activities and sediment samples were carried out upon arrival of the vessel “*Polarbas*” hired for the purpose. These activities involved sampling of the sediment at selected stations prior to the discharges from the platform, sampling in the water column for background values and deployment of the rigs.
- The drill cuttings and mud discharges from the drilling rig were surveyed by means of the ROV available on the drilling rig, operated by “Oceaneering”.
- When the actual discharges of cuttings and mud from the drilling rig commenced at the 9th of September 2003, the discharge was surveyed by turbidity measurements and water sampling for analysis of the content of barium (a constituent in barite).

The location of the drilling rig and its mooring system is shown in Figure A.2.5. The mooring system imposed restrictions on the deployment of the ocean current instruments and the cages. The preferred direction was in the NE direction (that is, in the downstream direction), but this was prohibited. The cages and the ocean current rig were therefore forced to be deployed in the NW sector instead.

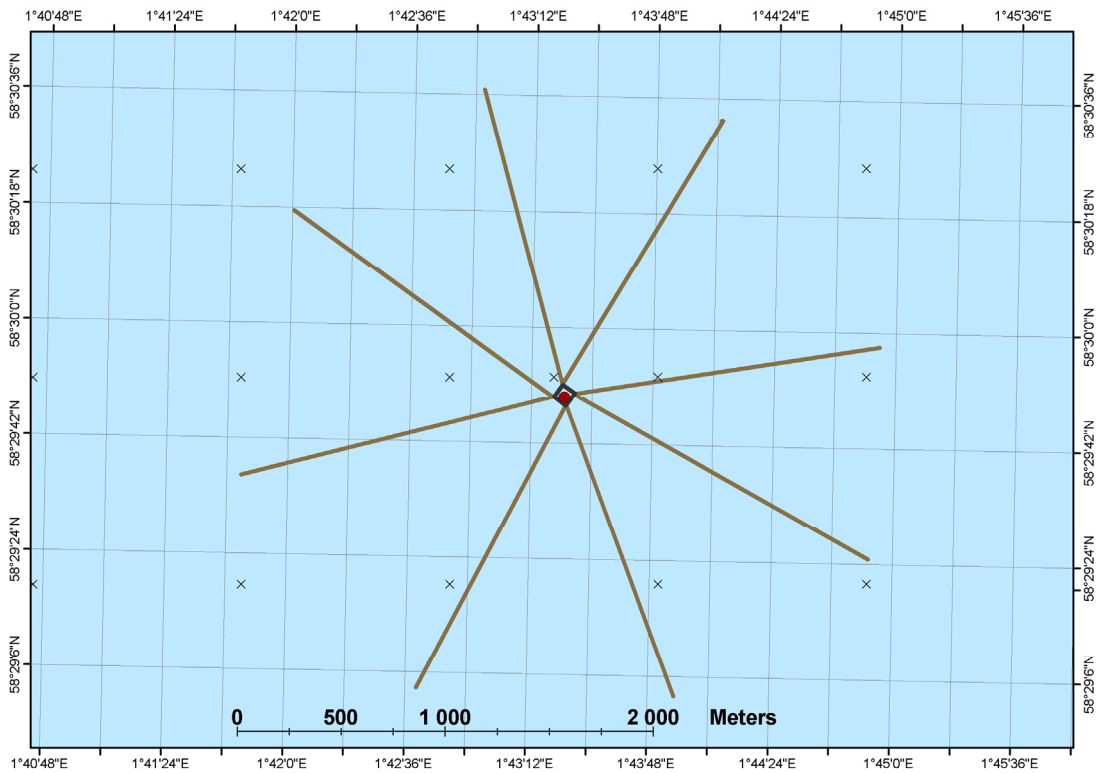


Figure A.2.5. Location of the anchor moorings for the Transocean Searcher drilling rig.

Figure A.2.6 shows the location of the actual deployment of the instruments. Note that the actual discharge point was located about 20 m SW of the actual center location of the rig. The distance from the discharge point to the ocean current rig is about 145 m. The distance from the discharge point to the shell rig A was about 250 m (shell rig B was lost).

The locations for the shell rigs were not the preferred one because the main current direction is towards NE and not towards NW. On the other hand, the locations are well within the “tidal sweeps” of the rotating tidal currents in the area. This is described in more detail later in the report.

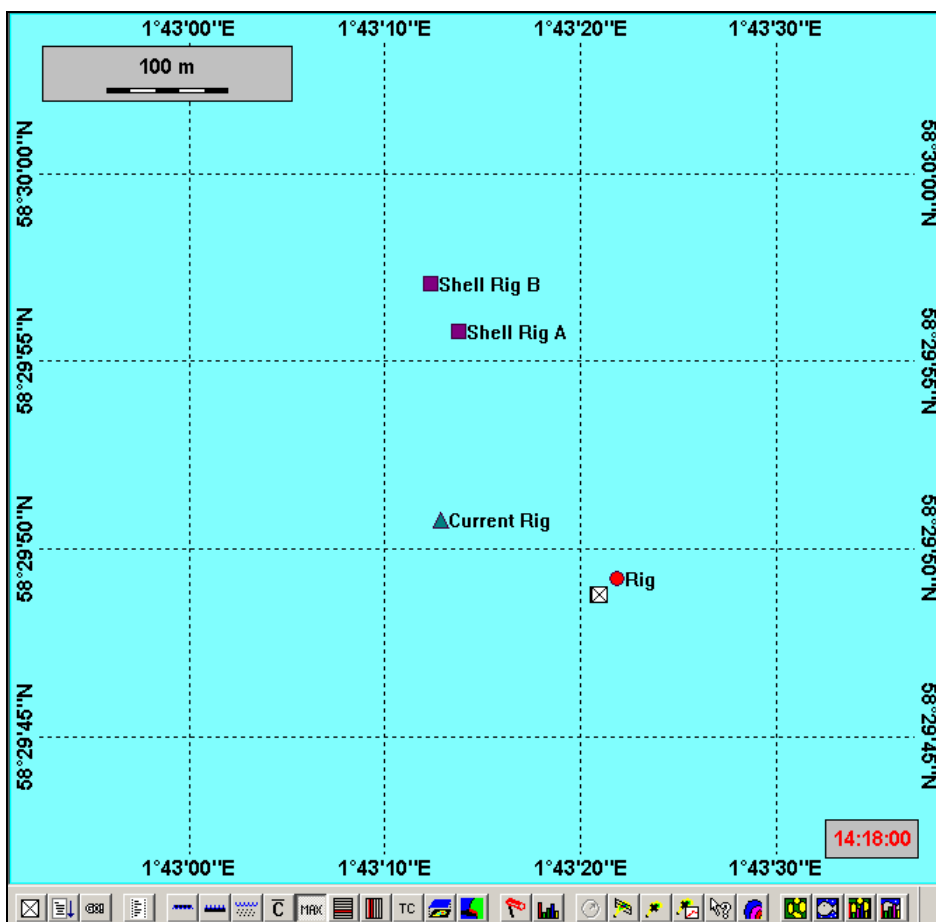


Figure A.2.6. The location of the shell cage stations A and B and the ocean current rig. The discharge location is denoted with a square with a cross inside.

Two reference stations, both for the cages (shell rig C) and the currents were also established about 6 km east of the drilling rig, as shown in Figure A.2.7.

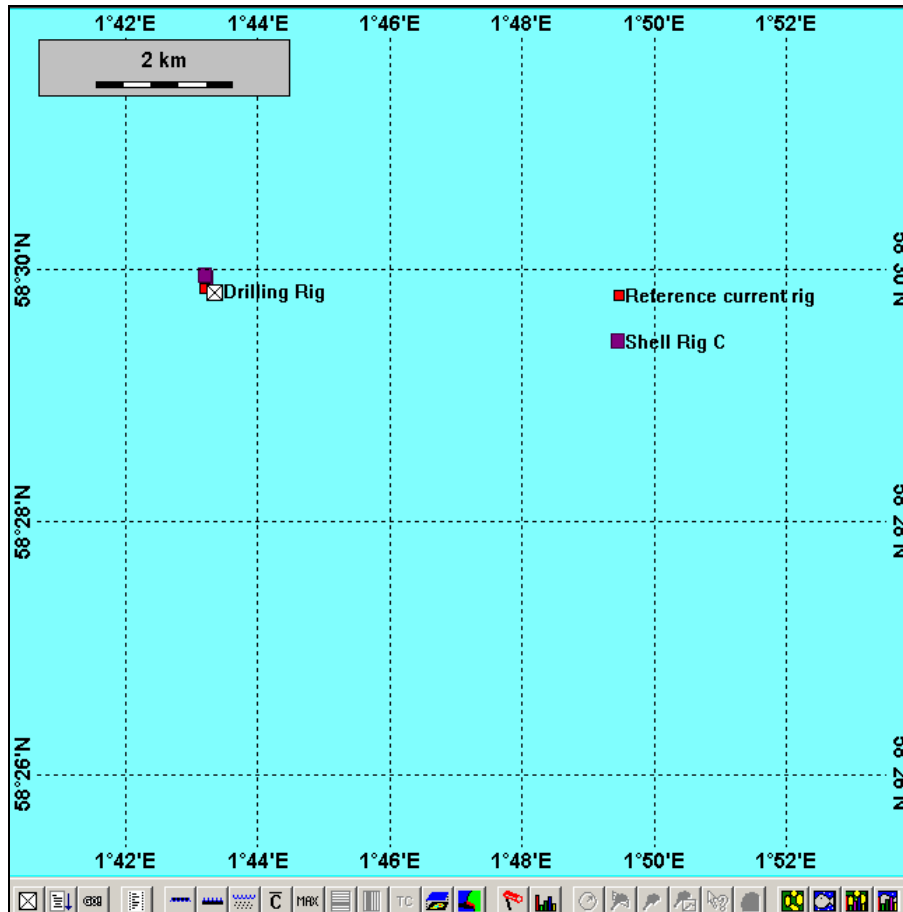


Figure A.2.7. Location of the reference shell cage rig C and the back-up ocean current rig. Discharge point is shown to the left denoted ("Drilling rig").

A.3. Deployment of cages with blue mussels and sea scallops.

Two shell rigs A and B were put out in the exposed area at a distance of about 250 m from the discharge point. The locations are for shell rig A (ED50; 58°29,930N. 01°43,230) and shell rig B (ED50; 58°29,951N. 01°43,206) NNW of the drilling rig (ED50; 58°29,821N. 01°43,363E, as specified by Statoil) at depths of; 10, 20, 40 m and 20, 35, 100 m, respectively. The locations of the cages are shown inn Figure A.2.6. A reference shell rig C was located at a distance 6 km towards E. The location is given as (ED50; 58°29,428N. 01°49,459) with cages at depths of; 10, 20 and 100 m. The

location is shown in Figure A.2.7. The cages were deployed at 5 September 2003 and retrieved at 12 October 2003.

Figure A.3.1 shows a layout of the cage mooring arrangements deployed. Rig B and the 10 m depth cage at Rig C (the reference station) were lost during the field trial. Therefore, only the 10, 20, and 40 m cages at rig A and the 20 and 100 m cages at rig C were retrieved. Less than 3% of the scallops and blue mussels placed in the cages died during the exposure period.

The equipment used in the field experiment was arranged to withstand the rough conditions in the North Sea. From the main buoy (Ø:75cm, CC5 upward pull: 210 kg) and marking flasher (Jotron MF 1114) a caching line (Danline 12 mm) and buoy was tied together with the main 12mm rope (Spectra Dynemika; 11 ton breaking load, working load ca 1,5 ton) which was anchored to the sea bed with 250-300 kg electro motors. Above each of the lantern nets which was tied to the main rope, two 11" trawl balls (buoyancy 18 kg) was spliced on to keep the nets and the rope in a vertical position (figure A.3.1).

Upon arrival to the field site the scallops and blue mussels cages were lowered at the pre-designated depths. After the first hydrographic measurements, it was discovered that the discharge plume would be expected to sink down to 35 – 40 m depth, rather than staying within the upper 10 – 20 m of the water column. The reason for this was the stratification conditions measured upon arrival to the site. The stratification is shown in Figure A.4.2, showing a relatively homogeneous water surface layer down to 30 – 40 m depth. This hydrographic situation was not anticipated before arrival at the site. Therefore, the depths of the cages close to the discharge site were changed to include the 30 – 40 m depth interval. However, this was not done at the reference station due to lack of time, leaving us with only one comparative reference depth of 20 m (figure A.3.1).

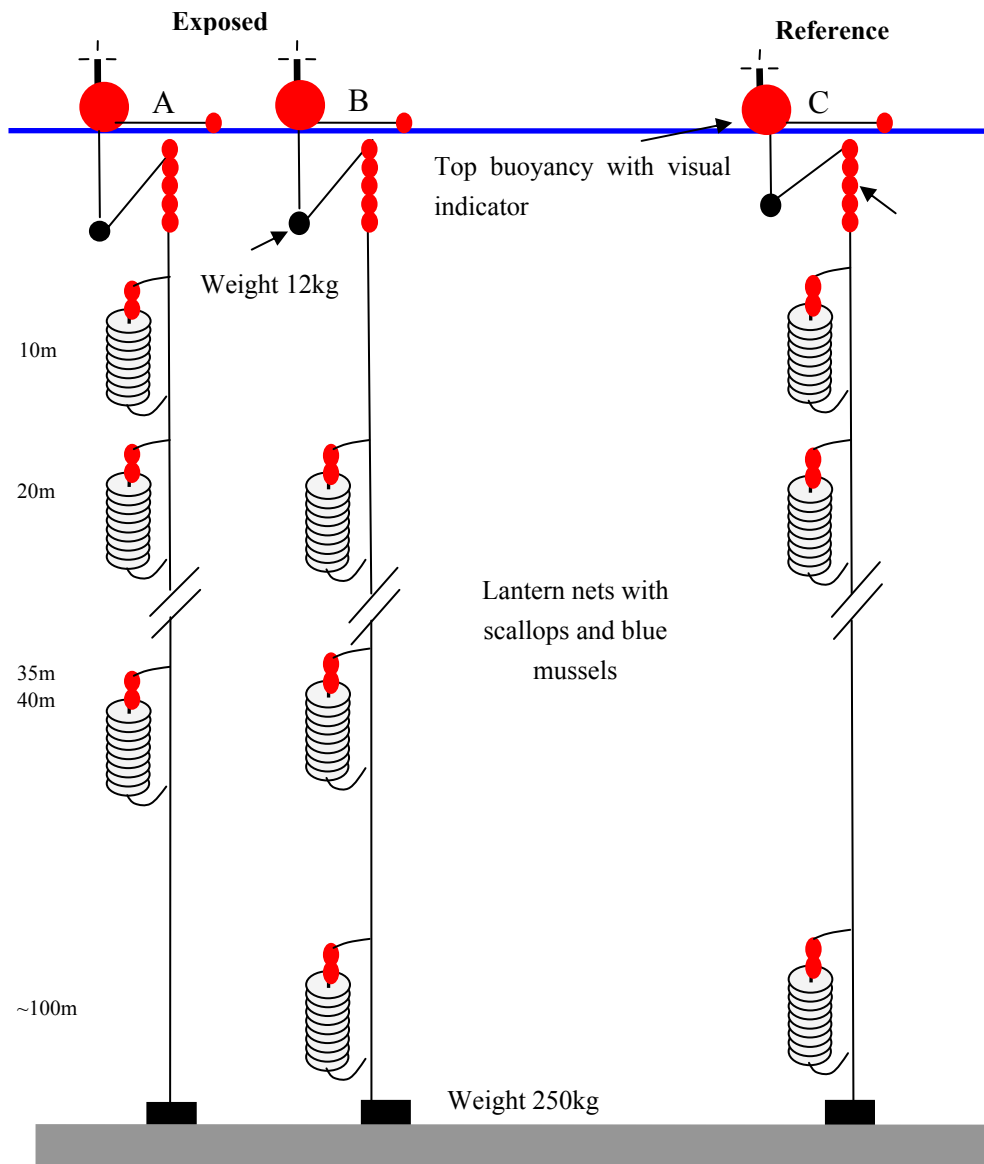


Figure A.3.1 Layout of the moorings and depths for the cages deployed. Note that the cages at rig B and the 10 m depth cage at rig C were lost¹ during the field trial.

¹ The reason why the shell rig A was lost is not clear. It simply wasn't there when it was to be retrieved.

A.4. Ambient data collection

This chapter contains an overview of the ambient conditions prevailing during the SVAN September 2003 field trial. The overview comprises:

- General weather conditions
- Temperature and salinity
- Ocean currents

A.4.1 General weather conditions.

Wind conditions during the 6 days cruise in September 2003 is shown in Figure A.4.1.

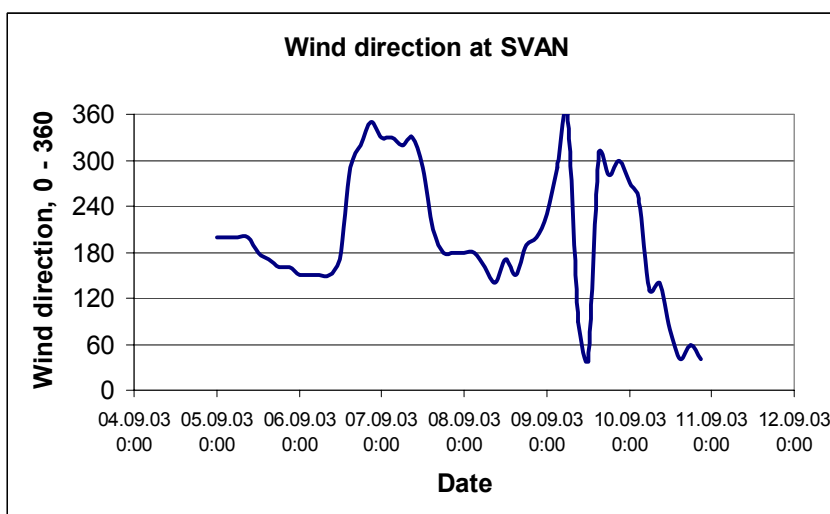
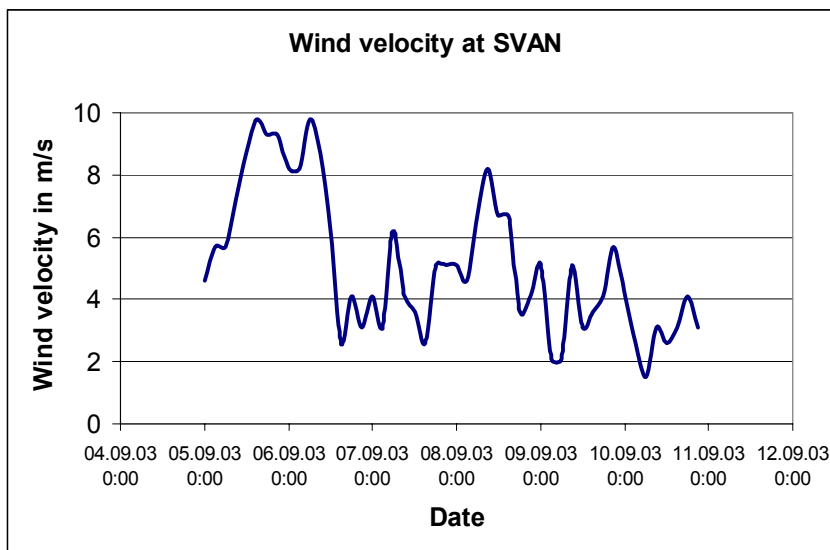


Figure A.4.1. Wind conditions during the 6 days SVAN cruise, September 2003.

The figure shows that there were generally calm winds during the field trial, in particular during the last days (9 – 10 September 2003) when cuttings and mud were discharged.

A.4.2. Temperature and salinity.

Vertical profiles of temperature and salinity were recorded daily during the cruise to the site. Profiling the water column with respect to salinity, temperature and turbidity was performed using a CTD from SAIV (model SD204), equipped with a turbidity sensor from Seapoint Sensors Inc.

Figure A.4.2 shows vertical profiles of temperatures measured during the cruise to the site. The figure shows a rather massive surface layer with temperatures at about 14 – 15 °C down to 30 – 40 m depth. Below 40 m depth the temperature was generally within the interval 8 – 11 °C. This stratification is rather unusual, with temperatures as high as above 14 °C down to 40 m depth. The reason for this was a build-up of warm water masses in the North Sea during the warm summer of 2003. This situation was not anticipated before the sea trial. It caused some re-arrangement of the layout of the field trial (change depths of cage locations, look for plumes at larger water depths than what was planned for originally) that had to be carried out on the site.

Salinity variations in the vertical were recorded to be small, within 34.6 – 34.9 ppt. These are typical ocean values for sites located far from land. Thus, it is the temperature variations that will cause a density change in the ambient water masses. These will be most pronounced close to 40 m depth.

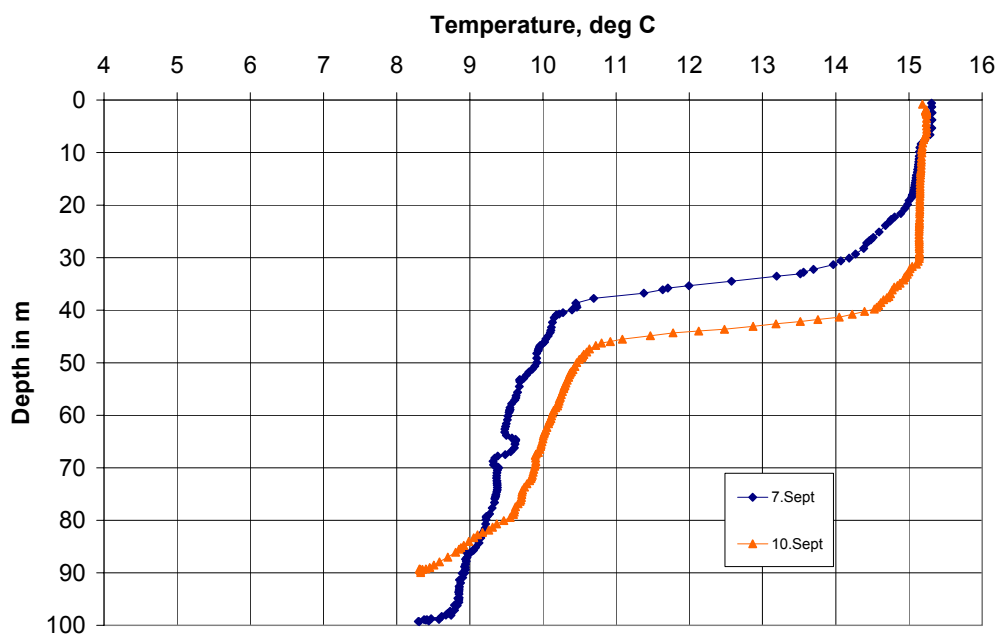


Figure A.4.2. Vertical variations of the temperatures recorded at 7. September and 10. September 2003.

A.4.3. Ocean currents

Aanderaa RCM-9 current meters were used for the current measurements. These meters measure the current speed and direction by a Doppler Current Sensor that sends out 600 pings during each recording interval of 10 min. The sensor measures the horizontal current in an area from 0.4 to 2.2 m from the instrument. The measurements are compensated for tilt, and referred to magnetic north by means of an internal compass. The 10-minute vector averaged current velocity (speed and direction) is then calculated and recorded.

The mooring was equipped with a surface buoy. For monitoring purposes the buoy transmitted the recorded data in real time to a nearby vessel by a VHF-radio connection.

The measurement position is shown in Figure A.2.6. The measurement depths were 10, 35 and 60 m. (In the period 5 – 7 September the meter in the middle was deployed at 20 m depth.) The deployment period was between the 5. of September to the 1. of October 2003. The mooring was accidentally cut after 20 days, releasing the upper meter and the surface buoy. The equipment was picked up by a stand-by vessel. Due to this event, the current meter at 10 m depth gave only reliable data for the time period 5 – 25 September. The other two meters in 35 and 60 m depth were in operation from deployment (5. September) until they were picked up 1. October 2003.

A back-up ocean current rig was also deployed at the reference station about 6 km east of the discharge point, but the data from this rig was never processed. The reason for this was that the data collected at the actual location was considered sufficient for the purpose. The location of the back-up rig is shown in Figure A.2.7.

Figure A.4.3 shows the relative numbers of current observations within 30°-sectors.

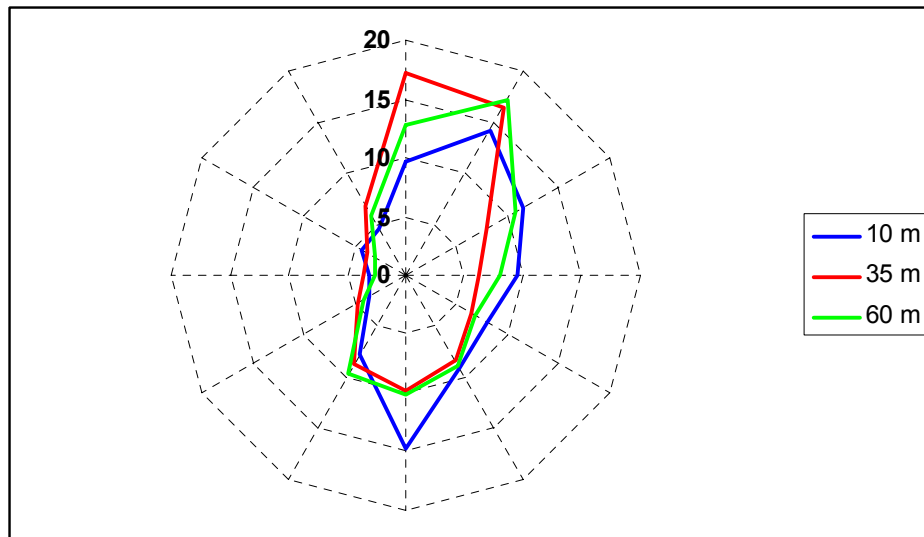


Figure A.4.3. The relative number of current observations within 30° sectors observed at the SVAN field during the recording period 5/9 - 1/10 2003. The current meter at 10 m depth recorded in the time period 5/9 – 25/9 only. The cages with the sea scallops and blue mussels were located towards NW, which are somewhat besides the main current directions (NE and towards S).

Figure A.4.4 shows one example of a time series recorded by the current meter at 10 m depth. The results show a dominating semi-diurnal tidal current rotating clockwise (in periods). Dominant tidal current directions were towards NNE and S (Figure A.4.3). This current compound was dominant at all recorded depths.

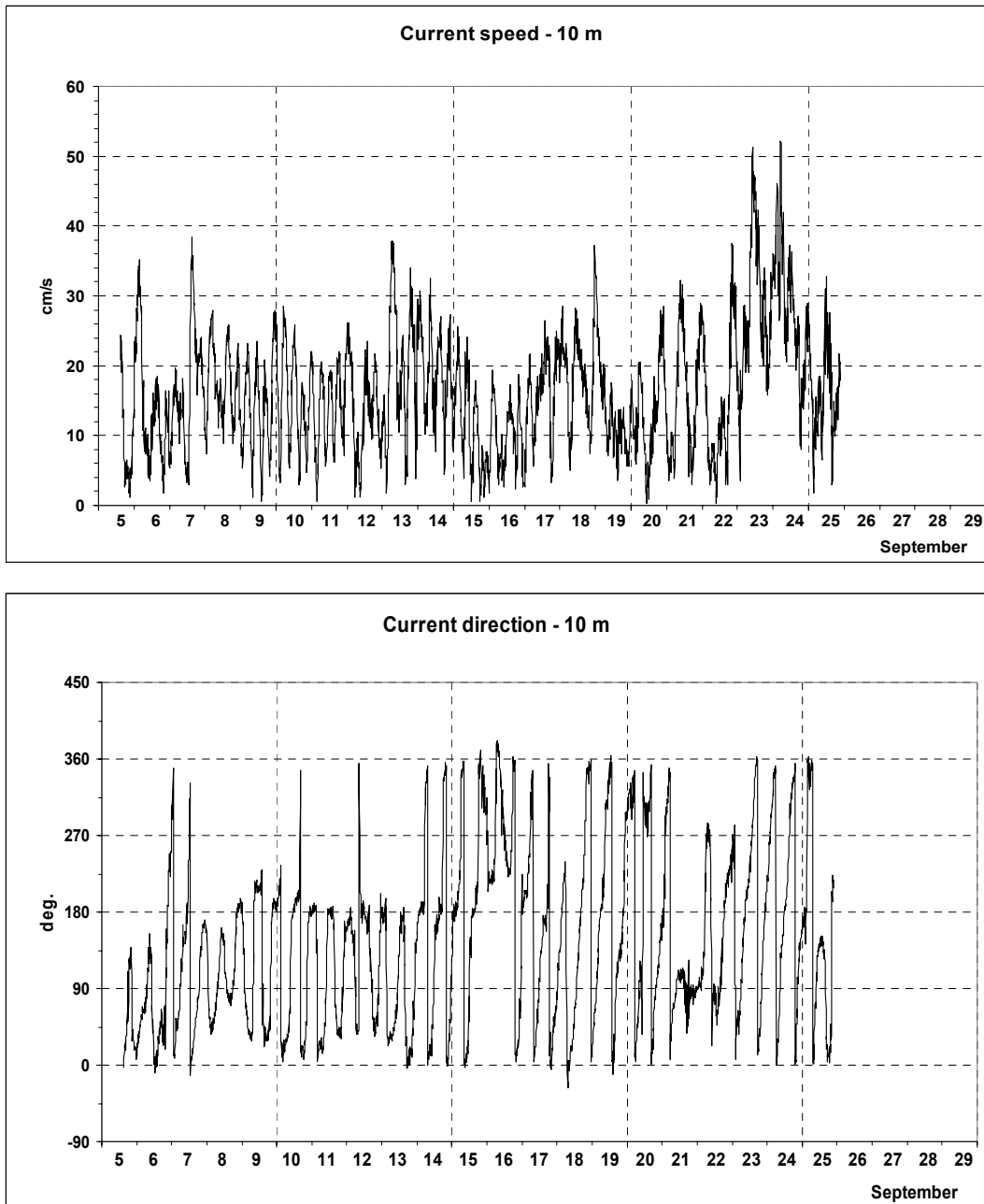


Figure A.4.4. Time series plot of currents recorded at 10 m depth at the SVAN field in the time period 5 – 25 September 2003. The figure illustrates the diurnal tidal motion of the currents in the area, with a tendency to move towards E (on the average) during the first 13 – 15 days of the measurement period.

A.5. Discharge conditions

A.5.1 Amounts of discharge

The discharge from the drilling rig commenced the 9th September at 1000 local time. Before that, the discharge had taken place directly to the sea floor (during drilling of the 36" and 26" well sections), deploying cuttings and water based mud (WBM).

The discharge took place from the drilling rig while drilling the 17 1/2" and 12 1/4" sections for three of the wells planned. The debris from the drilling hole was separated at the shaker, separating out the cuttings (to be discharged) from the mud (to be re-used). The cuttings (with some mud attached to it) were led through a pipe with an outlet opening located about 5 m below the sea surface.

There was some leakage from the pipe that caused some of the discharge to splash down directly on the sea floor instead of being discharged at 5 m depth. The relative amount that leaked out compared to the total amount discharged is not known, but is probably small compared to the amounts discharged through the main discharge opening. It was therefore assumed that this leakage would have little or no impact on the spreading of the underwater plume.

Upon arrival to the drilling rig, the existence of the actual discharge arrangement was not known to us. It was not possible to derive information of the design of the outlet arrangement on board the drilling rig either. Therefore, based on judgment, the diameter of the pipe was assumed to be 16" and the outlet depth to be 5 m (observed by an ROV).

During the deployment of the shell cages, discharges took place from the drilling rig during active drilling of four drilling sections during the following time periods (local time):

1st well, 17 1/2" section: Time period 9. Sept. 0930 – 12. Sept. 0900.

1st well, 12 1/4" section: Time period 16. Sept. 0400 – 18. Sept. 0600.

2nd well, 17 1/2" section: Time period 26. Sept. 0900 – 1. Oct. 0145.

2nd well, 12 1/4" section: Time period 6. Oct. 0300 – 13 Oct. 1100.

The cages were retrieved in the evening at 12 October 2003, that is about 14 hours before the completion of the fourth discharge period.

The reported mud contents of the discharges during these drilling periods as shown in Table A.5.1:

Table A.5.1. Content of discharge during drilling at the SVAN field trial in September – October 2003. Yellow line indicates a discharge of a non-PLONOR chemical. All other chemicals are categorized as PLONOR chemicals. PLONOR = “Pose little or no risk to the environment”.

Well			E3H	E3H	E1H	E1H
Drilling section			17 1/2"	12 1/4"	17 1/2"	12 1/4"
Barytt	BaSO ₄	kg	114000	96000	212000	60000
CMC LV;HV	Cellulose	kg				
Sitronsyre	Sitronsyre	kg	249	733	727	374
Duotec NS	Xanthan gummi	kg	937	1097	1668	1172
Glydrill MC	Polyalkylenglykol	kg	16723	16646	29204	13174
Kaliumklorid	KCl	kg	60250	54000	105483	46344
Kalsiumkarbonat	CaCO ₃	kg	1900	3717	5060	2351
Polypac	Cellulose + organisk støv	kg	5423	5599	10840	5004
Soda Ash	Na ₂ CO ₃	kg	375	637	890	536
Natriumbikarbonat	NaHCO ₃	kg	383	886	1028	642
Wyoming Bentonite	Leire	kg		550		
G-Seal	Grafit	kg	454	354	333	244
Mica	Mica	kg				800
Nutplug	Valnøtt skall	kg				500

The amounts of cuttings discharged can be estimated from the drilled volumes. The lengths of the drilled sections as well as the weights of the cuttings are shown in Table A.5.2.

Table A.5.2. Amounts of cuttings discharged during the measurement period 9 September – 13 October 2003. No wash-out of cuttings are included, which would increase the amounts of cuttings somewhat (order 10 %).

Drilling section	Length of section, m	Volume of section, m ³	Cuttings density, kg/m ³	Weight of cuttings, tons
1 st 17 1/2"	1321	205	3000	615
1 st 12 1/4"	662	50.3	3000	150.9
2 nd 17 1/2"	1445	224.2	3000	672.6
2 nd 12 1/4"	690	52.5	3000	157.5

The location of the discharge point is somewhat to the SW of the center of the drilling rig. This is also shown in Figure A.2.6, where the center of the discharge point is located on the SW side of the center position of the drilling rig. It should be noted that the dimensions of the drilling rig is rather large, of order 90 x 60 m for the outer frame.

A.5.2. Particle size distributions.

The largest amounts discharged comprise cuttings and barite; see the Tables A.5.1 and A.5.2. In sum, the cuttings amount to more than 1500 tons, while the barite amounts to more than 400 tons discharged during the period of the field trial. Both these discharges have particle nature. The fate of these two ingredients will therefore be dependent on their actual size distributions. If the particle sizes are small, the particles will have low sinking velocities and will thus be carried away with the currents. If the particle sizes are large, the particles will have large sinking velocities and will thus sink down on the sea floor close to the drilling site.

Samples of the cuttings and mud material were taken at the “shakers” at the drilling rig during drilling and transported to SINTEF for sieving. The results are shown in Figure A.5.3.

The particles in the mud (basically barite particles) have generally lower diameters. Their distributions were therefore determined by a Coulter Counter. A typical result is shown in Figure A.5.4 (actual distribution) and Figure A.5.5 (cumulative distribution). A summary of mud particle size distributions (essentially barite) is shown in Figure A.5.6. Particle size distributions for the mud are generally located between 0.1 and 200 µm diameter.

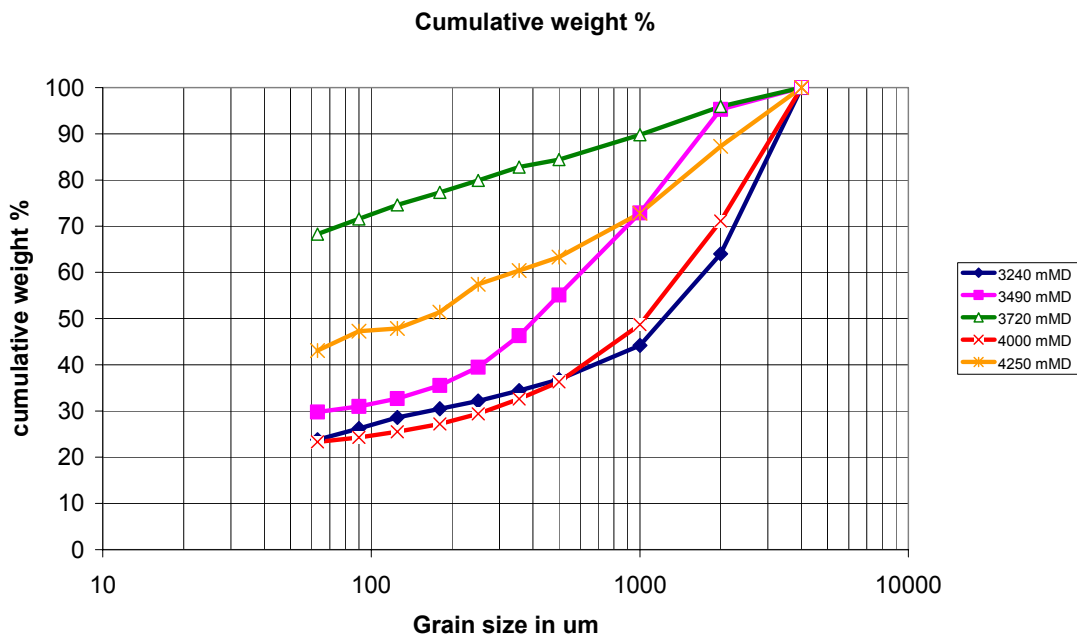


Figure A.5.3. Particle size distributions for the cuttings. The distributions are obtained by sieving. The distribution is detected between 0.063 mm and 4 mm. The samples were taken at the shaker. Numbers for mVD indicate the depth of the drilling when the samples were collected at the shaker.

COULTER® LS Particle Size Analyzer

Page 1

15:16 30 Apr 2004

File name:	2440m-3.\$01	Group ID:	2440m-3
Operator:	Stine Falkfjell	Run number:	5
Comments:	15/9-E-4H, MD MUDSAMPLE		
Optical model:	silika.rfd PIDS included		
LS 230	Small Volume Module		
Start time:	13:29 26 Mar 2004	Run length:	90 Seconds
Obscuration:	6%		
PIDS Obscur:	49%		
Software:	2.11	Firmware:	2.02 2.02

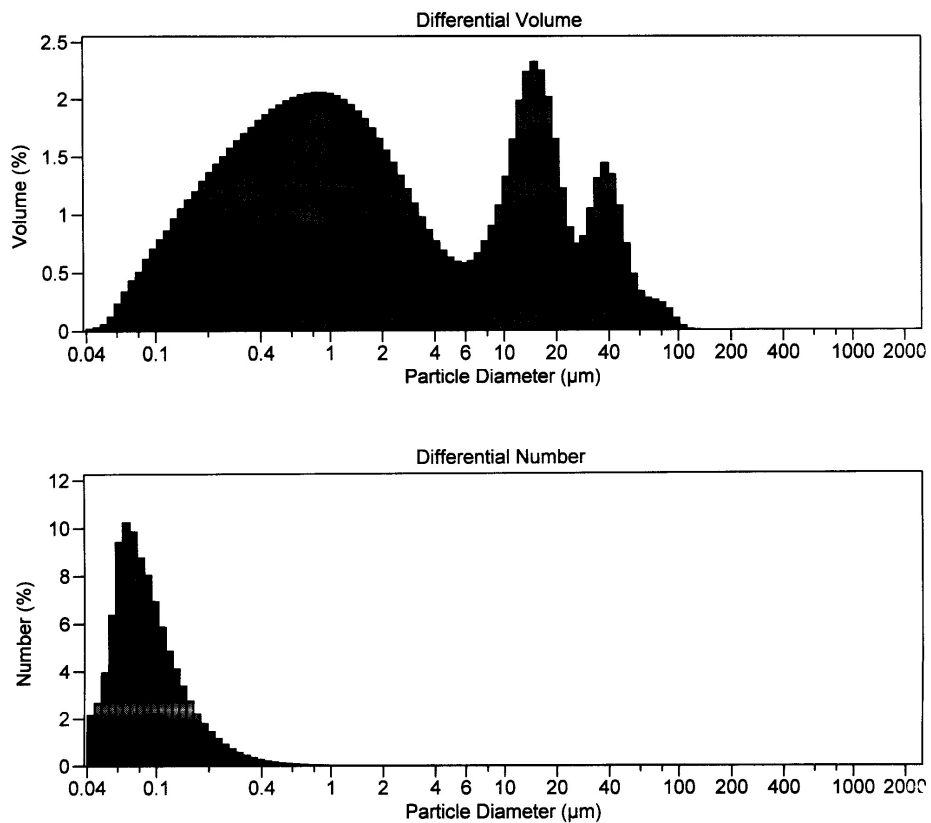
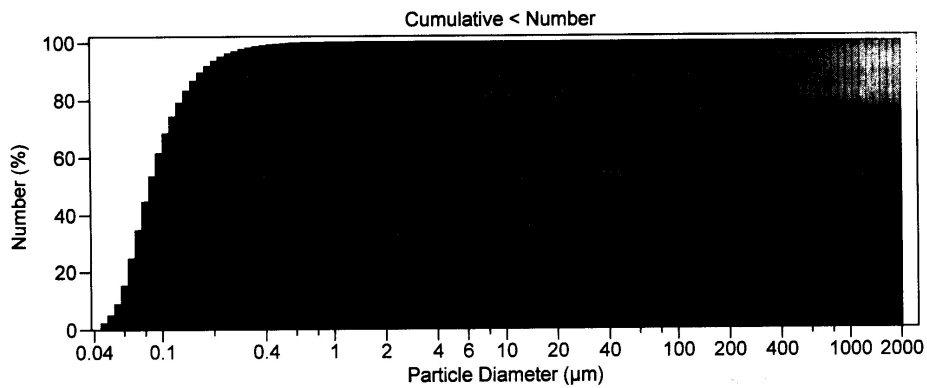
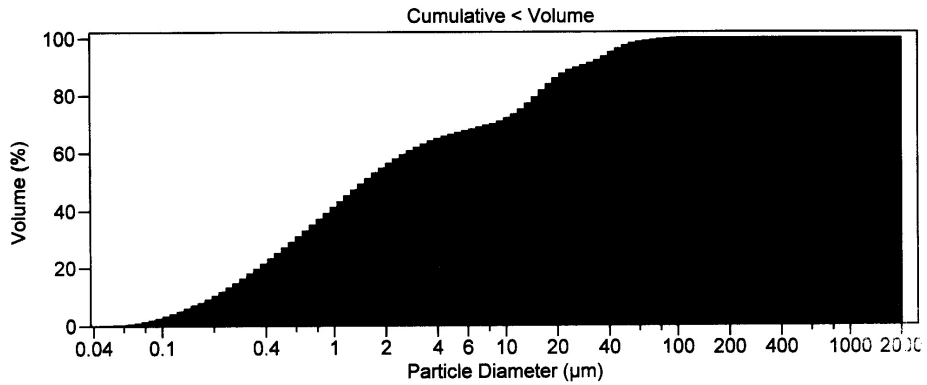


Figure A.5.4. Particle size distributions for mud sample collected at the “Transocean Searcher” drilling rig during drilling at the SVAN field in September 2003.

COULTER® LS Particle Size Analyzer

Page 2

15:16 30/09/2003



Volume Statistics (Arithmetic)

2440m-3.\$01

Calculations from 0.040 µm to 2,000 µm

Volume	100.0%			
Mean:	8.381 µm	S.D.:	14.16 µm	
Median:	1.451 µm	C.V.:	169%	
D(3,2):	0.548 µm			
Mode:	14.94 µm			

% <	10	25	50	75	90
Size µm	0.191	0.452	1.451	11.86	26.44

Figure A.5.5. Cumulative particle size distributions for mud sample collected at the "Transocean Searcher" drilling rig during drilling at the SVAN field in September 2003.

COULTER® LS Particle Size Analyzer

Page 1

12:22 2 Apr 2004

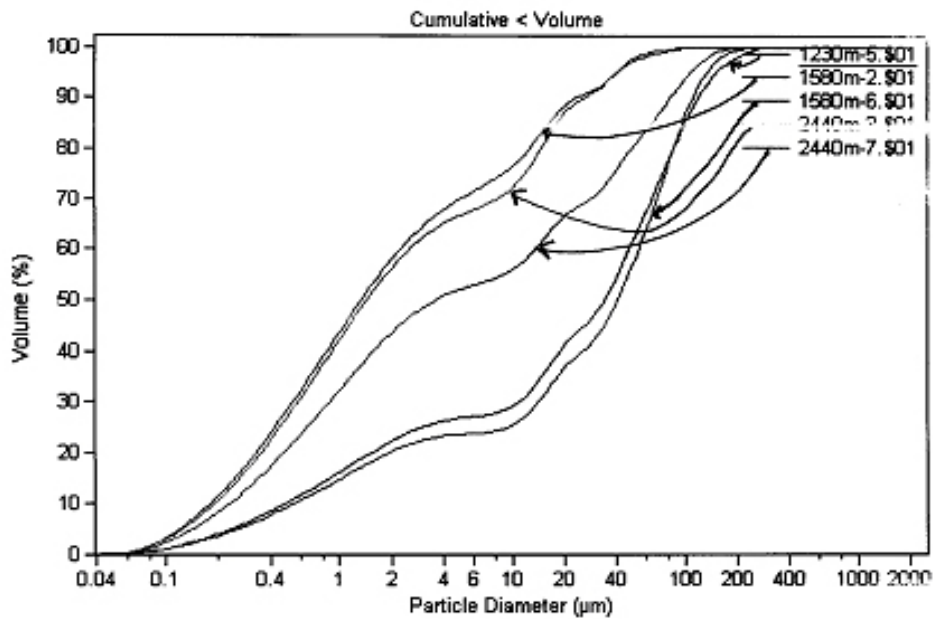


Figure A.5.6. A collection of particle size distributions for different mud samples collected at the “Transocean Searcher” drilling rig during drilling at the SVAN field in September 2003.

In the actual numerical simulations, it was made no attempt to differentiate between the different particle size distributions measured. The particle size distributions will vary, dependent on the geological structure drilled in and the type of drilling equipment used. The only differentiation made in the simulations was between cuttings particles and mud (barite) particles because these are varying significantly both in the density and size. The size variation within the cuttings samples (Figure A.5.3) and the mud/barite samples (Figure A.5.6) is relatively moderate, compared to the variations between the mud and the cuttings as a whole. Therefore, a median distribution for the particle sizes were used for both the cuttings and the mud (barite) in the simulations .

A.6. Numerical modeling of the discharges at the SVAN field.

A.6.1. About the (revised) DREAM model.

As a part of the ERMS project, the numerical model DREAM was developed further to simulate fate and behavior of the drilling discharges to the sea. The discharge is assumed to spread in the ambient water where the discharge depth (and location) acts as the source point. The discharge is assumed to form a “near field” underwater plume that spreads out in the recipient. The plume sinks down due to the content of the barite and cuttings particles which are heavier than the ambient water. The plume will stop sinking when the density of the plume equals the density of the ambient water (depth of “trapping” of the underwater plume, see also chapter A.6.3).

When the depth of trapping is reached, the discharge will separate into two parts. One part spreads out horizontally in the water column. This part will contain fine particles (with low sinking velocities) and dissolved chemicals. The other part will sink down on the sea floor. This part consists of coarser particles (with larger sinking velocities) and also chemicals/metals that are attached to the particles.

Figure A.6.1 illustrates the behavior of the discharge. The near field plume influence is seen at the upper left corner of the figure. The depth of trapping is at about 30 m depth.

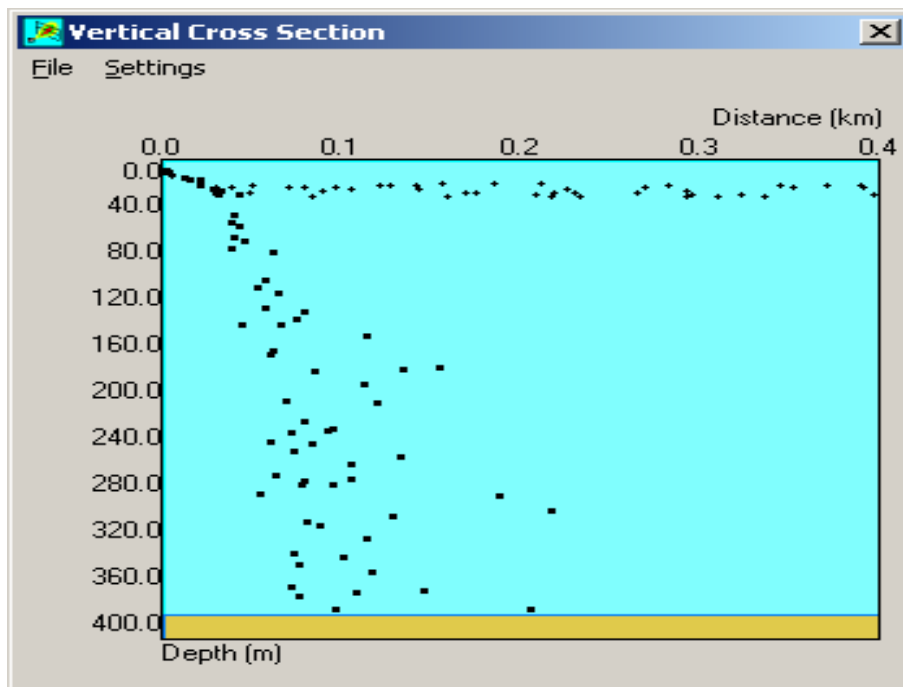


Figure A.6.1. Illustration of the influence of the near field plume, the spreading of the discharge in the water column and the deposition of the discharge on the sea floor. Note that the illustration is based on a general calculation and does not reflect the actual conditions at the Sleipner Vest Alfa Nord location.

Further details of the revised DREAM model developed as a part of the ERMS project are given in separate SINTEF reports (ERMS report No. 23 for the near field model and ERMS report No. 18 for the fates of the drilling discharges in the sea).

Feeding the model with the amounts of discharge as given in the Tables A.5.1 and A.5.2 (mud and cuttings) as well as the winds, currents and the stratification as observed during the field trial (see the figures A.4.1 – A.4.3), the expected concentrations of cuttings, barite and the non-PLONOR chemical *Glydrill MC* becomes as shown in the Figures A.6.1 – A.6.4². These four figures show how the plume develops for this particular discharge during the first 16 hours of the discharge period. Due to the tidal motions, the plume first travel in the SW direction (Figure A.6.1), then the tidal currents change toward NW and the plume starts to move towards NW (Figure A.6.2), then the currents start to move towards NE (Figure A.6.3) and then finally towards SE and finally towards SW again (Figure A.6.4). In this way a “spiral-like” plume pattern shape develops.

After a time period of 30 hours (which includes more than two tidal cycles, each with a period of 12.4 hours), the concentration field looks like as shown in Figure A.6.5. The concentration field contains a plume area with relatively large concentration (up to some ppm level), combined with a larger area where the concentrations are considerably smaller (typically order 5 – 50 ppb).

² Chemicals of the type “PLONOR” are not included in the calculations because they are not expected to have any significant impact on the biota in the recipient. The only compounds expected to have a potential impact are barite and the non-PLONOR chemical *Glydrill MC* for the discharge taking place when the cages were deployed.

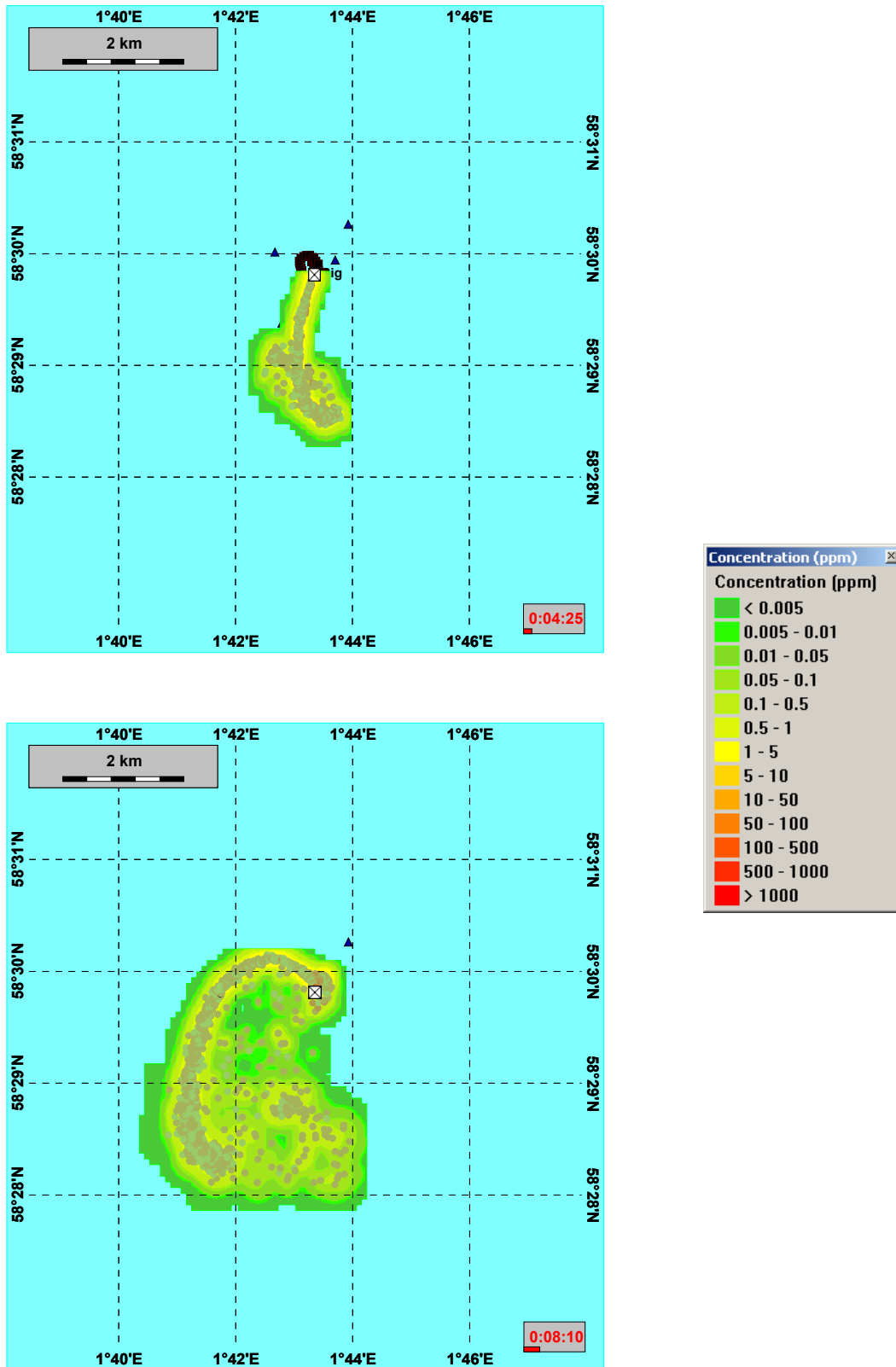


Figure A.6.1 and A.6.2. Numerical modeling with the revised DREAM model. Concentration field for particle concentrations (sum of cuttings and barite) 4 hours and 8 hours, respectively, after start of release from the drilling platform (9 September 2003).

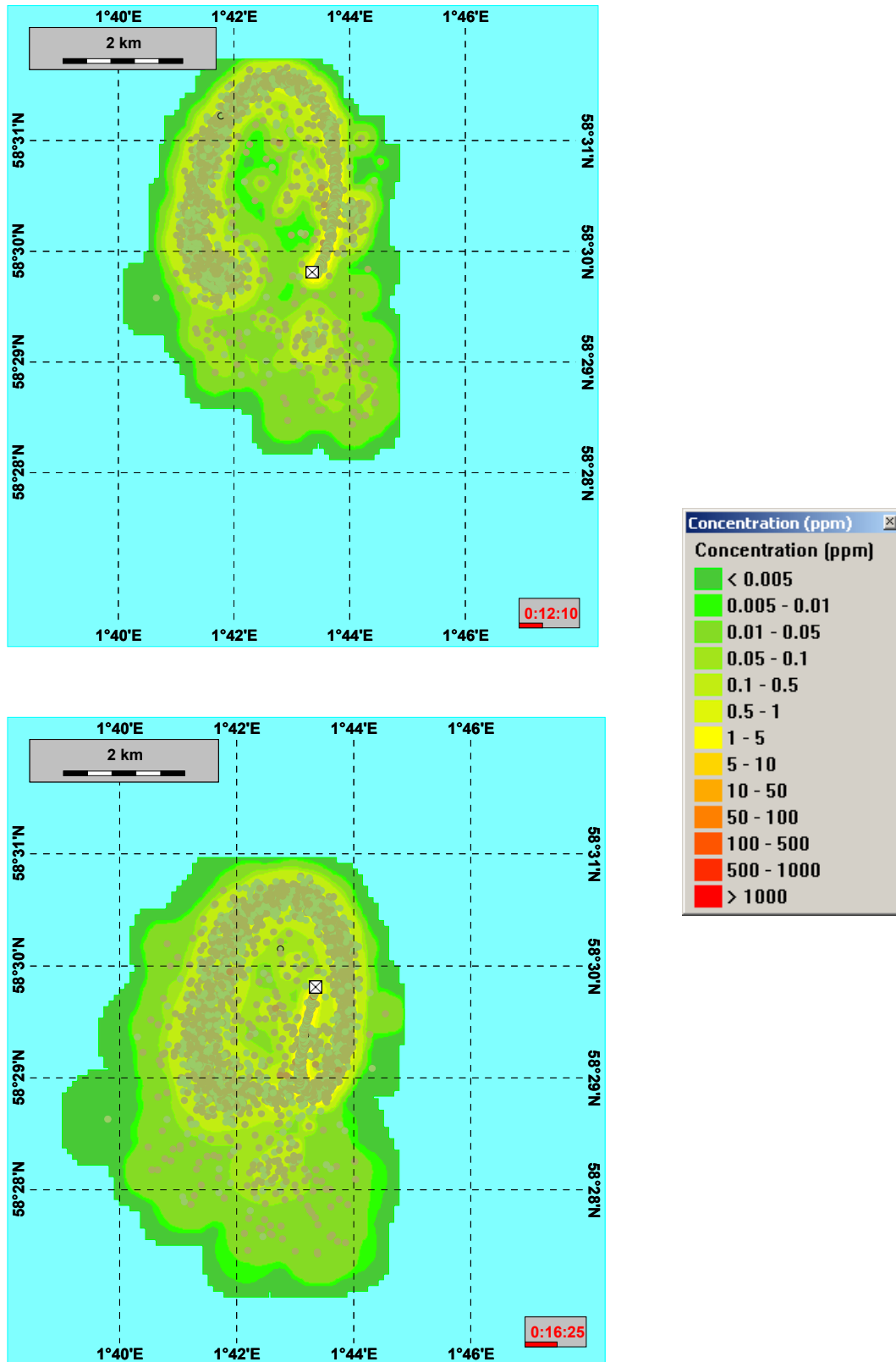


Figure A.6.3 and A.6.4. Numerical modeling with the revised DREAM model. Concentration field for particle concentrations (sum of cuttings and barite) 12 hours and 16 hours, respectively, after start of release from the drilling platform (9 September 2003).

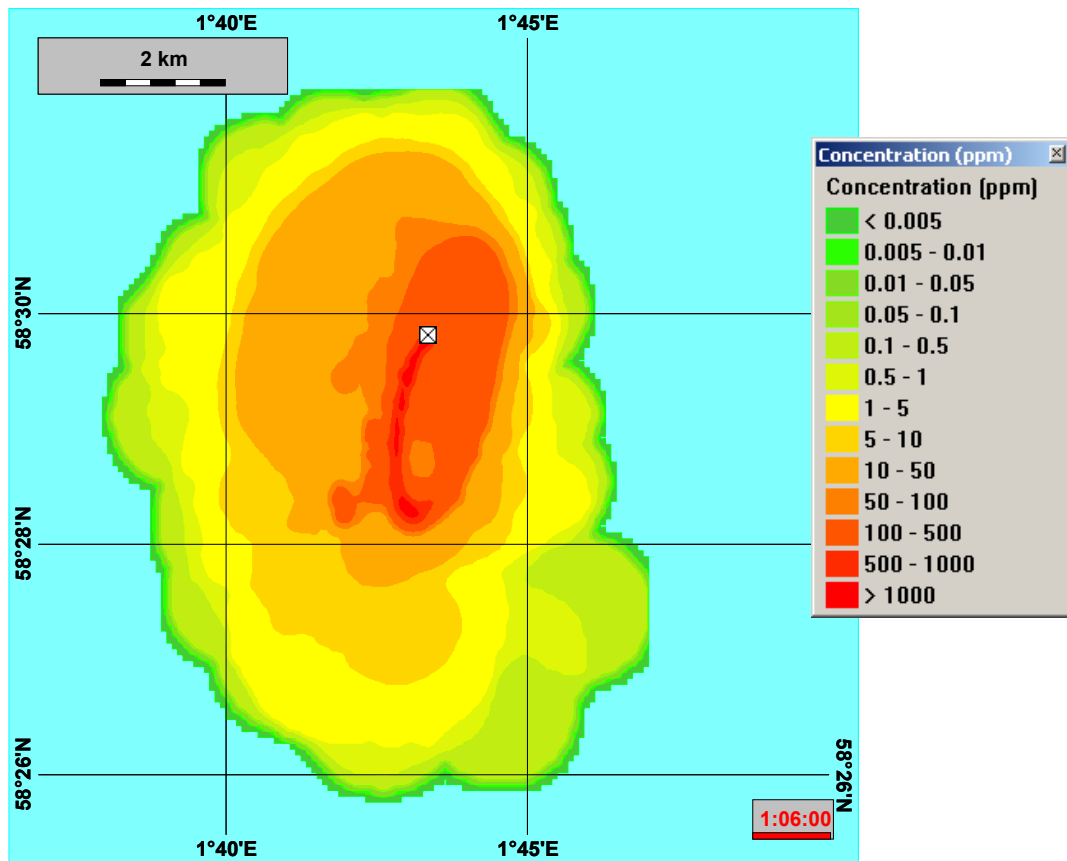


Figure A.6.5. Numerical modeling with the revised DREAM model. Concentration field for particle concentrations (sum of cuttings and barite) 30 hours after start of release from the drilling platform (9 September 2003).

Due to the presence of the stratification in the water masses (see Figure A.4.2), the maximum concentrations shown are not present in the surface layers. Due to the presence of the cuttings and the mud in the discharge, the discharge has a much larger density than the ambient water. The discharge plume will therefore sink down until the density of the plume equals the density of the ambient water. This happens in the depth interval 30 – 40m below the sea surface. Figure A.6.6 shows a vertical cross section of the plume calculated for the discharge at the SVAN field. The concentrations for the discharge (the sum of cuttings and barite particle concentrations are shown) tend to have a maximum at some distance below the sea surface. It is therefore expected that it will be the cage at 40 m depth at rig A (see the shell rig design in Figure A.3.1) that will experience the largest particle stresses.

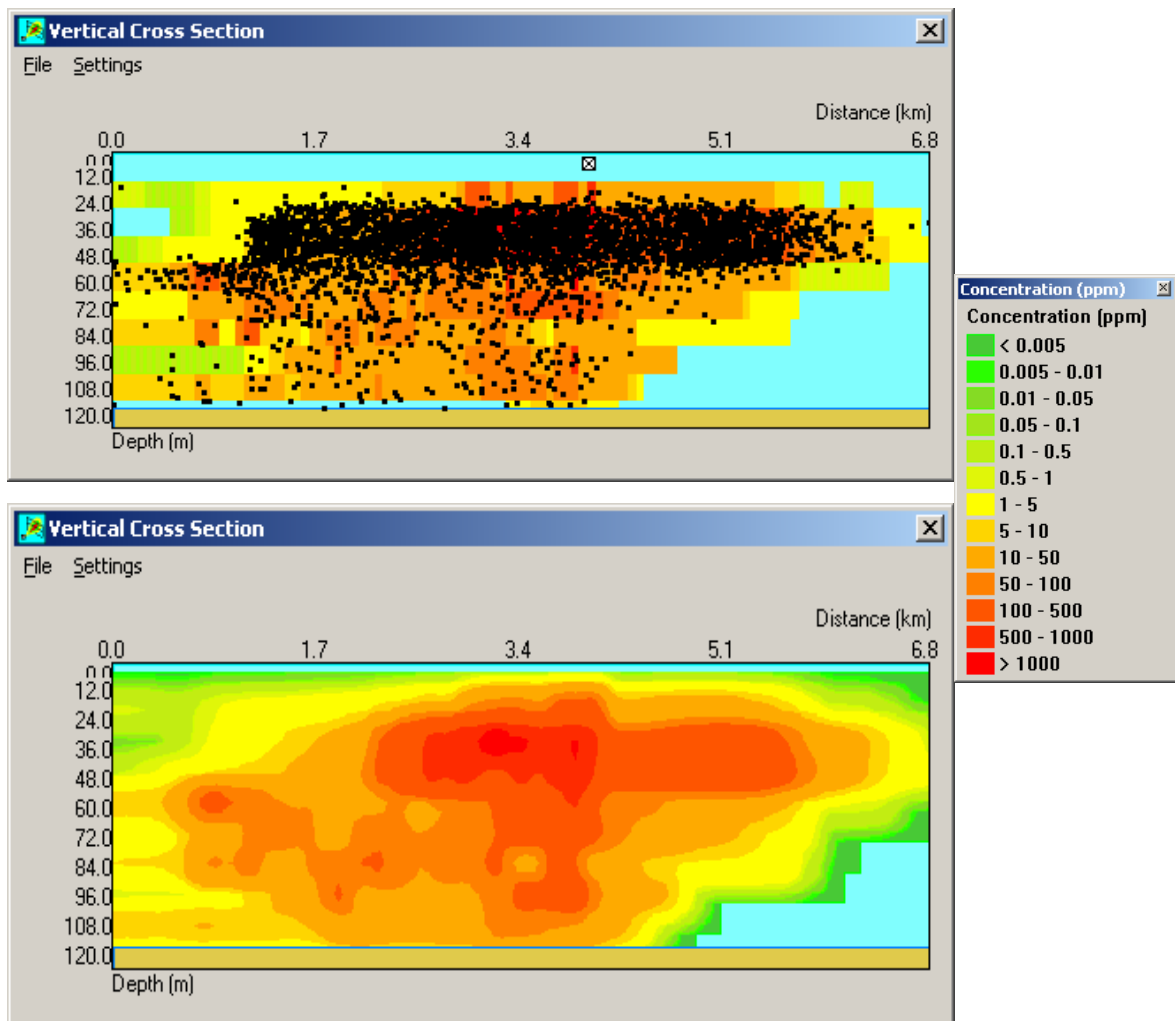


Figure A.6.6. Numerical modeling with the revised DREAM model. A vertical cross section of the plume calculated for the SVAN field release. The discharge point is shown with a cross inside a square (with a cross inside) at 5 m depth at the upper figure. The near field plume from the discharge will sink down to about 35 – 40 m depth. At this level, the discharge spreads out and is transported away with the currents. Upper figure: Concentration field (unsmoothed) together with particles representing the discharge. Lower figure: Smoothed concentration field only. Concentrations include both cuttings and barite particles.

Because the plume is sinking down to some “entrapment of the plume” level of about 30 – 40 m depth, the concentrations are expected to be at maximum at about the depth level where the 40 m shell cage is deployed. The actual depth of trapping will also be influenced by the current velocity (the depth of trapping tends to be shallower for larger current velocities). See further details described in Chapter A.6.3.

At the same time, the underwater plume is rotating due to the tidal action (as shown in Figures A.6.1 – A.6.4), so the 40 m depth cage will be exposed to “pulses” each time a plume is passing across the cage (“tidal sweeps”). Figure A.6.7 shows a calculation of a maximum particle concentration level at the location where shell cage A was deployed (see the location in Figure A.2.6). The concentrations are low in the periods between the pulses, and then rise to some level when the pulse is crossing the cage location. Each pulse will have durations of order 1 – 2 hours.

The actual concentrations experienced at each of the cages deployed and retrieved are shown in Chapter A.6.4.

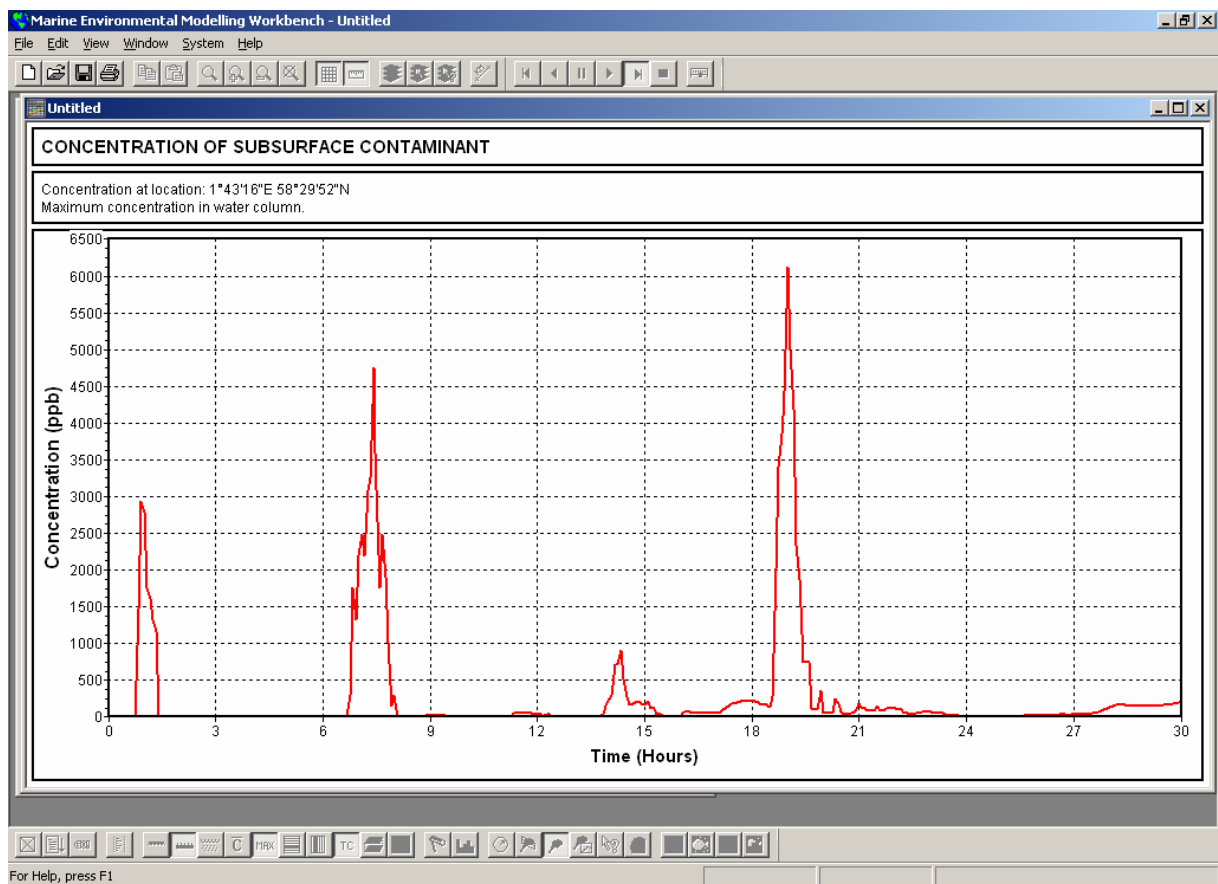


Figure A.6.7. Numerical modeling with the revised DREAM model. Particle concentration calculated for the shell cage at 40 m depth at location Shell cage A for the time period 9 – 10 September 2003 at the SVAN field.

A.6.2. Comparison between model simulations and measurements

The measurements were performed from the ship “*Polarbas*” during the first days of the discharge period (9 – 10 September). Measurements were carried out in the plume area at the SVAN field, comprising water sampling for determination of the barium (Ba) content in the water masses, and also profiling with a turbidity meter. This meter is in principle based on attenuation of light due to the presence of particles in the water masses. This may form a basis to determine the particle content (mostly cuttings and barite).

Evidence for the downwards sinking of the plume can be seen from Figure A.6.8, which shows the vertical profiles of temperature, salinity and turbidity collected near the shell cages located at rig A. A marked increase of turbidity is observed at 45 – 50 m depth (blue line), which corresponds reasonably well with the entrapment of the underwater plume close to 40 m depth as shown in Figure A.6.6.

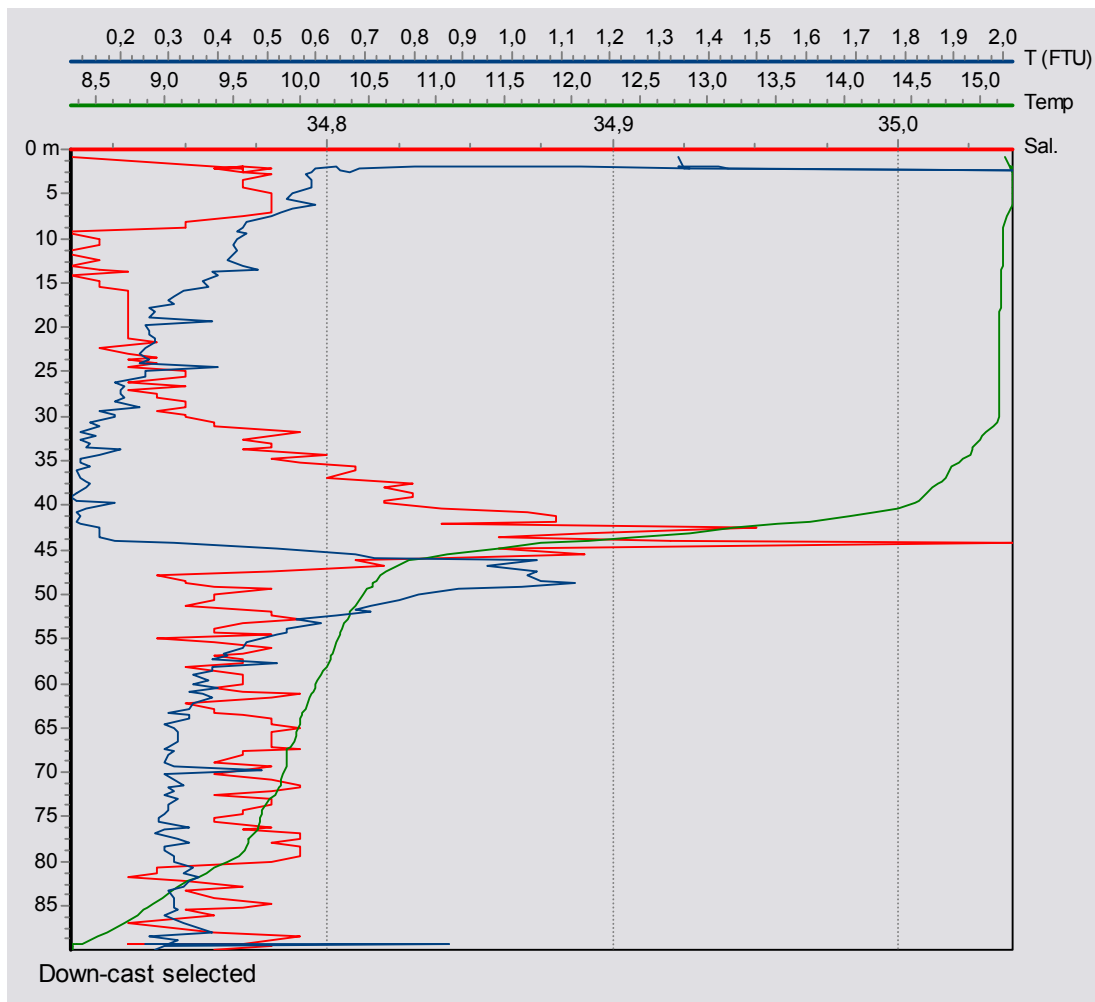


Figure A.6.8. CTD profile at shell station B, 10 September 2003, at time 1200. The shell cage station B was located close to shell cage station A, see map in Figure A.2.6. The vertical profiles collected at shell cage location B is assumed to be representative for shell cage location A as well. Turbidity (blue), temperature (green) and salinity (red).

In addition, as a supplement to the measurements and simulations that were carried out, an ROV (= *Remote Operating Vehicle*) was operated from the drilling rig to observe the discharge of drill cuttings and mud. The observations were taped to be examined after the field trial. One of the purposes of these recordings was to examine the sizes and behavior of the particles (and also the possible presence of flocculated material within the plume area). A ruler was also mounted in front of one of the cameras in order to observe particle sizes in the underwater plume.

At one occasion, the ROV was maneuvered to move just below the plume entrapped in the water masses (close to 40 m depth). The presence of the plume located at about 40 m depth was clearly evident from the ROV tape recordings, which then confirms both the model simulation results (Figure A.6.6) and the CTD measurements (Figure A.6.8).

An additional observation made by the ROV is also worth mentioning. From the position of the ROV just below the underwater plume at 40 m depth, it was evident that particle matter was leaving the plume area and moved downwards as individual particles. By closing in on these particles with the close-up camera (including the ruler mounted in front), the sizes were observed to be of order some mm, and the particles had a flake-like structure. These particles were most probably cuttings particles, originating from drilling in shalestone or clay layers. It was not observed any indications of (flocculated) barite particles from the ROV recordings. This observation confirms the revised DREAM model behavior, as illustrated in Figure A.6.1.

An attempt to compare measurements of Ba in the water column and Ba concentrations calculated was also made, as explained in the following. Measurement stations for the water column Ba concentrations are shown in Figure A.6.9. The color code shown in the locations measured indicates the concentration levels of Barium measured.

The measurements indicate that concentrations are generally low. For some of the stations, the concentrations are below 1 ppb, which indicates that the measurement has been carried out outside the plume area. Some of the other stations have measured within the area where concentrations are encountered, but outside the actual plume area (stations 2, 3 and 500 m downstream, see Table A.6.1 below).

However, at one occasion, the concentration was measured to be 200 ppb of Ba (which indicates a barite concentration close to 0.34 ppm). This measurement was carried out at Station 5 close to the discharge point, see Figure A.6.9.

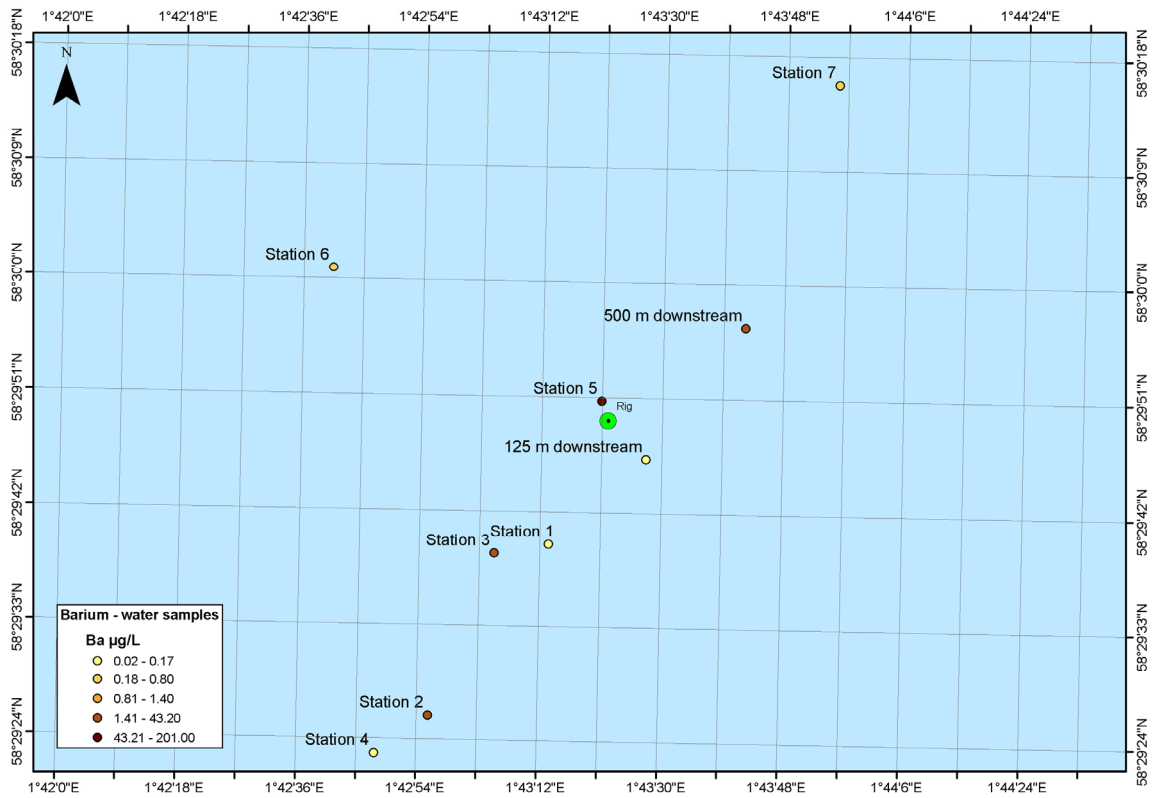


Figure A.6.9. Measurement stations for Ba concentrations in the water masses. Details of the results are shown in Table A.6.1.

Table A.6.1. Measurements of Ba concentrations in ppb measured in the SVAN area 9 and 10 September 2003.

Station	Position	Position	Sampling	Depth	Distance from discharge	Concentration
	N	E	Date	m	m	Ba, µg/L
Reference water 15m	58° 33.459	1° 51.117	10.09.2003	15	> 6000	0.61
Reference water 25m	58° 33.457	1° 50.923	10.09.2003	25	> 6000	1.4
Station 1	58° 29.657	1° 43.222	09.09.2003	15	321	0.02
Station 2	58° 29.43	1° 42.928	09.09.2003	30	835	24.3
Station 3	58° 29.644	1° 43.087	09.09.2003	15	428	43.2
Station 4	58° 29.38	1° 42.795	09.09.2003	20	984	0.17
Station 5	58° 29.845	1° 43.348	09.09.2003	20	64	201
Station 6	58° 30.014	1° 42.673	09.09.2003	20	770	0.54
Station 7	58° 30.263	1° 43.928	09.09.2003	20	995	0.8
125 m downstream	58° 29.77	1° 43.461	10.09.2003	15	128	0.03
500 m downstream	58° 29.943	1° 43.704	10.09.2003	15	407	22.5

The calculated maximum concentrations at Station 5 are shown in Figure A.6.10. The time instant of the recording at Station 5 was about 8 hours from the start. The concentration measured (201 ppb) is close to the observed max. value of 300 – 500 ppb for that time instant.

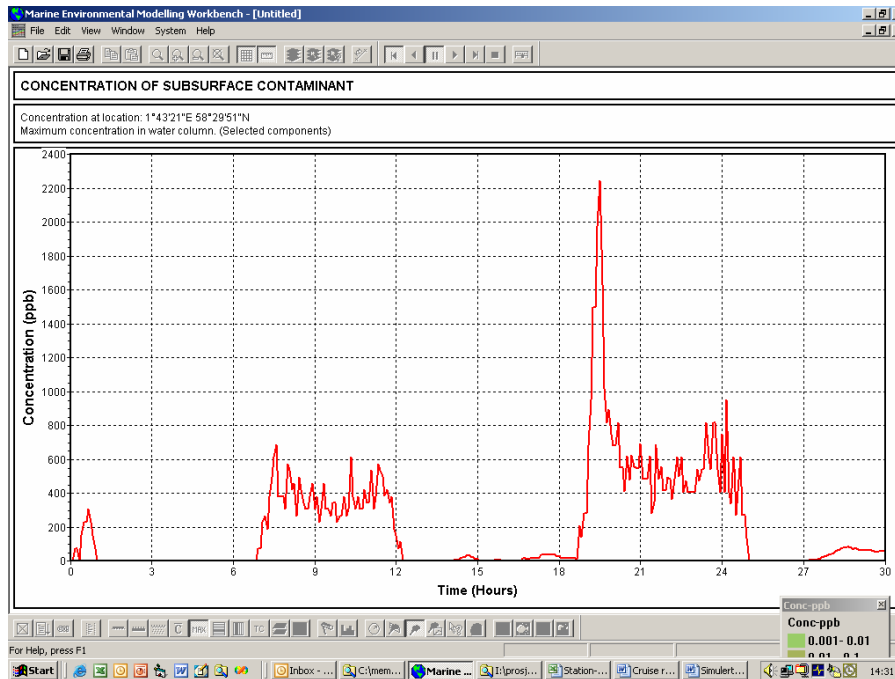


Figure A.6.10. Numerical modeling with the revised DREAM model. Time series plot for maximum Ba concentration calculated for Station 5 shown in Figure A.6.9.

One reason for the deviation between measurement and calculation of Ba concentration could be that the measurement depth was relatively shallow (20 m depth, see Table A.6.1). It may therefore be that the maximum concentration in the plume was located somewhat lower than 20 m depth. This assumption is supported by both the numerical simulation results as well as observation of the underwater plume by an ROV as explained below.

Numerical simulation results: Figure A.6.11 shows the corresponding concentration field calculated with the revised DREAM model. It turns out that the plume direction of the time instant where this measurement was carried out (about 8 hours after the commencement of the discharge) was in fact the same as the direction of the measuring point from the discharge point (towards NW). Station 5 was located lower than 100 m from the discharge point. The depth of the maximum concentration seems to be located somewhat below the recording depth of 20 m. The depth of the maximum concentrations calculated seems to be located close to 40 m depth. This seems also to be more in line with the turbidity measurements shown in Figure A.6.8.

Observations by ROV: From the observations of the ROV, the presence of the plume close to 40 m depth was evident from the tapes recorded, as explained earlier in this chapter.

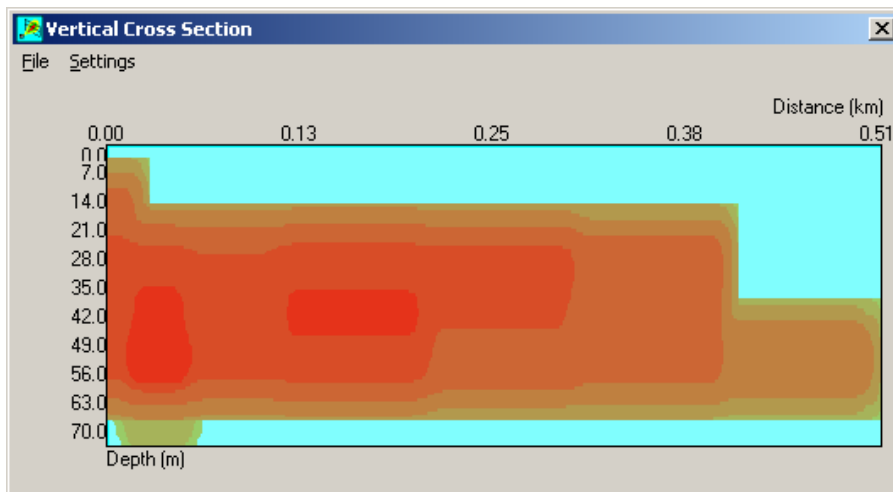
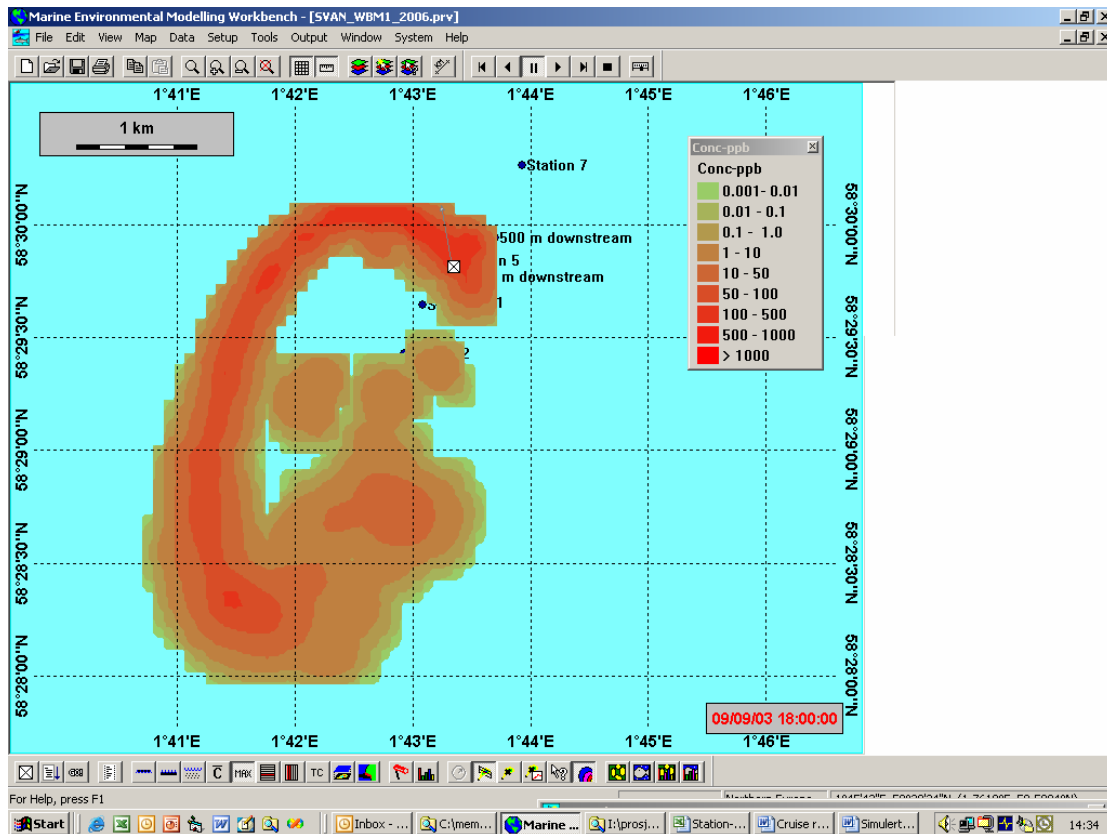


Figure A.6.11. Numerical modeling with the revised DREAM model. Concentration field for Ba at about 8 hours after start of simulation. Horizontal section (above) and vertical section (below).

A.6.3. Modelling the near field dilution of the discharge

As shown in Figure A.6.6, the discharge is sinking down to a water depth larger than the discharge depth. The discharge is carried downwards as a near-field plume, generated basically by its own density. On its way downwards, it will entrain ambient water into the plume. The dimension of the plume is rapidly increasing. When the density of the plume equals the density of the ambient water, the plume will level out and the sinking will cease to occur.

The reason for the descent of the plume is that the density of the plume is relatively large, of order twice as large as the density of the ambient water. The cuttings and the barite are both ingredients with large densities. As shown in the Table A.5.2, the density of the cuttings is close to 3000 kg/m³. Also, the barite contributes to the large density of the plume with a density of about 4200 kg/m³. The barite is the chemical that appears in the largest amounts, as shown in Table A.5.1.

Figure A.6.12a shows the results from a typical track of a plume for the SVAN discharge case, calculated with the revised DREAM model. The plume sinks down to about 40 m depth when the density of the plume equals the density of the ambient water. This depth is in accordance with the density stratification (caused by temperature) as shown in Figure A.4.2. This figure shows a sharp temperature gradient at about 40 m depth. The plume is not able to penetrate this gradient, and is therefore “entrapped” in the water column at this depth.

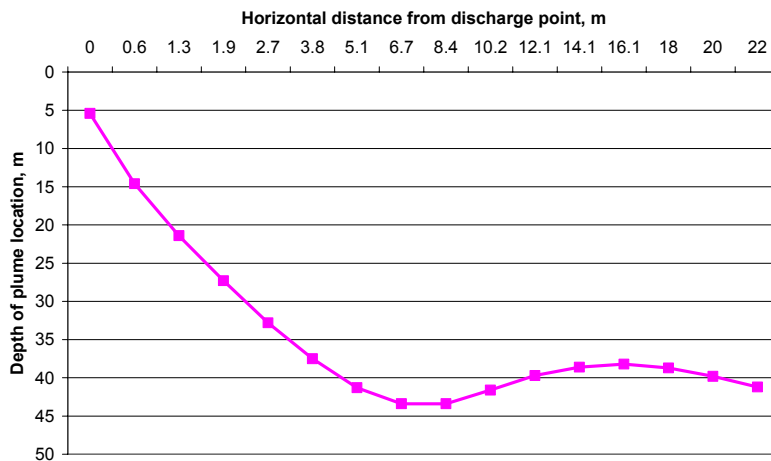


Figure A.6.12a. Numerical modeling with the revised DREAM model. The near field plume path for the discharge at the SVAN field. The plume reaches down to the level of 40 m depth when the entrainment of the plume is taking place. Discharge depth is 5 m.

Figure A.6.12b shows the radius of the plume for the same near field calculation. Note that the radius of the plume is increasing from order 0.1 m to about 10 m at the point of entrainment. This increase represents of order $100 \times 100 =$ order 10 000 increase in the cross section area of the plume. The increase in this cross section is due to entrained water from the ambient. The entrained water is generally of relatively high temperature in the present case (order $14 - 16$ °C, see Figure A.4.2), and is thus less dense than the water masses below 40 m depth. Therefore, the density difference between the ambient water and the plume is reduced significantly due to the entrainment of ambient water. The reduction is sufficient to stop the plume to cross through the density stratification, although the density difference caused by the temperature stratification is only of order 0.1 % of the over-all density of the water.

The entrainment depth of the plume will also be dependent of the ocean current velocity. Generally, the depth of entrainment will be more shallow when the ocean current velocities are large.

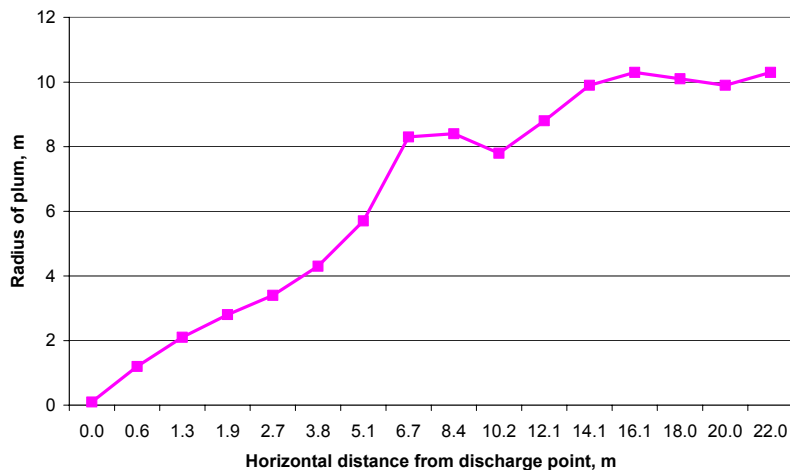


Figure A.6.12b. Numerical modeling with the revised DREAM model. The radius of the plume for the discharge at the SVAN field.

A.6.4. Calculations of barite concentrations at cage locations.

One of the purposes of the field trial was to compare environmental impact at the cage locations with biomarker responses determined for the sea scallops and the blue mussels. Particular attention was drawn to the presence of the barite, which may have a particle effect on filtering organisms (Cranford and Gordon 1999).

Since no continuous measurements of the barite concentrations were carried out at the 5 different cage locations that were retrieved (cages from three depths at Shell rig A and two depths at Shell rig C, the reference rig), the concentrations experienced at the different cage locations were deduced from the numerical simulations of the barite (or particle) concentrations.

The results from the revised DREAM model shows that the model is able to reproduce essential features of the drilling discharges measured at the SVAN field in 1993 (plume formation, entrapment of the plume below discharge depth, deposition of large cuttings particles on the sea floor). The simulations also indicate that the concentration levels are reasonably well reproduced.

The numerical model developed (the revised DREAM model) was therefore run for the whole period where the Shell rigs were deployed (9 September – 12 October 2003). The ocean currents recorded (at three depths) were used as input, along with stratification in the water masses (for the entrapment of the underwater plume), winds and the content of discharge as specified by Statoil. The currents represent the real currents experienced, except for the 12 last days, where the current recordings are missing. For this last time period, the ocean current time series used in the simulations were elongated with the (basically tidal) currents recorded from the same location before retrieval.

The results for each of the cages deployed consist of:

- Average particle concentrations for the whole deployment period
- Average particle concentration for the 5 last days of the deployment period
- Time series plots for the particle concentrations for the whole deployment period.

The actual discharge is such that first the discharge is taking place during some days, then the discharge is absent for some days. After that, the discharge is turned on again. During the absence of the discharge, the scallops and the blue mussels may recover before the next discharge is taking place. Because there was a more than a 5-day period with discharge taking place before the actual retrieval of the cages, the last 5-day average concentration levels might be the most relevant parameter to compare with (some of the) biomarker responses.

Table A.6.2 shows the results for the average particle content for each cage for the whole deployment period and for the 5 last days of the deployment.

Figures A.6.13 – A.6.17 show the time series plots for the particle content for the location of the 5 cages. These results form the basis for calculating risks for environmental damage on the biota in the cages, as presented in Part C of the present report. (Similar results for the corresponding risks are shown later in the report in the Figures C.1.6 – C.1.10.)

Table A.6.2. Average concentrations for the cage locations A and C. The concentrations include both cuttings and barite particles, where the barite is assumed to represent the most important contribution.

Concentrations calculated at the cages (ppb)		
Station	Average over 33 days	Average over the 5 last days
Cage Rig A 40 m depth	148.8	96.6
20 m	2.33	13.1
10 m	0.54	3.22
Cage Rig C 100 m	0.341	0.018
20 m	1.03	3.89

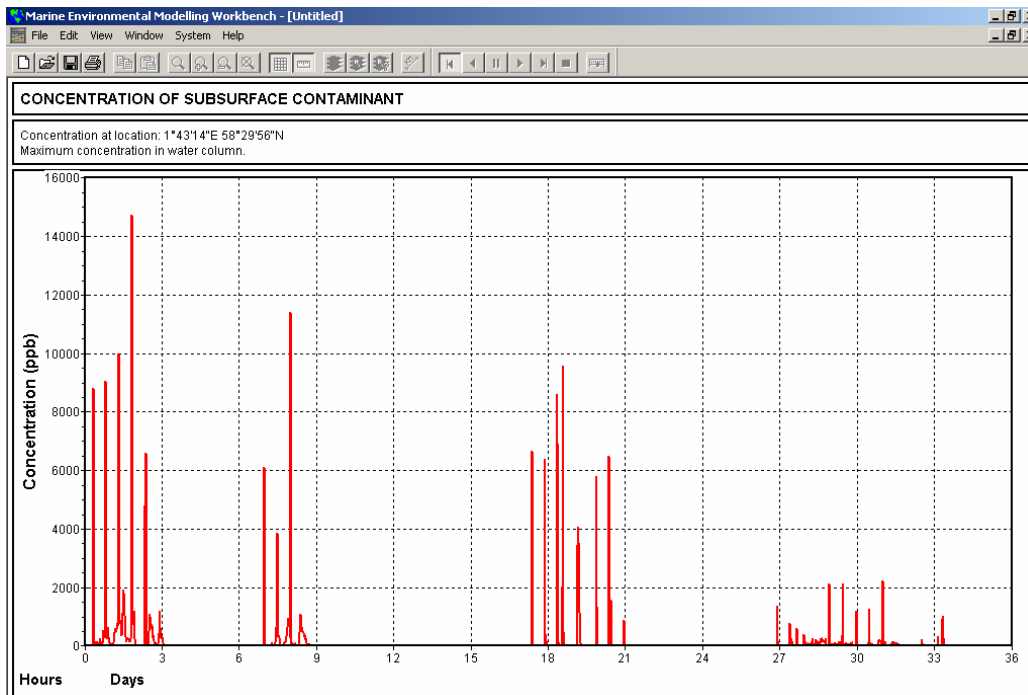


Figure A.6.13. The time series particle concentrations (essentially barite) calculated for the cage at 40 m depth at shell rig location A.

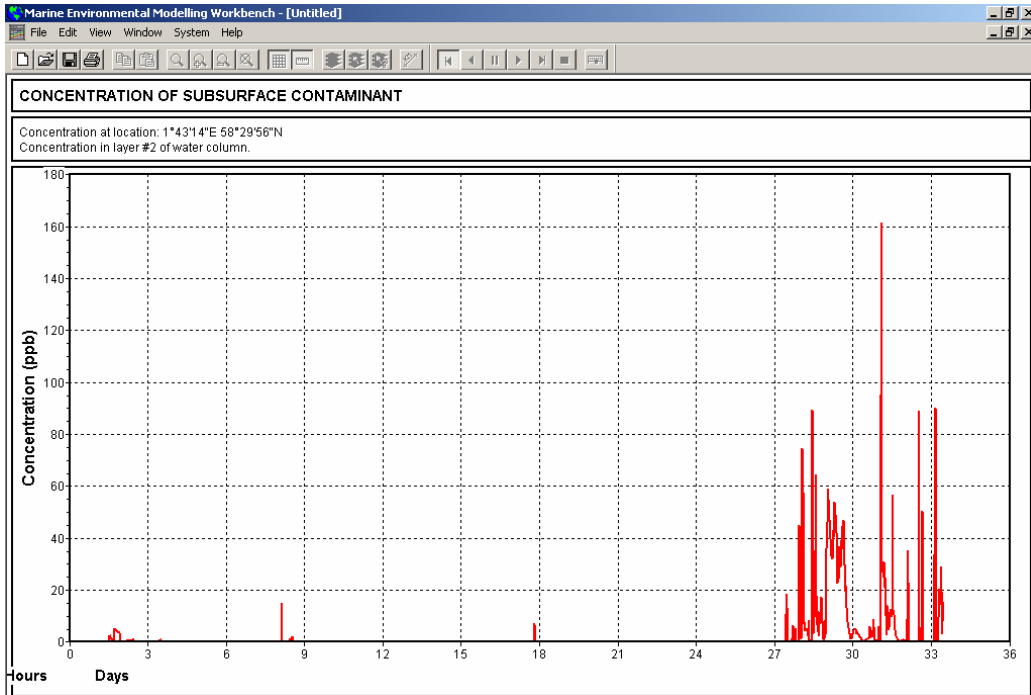


Figure A.6.14. The time series particle concentrations (essentially barite) calculated for the cage at 20 m depth at shell rig location A.

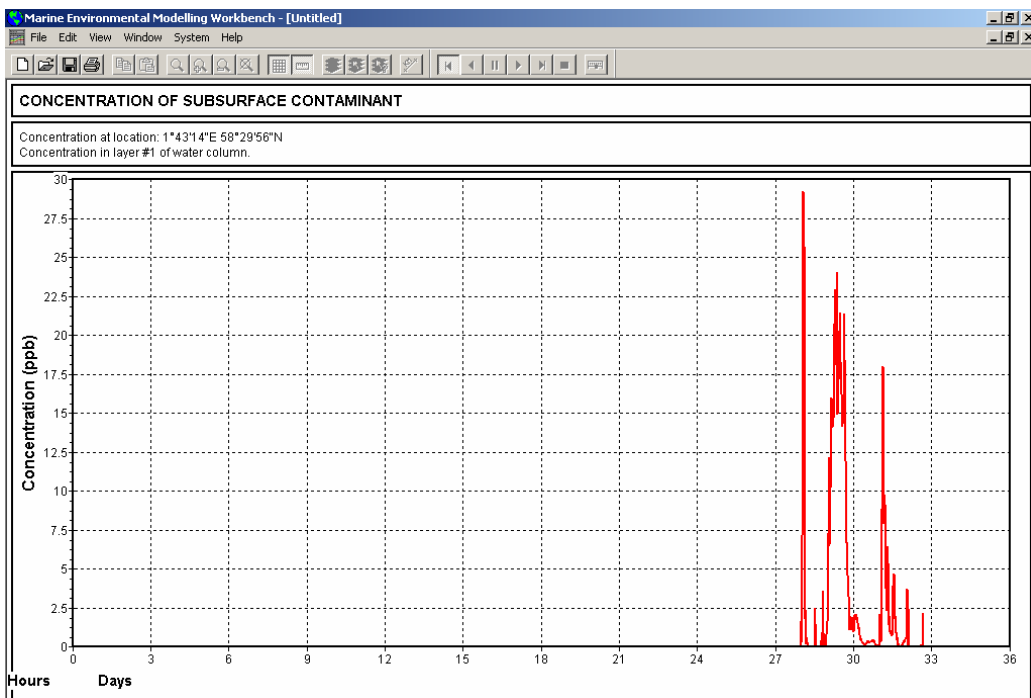


Figure A.6.15. The time series particle concentrations (essentially barite) calculated for the cage at 10 m depth at shell rig location A.

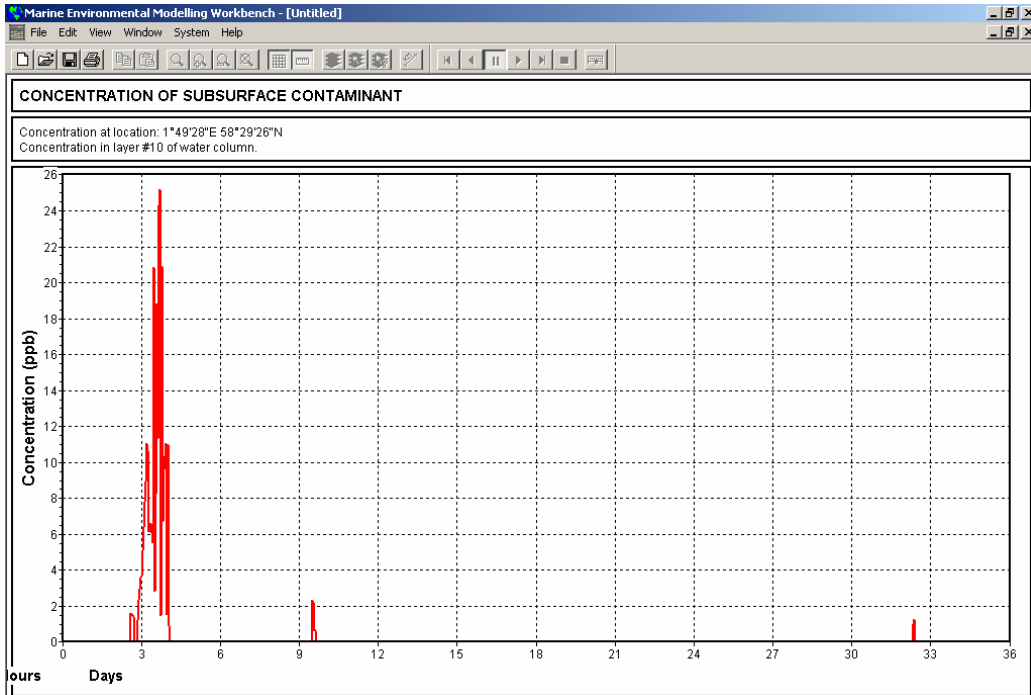


Figure A.6.16. The time series particle concentrations (essentially barite) calculated for the cage at 100 m depth at shell rig location C.

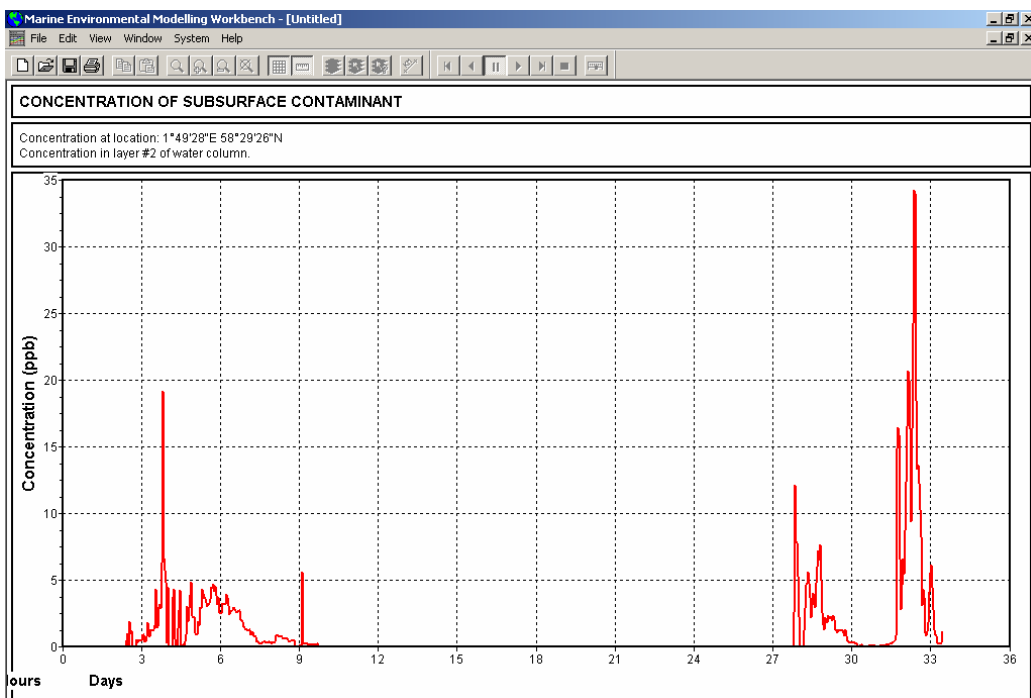


Figure A.6.17. The time series particle concentrations (essentially barite) calculated for the cage at 20 m depth at shell rig location C.

PART B

The validation of biological effects in blue mussels and scallops.

B.1. Introduction

The aim of this part of the research was to examine chronic toxicity and physical disturbance of discharged drilling fluids on transplanted adult scallops and mussels. The approach chosen is based on the use of biological effect parameters, so called biomarkers, which have been selected based on a scientific evaluation of biological relevance, to measure physical and chemical stress during exposure to drilling waste (table B.4.1). Several classes of chemical compounds in the drilling fluid, including barite and other known non toxic drilling wastes, can during chronic exposure affect growth, reproductive success and survival by altering the physiological state and nutrition condition of the organism (Cranford and Gordon 1991; Cranford and Gordon 1999). Other chemicals such as PAHs are known to enhance the intracellular formation of non stable reactive oxygen species which could increase to a toxic level, generating both DNA-, protein- and membrane damages in addition to altering enzyme systems (Regoli, Nigro et al. 2000; Regoli, Nigro et al. 2000; Camus, Jones et al. 2002; Regoli, Gorbi et al. 2002; Regoli, Winston et al. 2003). Weltens et al.(2000), showed that particle bound fractions of metals can become available within the body of filter feeding *Daphnia*. Adsorbed metals might desorb in the gastrointestinal tract due to different physical and/or chemical conditions and exert toxic effects, leading to unexpectedly high tissue concentrations (Weltens, R. et al. 2000). The digestive physiology of the animal and the behaviour of the chemical within the animal's gut influence contaminant assimilation (Weltens, R. et al. 2000). For suspension feeders such as mussels and copepods, uptake of metals from the dissolved phase and food ingestion can be equally important to metal accumulation (Wang and NS. 1999). Particle bound contaminants can also be bioavailable to fish (Van den Belt, S. et al. 2000).

B.2. Biological material

In this project two invertebrate filter feeders were chosen since impact from drill cuttings would probably affect these animals through; particle adsorption to gills, skin and filtration organs, disturbance of the feeding mechanism and the total energy budget, or through physical and chemical interactions. The use of filter feeders simplifies the experiment setup since scallops and mussels need no extra food supply and both have the ability to tolerate high pressure. Both species have the capability to reject inorganic particles as faeces, but only mussels are capable of “sealing” their valves during unfavourable conditions, and surviving without exchanging the mantle water for a prolonged period (Hovgaard 1984).

B.3. Test organisms

Blue mussels are often used as indicator organisms that are particularly vulnerable in connection with pollution in the sea, since they have restricted or no opportunity to move away when the conditions become unfavourable. Both particles and dissolved chemicals will enter the shell and depending on the property, the material will be accumulated, metabolized or rejected. Scallops and mussels reject particles based on the ability to discriminate against size and inorganic material. The production of faeces is efficient when the content of organic material is higher than 50 %, but reduced significantly when the organic content is less than 25 %. The production of faeces is also more efficient for larger particles (greater than 10 µm) compared to small particles (Hovgaard 1984; Hardy 1991).

Adult great scallops (*Pecten maximus*) have a complex system of ganglions supporting the many sensor organs (eyes, mantel, tentacles) which are used during movement, controlling the water flow and increasing the possibility of selecting and rejecting particles, making it a selective and sensitive organism with respect to feeding (Hovgaard 1984). The feeding conditions are optimum for these animals when the temperature is between 15-18°C, salinity > 29 ‰ and when the feeding particle size is 5-6 µm. Scallops are hermaphrodites and produce sperm and eggs from when they are 2 years old, spawning in Hordaland between April and August, with the main gonad development period between August and October (Hovgaard 1984; Hardy 1991).

Blue mussels live in the intertidal zone and are adapted to dry periods, wave actions and fluctuating food supply, temperature and salinity conditions. Mussels are highly flexible grazers that efficiently utilize variations in food supply and quality with an efficient filtration of particles down to 2-3 µm. Mussels have distinct genders and they produce eggs or sperm from the age of 2 years. The main spawning is between April and June, with a gonad development period in the winter months (Hovgaard 1984; Hardy 1991).

B.3.1. Storage and transport

Sea bed farmed 3-4 year old scallops and 2-3 year old rope farmed blue mussels were collected and brought to Akvamiljø. Because of a drilling start-up delay, the organisms were stored for 14 days in fish tanks (1 m*1 m*0,5 m) at Akvamiljø. During this time the test organisms were sporadically fed with algae (*Skeletonema sp.*) before being transported by truck under stable temperature conditions (10-13 °C) to Bergen in boxes containing moistened shavings. Onboard the mussels and scallops were distributed in strengthened lantern nets (figure B.3.1) and stored at 13-15 °C in 90 m³ sea water tanks until arrival at the drilling area 22 hours after departure from Akvamiljø. In each lantern net 68 individuals were randomly distributed in 18 compartments with 3 nets per station.

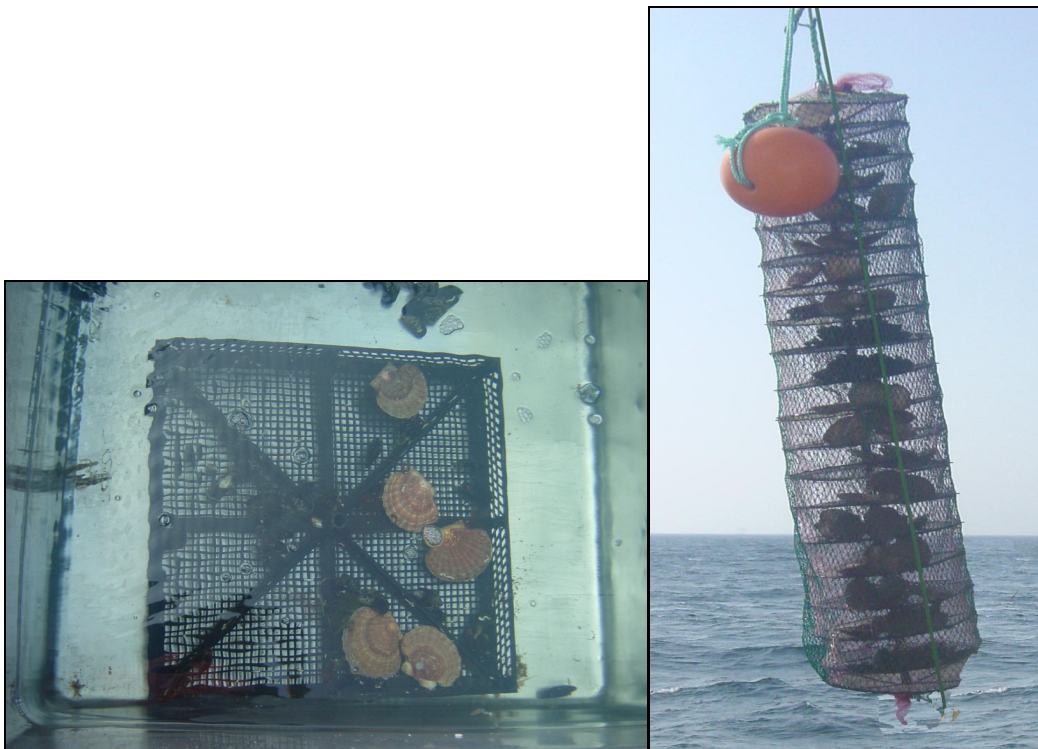


Figure B.3.1. Transportation vessel and the net used during the exposure at SVAN field.

B.4. Biological measurements

For each group analyzed, 3 to 25 individuals were sampled (table B.4.1). Each individual was opened and the seawater content within the shell was poured out. Blood samples were collected from the adductor muscle using a 1 ml syringe (figure B.4.1) and used to perform the proteomic analysis and the comet assay. Another 10 individuals were sampled from each group to collect samples for the lysosomal test, clearance rate and for the stress on stress parameter. Following this, the different sample tissues (gonad, digestive gland and muscle) were dissected, weighed and stored in a -80°C freezer until further pre treatment and analysis of GST, TOSC, glycogen and heavy metals. Sampling for glycogen analysis was performed but owing to economy priorities it was not taken any further. A detailed description of the methods used to analyze the biomarkers (table B.4.1) can be found in the biomarker handbook (Beyer 2003).

One-way ANOVA with Dunnett's or Turkey post-hoc test ($p < 0.05$) was performed to test statistical difference between treatments. A Kaplan-Meier plot with Wilcoxon and Log-rank test was performed on survival data (stress on stress parameter) to test statistical difference between treatments.

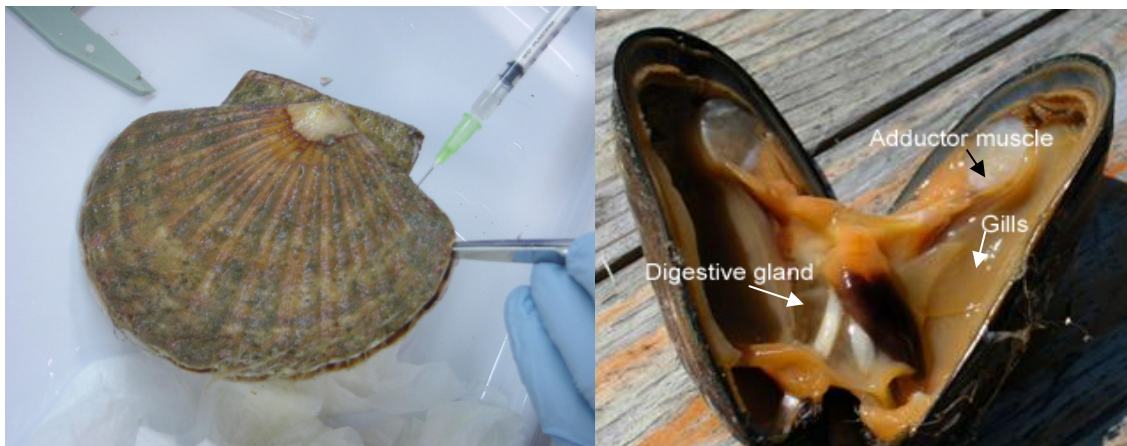


Figure B.4.1 Blood sampling of scallop and an open blue mussel ready for tissue sampling.

Table B.4.1. Sample and analysis overview. Red numbers refers to lost or none analyzed samples. The whole shellrigg B (cages at; 20 m, 35 m, 100 m) was lost offshore. * blue mussels only.

Parameters	Sample tissue	No. of replicates	Stations exp A/B	Depths (m)					No. of shells Scallops	No. of shells Blue mussel	Analysis.
				10	20	35	40	100			
Lysosomal membrane stability	Haemolymph	10	exp. ref.		10 10	10 10	10 10	10 10		40	40
GST	Hepatopancreas	10	exp. ref.		10 10	10 10	10 10		40	40	80
TOSC	Hepatopancreas	10	exp. ref.		10 10	10 10	10 10		40	40	80
Clearance rate	whole live mussels	10	exp. ref.		10 10	10 10*	10 10*		20	40	60
Stress on stress	whole live mussels	10	exp. ref.		25 25	10 25	25 25	10 25		100	100
Proteomic pattern	Haemolymph	25	exp. ref.		25 25	25 25	25 25		75	75	150
Glycogen	Muscle	10	exp. ref.		10 10	10 10	10 10				
Comet assay	Haemolymph	9	exp. ref.		9 9	9 9	9 9			27	27
Barite (metals)	Whole tissue	3	exp. ref.	3 3	3 3	3 3	3 3		15	15	30
Scallop; Length, tissue, gonad and muscle weight		25	exp. ref.	25 25	25 25	25 25	25 25		75		75
Blue mussel Length and tissue weight		25	exp. ref.	11 25	11 11	25 25	11 11			55	55

B.4.1. Fitness parameters

The fitness parameters shell length, muscle, gonad and total weight were measured for 25 mussels and scallops per tested depth. The sex was difficult to determine in mussels due to poorly developed egg and sperm cells. Scallops are hermaphrodites with both sperm and eggs.

B.4.2. Lysosomal membrane stability

Lysosomal membrane stability is an assay employing the supravital dye, neutral red for the study of lysosomal injury in isolated digestive cells and blood cells (haemocytes) developed by Lowe et al. (Lowe, Moore et al. 1992; Lowe and Pipe 1994; Lowe, Fossato et al. 1995). This assay, as a measure of contaminant-induced lysosomal membrane damage, makes use of the fact that only lysosomes in healthy cells can retain neutral red after initial uptake. A healthy sample set of *M. edulis* normally has a retention time from 150-180 minutes.

B.4.3. Comet assay

The comet assay, also called the alkaline single-cell gel electrophoresis (SCGE) technique, measures DNA damage in individual cells from experimental animals exposed to potentially genotoxic compounds. The assay is capable of detecting various forms of DNA damage, e.g. single strand breaks, oxidative DNA base damage and single strand breaks associated with incomplete excision repair sites. The comet assay was developed by Singh *et al.* (Singh, McCoy et al. 1988) for use on human cells, but has been applied successfully with several aquatic species (Steinert 1996; Steinert, Montee et al. 1998; Steinert, StreibMontee et al. 1998; Rank 1999).

The assay was performed on mussel haemocytes which was extracted into a physiological saline solution (Lowe, Moore et al. 1992) to maintain the integrity of the cells. The final ratio between haemolymph and buffer was 1:1.

B.4.4. Protein (Bradford method)

The Bradford assay is based on the change in absorption of Coomassie Brilliant Blue G-250, from 465 to 595nm, which occurs when this dye binds to protein. The amount of absorption is proportional to the protein present, and therefore protein concentration can be calculated from a standard curve created using a serial dilution of bovine serum albumin (Bradford 1976).

B.4.3. Glutathion-S-transferase (GST) activity

To convert lipophilic xenobiotics to more hydrophilic and usually more readily excretable metabolites, organisms have developed several biochemical processes, termed biotransformation. These biotransformations are mostly enzymatic in nature and involve hydrolysis, oxidation, reduction, conjugation and synthetic reactions. One of the major enzyme systems that act as a catalyst of a large range of conjugation reactions is Glutathione-S-Transferase. Characteristic of the biotransformation enzymes is that

following exposure to xenobiotics, the enzyme activity can be enhanced. These responses are used as a tool to identify the effect of pollution on various organisms.

The absorbance slope from the reaction between the reagents (CDNB, GSH) and cytosol samples (50 μL) is measured at 340nm and the enzyme activity is calculated and normalized against the sample protein concentration.

B.4.5. Total Oxyradical Scavenging Capacity (TOSC)

Reactive oxygen species (ROS) are continuously and naturally produced during aerobic metabolism and their toxicity to the main cell components (DNA, membrane lipid, proteins) is counteracted by activity of antioxidant enzymes and specific low molecular weight scavengers. The balance between prooxidant forces and antioxidant defences is altered by several classes of environmental pollutants (both organic and metallic) which, through different mechanisms, enhance intracellular generation of ROS and/or affect the efficiency of antioxidant defences, possibly leading to a pathological condition generally referred as oxidative stress.

The principle of the TOSC-assay consists of measuring the efficiency of body fluid to scavenge selected ROS (peroxyl, hydroxyl and peroxynitrite) generated at a constant rate. Non scavenged ROS will oxidise substrate α -keto- γ -methiolbutiryc acid (KMBA) to produce ethylene measured by gas chromatography. The method is based on (Regoli and Winston 1998; Regoli and Winston 1999), except that buffers were adjusted for marine invertebrates.

B.4.6. Clearance rate (Algae density estimation)

Each mussel and scallop group (exposed and reference) was measured 1-2 days after pick-up according to a modification of the method described by Widdows et al. 1987. The modification was due to transport time and limited capacity for analysis.

The clearance rate experiment was performed in a climate room at 10°C. Two different sized beakers \varnothing 12cm and 18cm (DURAN glass), each with a volume of 1L, were filled with filtered seawater at a temperature of 10°C. A Coulter multisizer (Coulter, Toronto, ON, Canada) equipped with a 70 μm probe was used to estimate the density of particles. For each treatment, the seawater was first rapidly mixed with a spoon and a seawater subsample was poured in an 80 mL beaker where the number of particles between 3.5-10 μm was counted.

First, a seawater blank sample with neither algae nor shells was made. Then a known volume of seawater (400 and 1000 mL) plus an algae culture of *Isocrysis galbana* was added to 3 beakers at a level which would completely submerge the mussels and scallops by at least 2cm. Beakers without mussels were used to estimate the mean initial concentration of the algae solution which should be between 30-50 cells/ μL , before the beginning of the filtration rate measurement.

In each beaker the algae suspension was well stirred before 10 individuals from either exposed or reference organisms were carefully placed in each beaker. When the shell

valves opened, a 10 ml sample was carefully collected from behind the mussels to avoid filtration disturbance. Further samples were collected for multisizer measurements after 5 and 15 minutes. Any change in the mussels and scallops behaviour was carefully noted to assist the interpretation of the filtration values.

B.4.7. Stress on stress (survival time in air)

Stress on stress response is a simple monitoring tool in the assessment of a general stress syndrome in mussels. When mussels are exposed to air they switch their aerobic metabolism over to anaerobic, thereby generating an extra biochemical stress which in turn affects the survival time. Different survival times reflect the mussels' fitness before they were exposed to air, and exposed mussels die faster or in greater numbers at a given time. Median survival time (LC50) was calculated for each mussel group.

To determine survival in air, 25 blue mussels from each group were put on moistened paper and incubated dark in sealed boxes at 10°C. Mussels were considered dead during daily mortality checks when they began to gape and closing the valves did not diminish the gape.

B.4.8. Proteomics

The proteomic pattern was studied using Surface Enhanced Laser Desorption/Ionisation Time of Flight Mass Spectrometry (SELDI-ToF MS). The proteomic method is sensitive and will pick up all types of stress responses, it is a very fast screening method, and possible specific individual biomarkers as well as common responses can be found quickly. If interesting proteins are found, one option is to get them sequenced and possibly identified. Another option is to use multivariate analysis to distinguish between groups. In this case, one does not necessarily have to know what these proteins are or which role they play in the animal, as it is the *pattern* or exposure specific protein combination which is the biomarker itself, not the response of individual proteins (Bjørnstad, B.K. et al. 2003; Larsen, A et al. 2003).

B.4.9. Body burden of barite

The analysis was performed on the whole organism. The wet tissue was homogenised and then digested. For the digestion about 2 grams of the homogenised tissue were placed in a Teflon pressure vessel. Nitric acid (5 ml conc. HNO₃) and hydrogen peroxide (1 ml 30 % H₂O₂) was added. The vessel was placed in a microwave oven using a temperature/effect program that lasted 30 min. After cooling, the samples were diluted to 50 ml in polypropylene vessels. All quantification was performed on wet weight basis. For the samples where individual organs were analysed, the same procedure was used with the homogenisation step omitted. For the shell analysis pieces of the outer part of the shell were used. The shell pieces were carefully rinsed in Milli-Q water to remove most of the adsorbed particles. Small particles usually have strong adhesive forces and it is very likely that if the shells are exposed to barite there are barite particles adsorbed on the shell. The shell pieces were not totally dry when the dissolution was performed. To compensate for this, results are normalized to a major

component, which in this case was Sr, which is a base component in the carbonate shell. About 0.2g of shell was dissolved in dilute nitric acid (0.2 M). The dissolution was made in a polypropylene test tube. The capped test tube was placed in a water bath for 2 hours and the sample was then left at room temperature for 24 hours.

For the analysis a VG PQ 2+ ICP-MS equipment was used. A standard Ni skimmer and sampling cones and a Meinard nebulizer attached to a water cooled quartz spray chamber were used. The spray chamber was regulated at 10 degrees. The dissolved or digested samples were then further diluted with Milli-Q water to concentrations suitable for the ICP-MS. In this procedure an internal standard (5 µg/l Indium) was added. In the ICP-MS procedure a peak-jump program containing the elements of interest was used. The results were standardised against Spex water standards and the added Indium was used to compensate for instrument drift during the analysis.

B.5. Results and discussion

B.5.1. Fitness results

The shell length, muscle, gonad and total body weight were measured on 25 scallops and blue mussels from each group.

After 1 month exposure none of the scallop groups seemed to have increased their shell length significantly, and the shell length was uniform distributed (scallops; 101 ± 6 mm). For scallops, the total weight seems to decrease with depth and significant differences were found between reference scallops at 20 and 100 m (figure B.5.1.). It is natural to connect this to decreasing food supply, temperature and the increased influence of pressure (Hovgaard 1984; Hardy 1991; Gosling 1992).

After 1 month growth no significant differences in shell length was found for blue mussels (mussels; 60 ± 6 mm) or in the total weight towards depth. This seems inconsistent with the food supply explanation, favouring mussels in the upper water column (figure B.5.2.). Some plausible explanation to this could be that 1 month exposure time is too short under the existing feeding regime to find any significant differences towards body weight and shell length. It is also known that mussels can save energy and loss of body weight by sealing their shell for a period of time during unfavourable conditions. Mussels could also be entering a hibernation state as a result of low temperature in relation to depth (Hovgaard 1984; Hardy 1991). The effect from starvation on biomarkers is not fully understood. Although effects generated on biomarkers by other agents than the exposure reagent would be balanced by the use of a reference group. In this experiment the body burden results show that mussels have been exposed to barite by filtrating particles, but that this exposure have no significant effect on the total body weight and shell length during ~1 month exposure time.

The Scallops have not the same opportunity as blue mussels to save energy and they are more selective towards particle size, pressure drops, mechanical influences and changes in their environmental conditions (Hovgaard 1984; Hardy 1991).

In the exposed area a significant gonad weight reduction was found for scallops sited at 40 m depth as compared to the 100 m reference group, suggesting that the exposure to drilling wastes had a stronger negative effect than depth on gonad weight development (figure B.5.1.). It seems that the filtration and rejection of non nutritional particles (in the plume) affects the build up of gonads and muscle mass in scallops or affects it indirectly by mobilizing energy (glycogen) stored in these tissues. However, scallops located at 20 m depth (exposed and reference) had a significantly higher muscle weight than the others (figure B.5.1.), reflected by a small increase in the total weight (figure B.5.1.), probably as a response to more favourable food conditions.

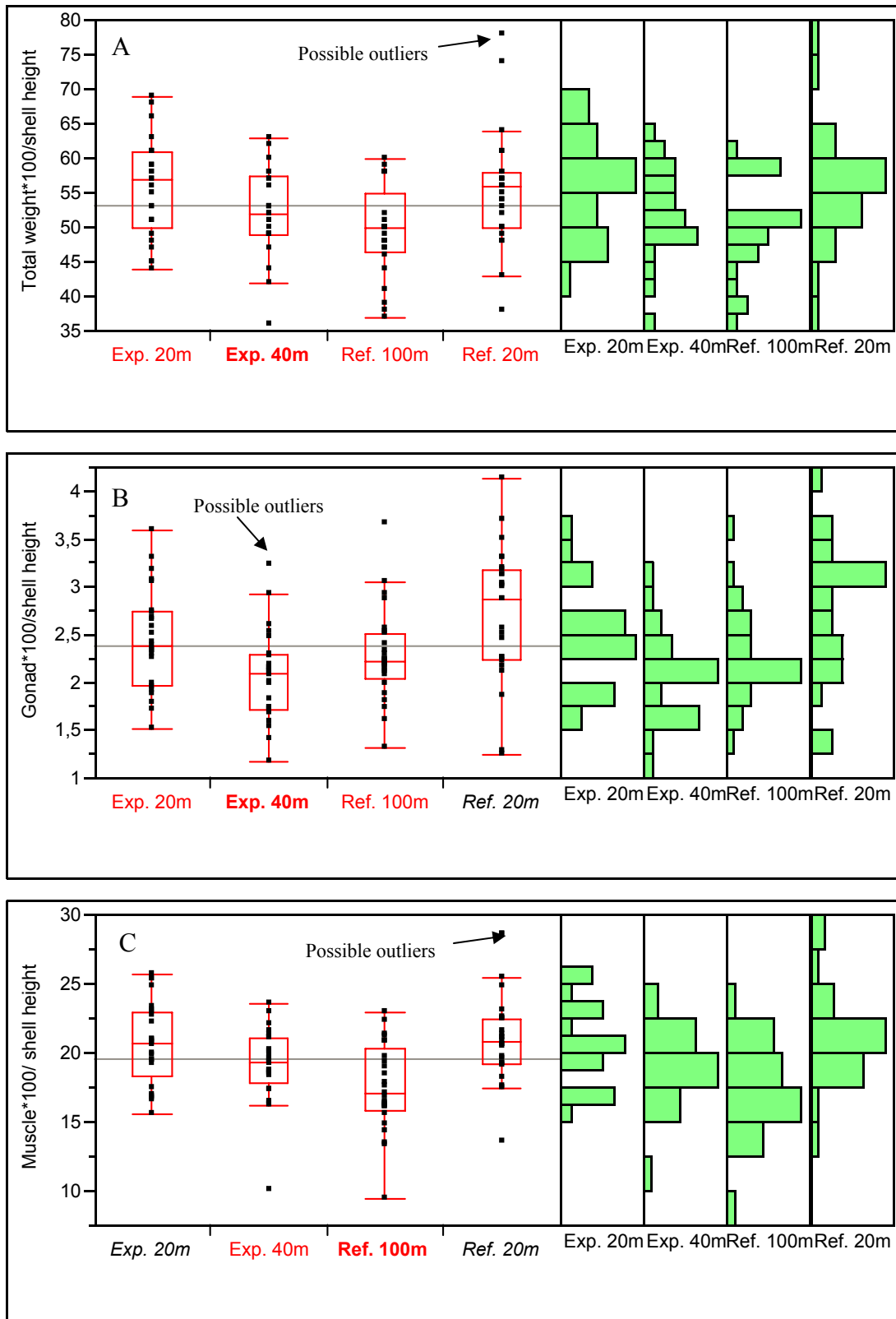


Figure B.5.1. Scallops caged at different depths during 5 weeks discharge of drilling fluids (mainly barite). Figure A; total weight, B; gonad weight and C; muscle weight/height (g/mm). Quantiles boxes with median values and whiskers (values within 1,5x interquartile rang). Outliers are present if a value are higher or lower than the whiskers range (Turkey 1977).

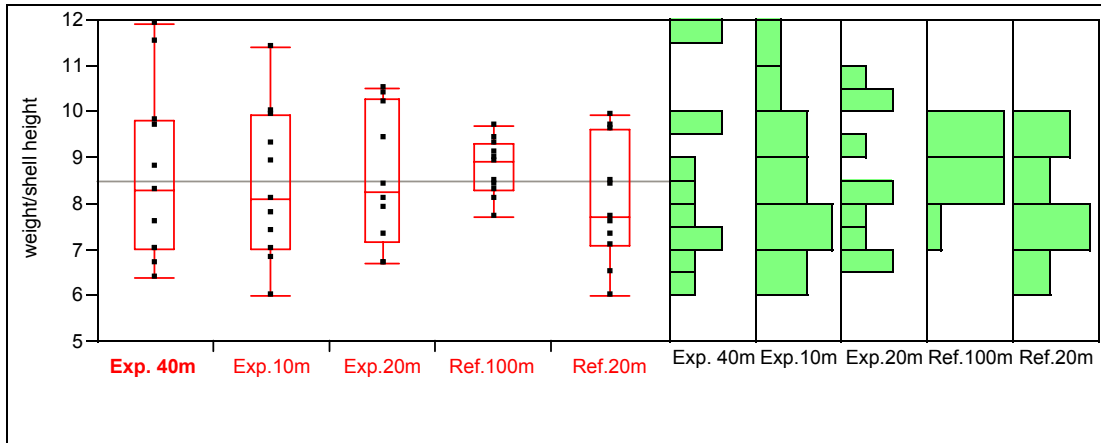


Figure B.5.2. Total weight/height (g/mm) of blue mussels caged at different depths during 5 weeks discharge of drilling fluids (mainly barite). Quantiles boxes with median values and whiskers (values within 1,5x interquartile rang). Outliers are present if a value are higher or lower than the whiskers range (Turkey 1977).

B.5.2. Lysosomal membrane stability

The average retention times observed in the caged mussels varied from 117 min (ref. 20 m-a) to 77,3 min (exp. 20 m), a 34 % reduction in membrane stability (figure B.5.3.). Not only the exposed mussels at 20 m showed a decrease in membrane stability, the control organisms also had reduced retention times (114,6 and 117 min.) compared to what is expected from a healthy organism (150-180 min). This is most likely “travel” stress rather than chemical stress.

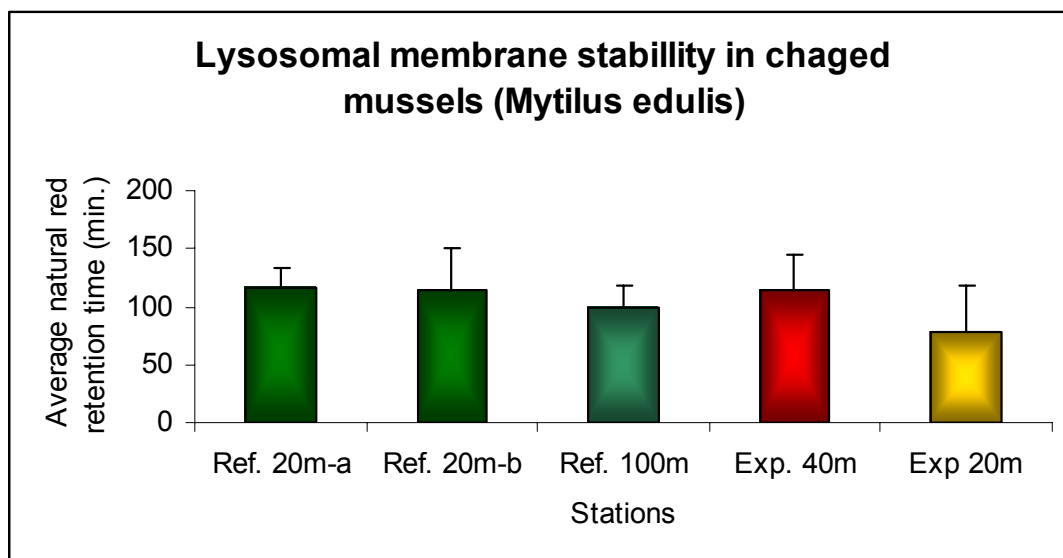


Figure B.5.3. Lysosomal membrane stability in blood cells. Scallops caged at different depths during 5 weeks discharge of drilling fluids (mainly barite). -a and -b are parallel samples. Mean values with standard deviation lines.

B.5.3. Comet assay

To our knowledge, no genotoxicity study on marine organisms exposed during drilling operations has been performed before. However, evidence of long-term adverse effects, such as cancer, due to relatively high concentrations of heavy metals in marine animals has been shown in field and laboratory studies (Bolognesi, Rabboni et al. 1996). Genotoxic effect may be involved in the mechanism of metal carcinogenicity. The comet assay has been used to detect DNA damage caused by metal exposure of fish (Risso-de Faverney, Devaux et al. 2001) and mussels (Bolognesi, Rabboni et al. 1996), (Black, Ferrell et al. 1996).

Figure B.5.4. shows the results from comet run 1 with reference mussels from 20 m depth and mussels exposed at 20 m, showing that exposed mussels displayed no statistically significant ($p < 0.05$) increase in % DNA in the comet tail compared to the reference group. The comparison is based on all cells measured.

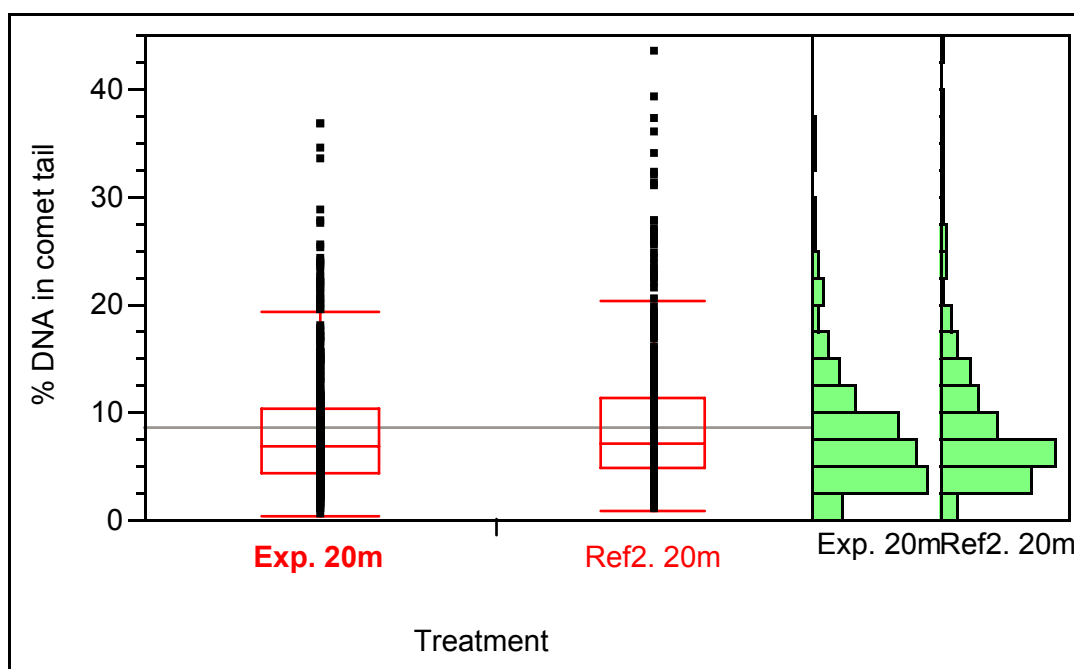


Figure B.5.4. Results from comet run 1. Comparison based on all cells measured from mussels exposed at 20 m depth with all cells from reference mussels (20 m) sampled for comet run 1. Grand mean is given as a horizontal line (grey) as well as quantiles boxes with median values and whiskers.

The comet results from run 2, measured for reference mussels from 20 m depth and mussels exposed at 40 m (figure B.5.5.), show that exposed mussels had a statistically significant ($p < 0.05$) increase in % DNA in the comet tail compared to the reference group. The average value of haemocytes from reference mussels is higher than in the first comet run and also higher than in control mussels (table B.5.1.) from previous studies in our laboratory (~10 % DNA in the comet tail of mussel haemocytes). Two

individuals from both the reference group and the group exposed at 40 m had distinctly elevated levels of DNA damage. Removing these individuals results in a mean reference value of 10.5 ± 3.2 % DNA in the comet tail, close to what has been obtained in control mussels from previous studies. Removing the two individuals from the group exposed at 40 m, reduces the mean value for this group to 12.1 ± 3.9 , which is still significantly higher than the reference group ($p < 0.05$).

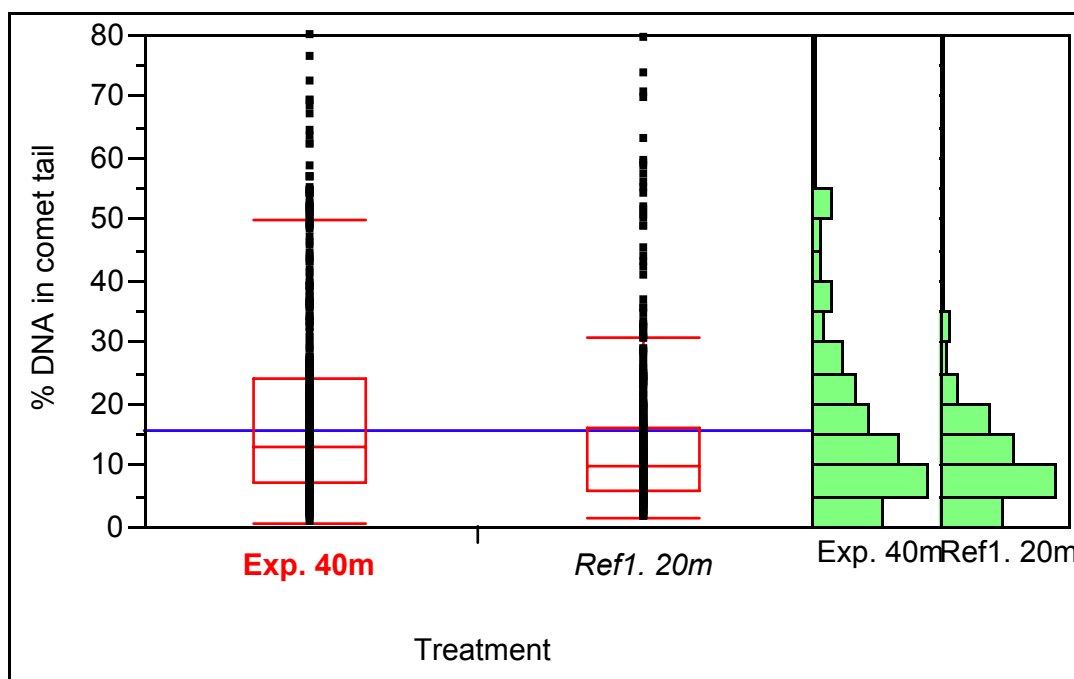


Figure B.5.5. Results from comet run 2. Comparison based on all cells measured from mussels exposed at 40 m depth with all cells from reference mussels (20 m) sampled for comet run 2. Grand mean is given as a horizontal line (blue) as well as quantiles boxes with median values and whiskers.

Table B.5.1 shows the overall results of the comet assay, measuring DNA damage on mussel haemocytes generated by depth and/or the exposure to an average barite concentration higher than 0.09 mg/l (table B.5.3). Significant DNA damage has been found at lower barite concentrations (0.5 mg/l, for 4 weeks) (Bechmann, Westerlund et al. 2006) and DNA damages have only been reported from experiment where the pressure difference was higher (850 m to surface, (Dixon, Pruski et al. 2004) than the pressure between the reference- (20 m) and the exposed group (40 m). The results from the present study show that DNA damage could be found in haemocytes from mussels exposed to drilling chemicals and barite particles.

Table B.5.1. Summary of comet results. Samples of Mytilus edulis haemocytes were taken after 5 weeks exposure in the Sleipner drilling area. The standard deviations are calculated based on cells from each treatment (cells from individual mussels from the same treatment have been combined) based on the mean % DNA in the comet tail of cells from each individual mussel.

	Comet run	Mean % DNA in comet tail \pm St. Dev.	
		Based on all cells from each treatment	Based on mean from each individual animal
Reference 20 m	1	7.7 \pm 4.9	7.7 \pm 0.9
Exposed 20 m	1	8.4 \pm 5.8	8.4 \pm 1.5
Reference 20 m	2	13.5 \pm 12.2	13.5 \pm 7.0
Exposed 40 m	2	18.4 \pm 15.7	18.4 \pm 12.9

B.5.4. GST

To convert lipophilic xenobiotics to more hydrophilic and usually more readily excretable metabolites, organisms have developed several biochemical processes, termed biotransformation. These biotransformations are mostly enzymatic in nature and involve hydrolysis, oxidation, reduction, conjugation and synthetic reactions. One of the major enzyme systems that act as a catalyst of a large range of conjugation reactions is Glutathione-S-Transferase (GST). Characteristic of the biotransformation enzymes is that following exposure to xenobiotics, the enzyme activity can be enhanced. These responses are used as a tool to identify the effect of pollution on various organisms.

For caged scallops a significant increase in the enzyme activity was measured for the exposed 40 m group, compared to both reference sites at 20 m and 100 m (figure B.5.5.). Since depth alone had no major effect on the GST activity in scallops, the release of drilling mud and chemicals is likely to be responsible for the increased enzyme activity.

The GST response for blue mussels caged at 40 m was significant higher than reference mussels caged at 20 m depth. However, blue mussels responded to depth by increasing the enzyme activity (although not significantly) from 20 m to the 100 m reference group, making depth and the sea bed habitat a co-factor for the increase in GST activity.

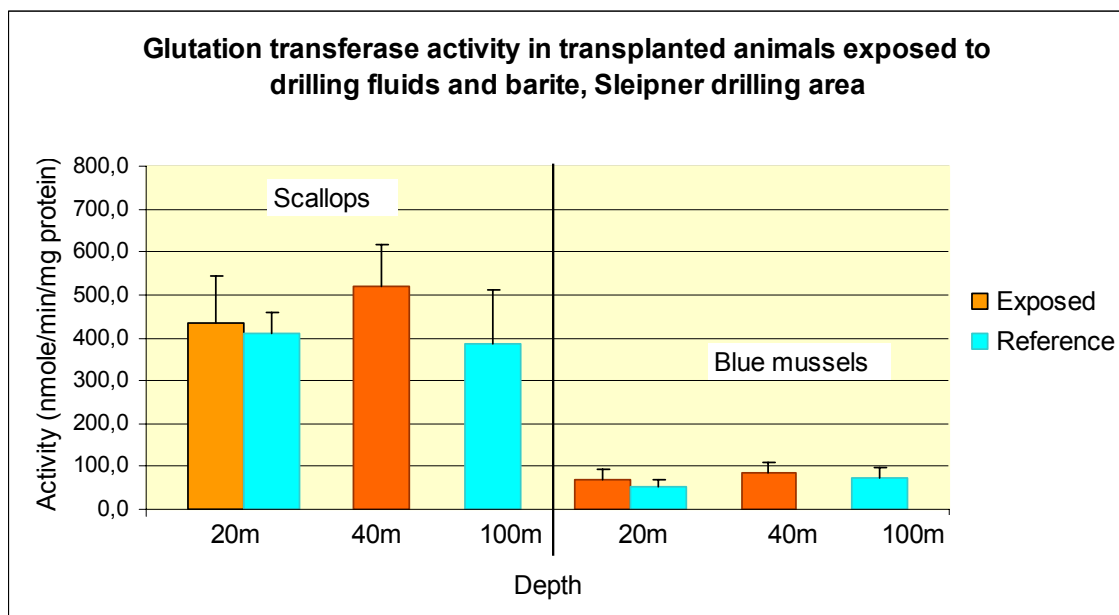


Figure B.5.5. GST activity measured in scallops and blue mussels caged at different depths, after the exposure to drilling wastes in the North Sea. Mean values with standard deviation lines.

B.5.5. TOSC

Several classes of environmental pollutants can through different mechanisms enhance the intracellular generation of reactive oxygen species (ROS) and/or affect the efficiency of antioxidant defences leading to antioxidative stress. Metals constitute a class of pollutant that alter the balance between prooxidant forces and antioxidant defences, generating ROS. Organic and/or metallic pollution have a significantly reduced capacity to neutralize specific ROS in mussels at 40 m compared to the 20 m reference group. High levels of ROS were found in all exposed groups, which indicate an oxidative stress response (figure B.5.6.).

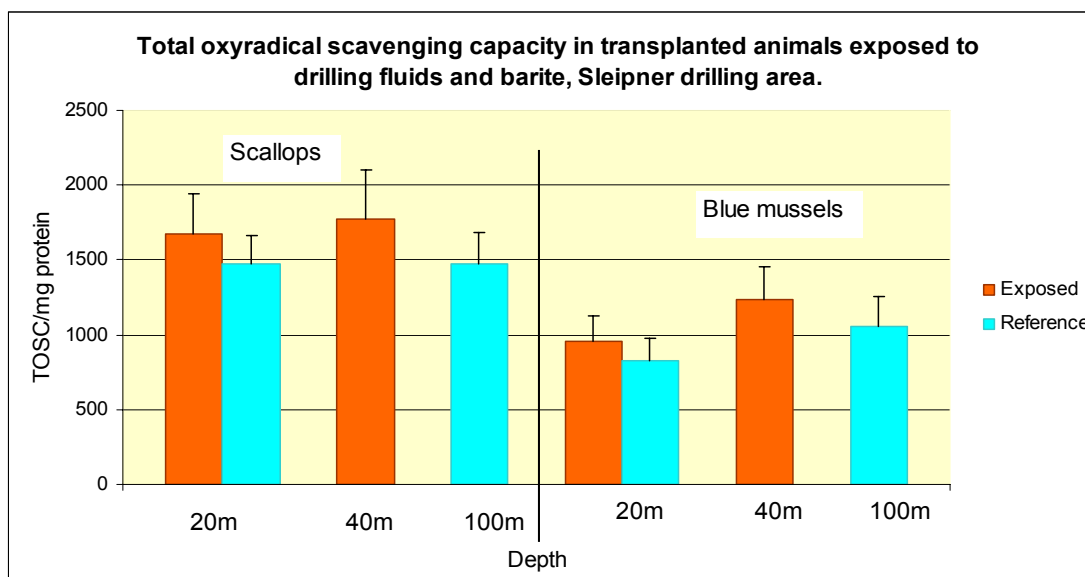


Figure B.5.6. TOSC activity measured in scallops and blue mussels caged at different depths, after the exposure to drilling wastes in the North Sea. Mean values with standard deviation lines.

B.5.6. Clearance rate of exposed mussels and scallops

Both scallops and mussels have lamellbranched gills with a large surface area which makes it possible to filter huge water volumes (mussels ~70 ml/min and scallops ~140 ml/min (Walne 1974)) for feeding and for the exchange of gasses and dissolved materials. Damage to the gills would alter the respiration rate, nutritional uptake and the possibility to reject excess particles as pseudofaeces (Hovgaard 1984; Barlow and Kingston 2001). The discharge of particles can reduce the filtration activity as a consequence of disruption of the filtration or the digestive systems caused by rejecting non nutritional particles (Hovgaard 1984). The filtration organs could also be damaged directly, since barite particles are rough and edged.

In this field study a significant reduction in clearance rate was measured for both exposed scallops and mussels (figure B.5.7. and B.5.8.). This reduction was not influenced by depth or the decreasing temperature towards depth, since the reference organisms sited at 20 and 100 m maintain a natural filtration rate (table B.5.2.). Laboratory experiments performed under different barite exposure regimes (Bechmann, Westerlund et al. 2006) support the result that barite has a negative effect on the ability of filter feeders such as mussels and scallops to sustain a normal feeding regime. The laboratory exposure showed a reduction in scallops exposed to 0.5 mg/l barite and at 20 mg/l barite for mussels (Bechmann, Westerlund et al. 2006). During the SVAN field exposure the barite concentrations at 40 m reach pulses above 14 mg/l barite (figure A.6.13), with an average exposure level varying from 0.09-0.7mg/l barite (table A.6.2 and figure A.6.13) the remainder of the time. Since the discharge is below 2 mg/l most of the time (figure A.6.13-16), and earlier lab experiments show an effect for mussels only at 20 mg/l (Bechmann, Westerlund et al. 2006) a short term exposure pulse could be the main cause of the reduced filtration rate. If so the effect from these pulses (figure

A.6.13) is an important factor, and could explain why a reduced filtration rate was seen even after 14 days (figure B.5.7 and B.5.8). The discharge of barite at 20 m (figure A.6.14) is much lower than at 40 m and had no effect on the filtration rate for blue mussels (figure B.5.7). At this depth the average exposure was under 0.01 mg/l with barite pulses up to 0.16 mg/l (figure A.6.14). This exposure regime gave a significant reduction in the filtration rate for scallops. This could mean that scallops are sensitive to barite concentration as low as 0.01 mg/l or that the pulse discharge caused and sustained a reduced filtration rate.

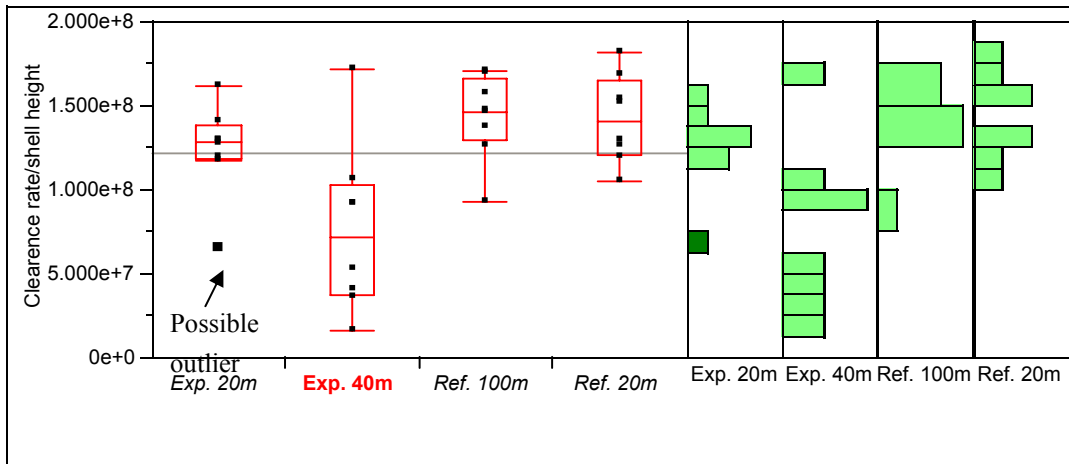


Figure B.5.7. Clearance rate (algae/L/h/length in mm) measured for blue mussels under stable lab conditions after a caged period at different depths during exposure to drilling wastes. Significant reduction for mussels in Exp. 40 m. Quantiles boxes with median values and whiskers (values within 1,5x interquartile rang). Outliers are present if a value are higher or lower than the whiskers range (Turkey 1977).

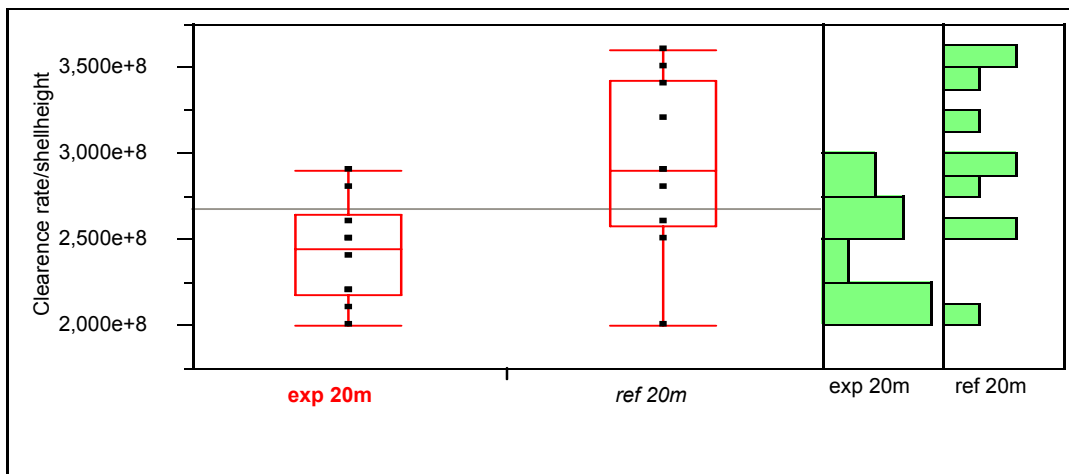


Figure B.5.8. Clearance rate (algae/L/h/length in mm) of scallop under stable lab conditions after a caged period at different depths during exposure to drilling. Significant reduction for scallops in group Exp. 20 m. Quantiles boxes with median values and whiskers (values within 1,5x interquartile rang). Outliers are present if a value are higher or lower than the whiskers range (Turkey 1977).

Table B.5.2. *Filtration rate of scallops and mussels caged at different depths in an area exposed to drill cuttings (n=8-10).*

Filtration (ml/min.)	Ref. 20 m	Ref. 100 m	Exp. 20 m	Exp. 40 m
Blue mussel	59,2 ± 8,9	60,8 ± 8,3	44,8 ± 18,6	27 ± 27,4
Great scallop	119,7 ± 19,4		79,3 ± 16,1	

B.5.7. Stress on stress (survival in air for blue mussels)

Physiological responses indicate the disruptive effects of pollutants on “normal” function, they are generally non-specific and are directed at evaluating effects on energy metabolism or influence on growth and reproduction. An impairment of physiological processes inevitably reduces the survival potential of an organism and it is likely to have relevance for the population as whole (Depledge, Aagaard et al. 1995; Depledge and Billingham 1999).

A set of co-factors other than exposure, temperature and pressure involving transport, caging, wave actions, change in environment and food supply will in general affect the mussel’s survival time and the overall outcome of the test. In this case the survival time in air showed a high capability of mussels caged at 100 m to deal with additional stress, while the reference group at 20 m have a significantly higher death rate (figure B.5.9.). In addition to depth the comparison between exposed and non exposed mussels at 20 m shows that the exposure to particles as barite significant increases the survival time for blue mussels. These results suggest that the mussels may be adapted by unfavourable conditions such as increased depth and particle exposure, preparing the mussels for further influences (as stress on stress) by lower the metabolism. This was not supported by comparing the survival time measured for mussels exposed at 20 m and 40 m (B.5.9). Although the survival time data demonstrates that mussels caged at 100 m could prolong the survival time, as could those exposed to barite. If this increase is attributed to hibernation like state, this could prevent a normal growth over time, generate an oxygen deficiency, and disturb the yearly progress of energy construction in growth periods, affecting spawning and survival.

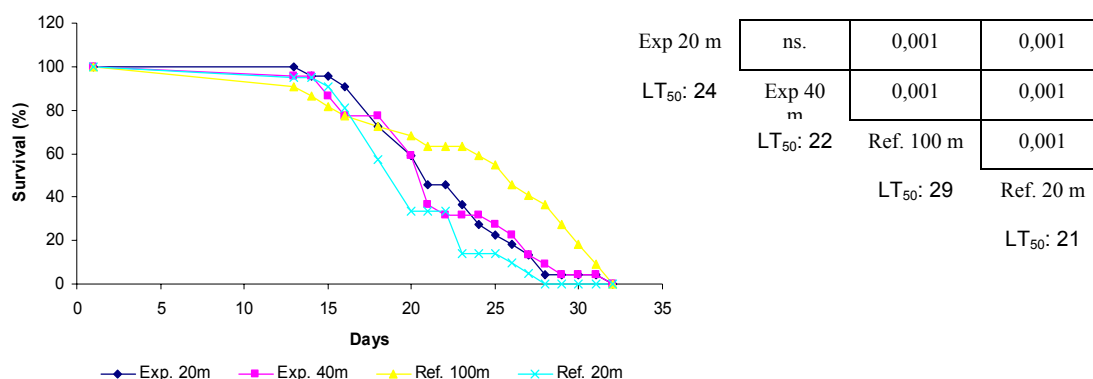


Figure B.5.9. Survival in air curves for mussels caged at different depths in an area exposed to drill cuttings. Median survival time LT_{50} , using Kaplan-Meier plot. Statistical comparison using Kaplan-Meier plot, log rank and Wilcoxon tests.

B.5.8. Proteomic analysis

In this study, hemolymph from 4 groups of 25 individuals was analysed for both blue mussels and scallops. These were then compared pair wise in order to tell whether exposure to drill cuttings caused significant changes in peak intensity. It was also important to clarify whether different depths (and/or temperature) would lead to altered protein intensities. These comparisons are all shown in Appendix B and C.

Unfortunately due to spawning it was difficult to determine gender for mussels, and also to determine whether the scallops had predominantly male or female reproductive cells at the time of sampling. As protein signatures are gender specific and protein responses to an exposure are not necessarily the same for both sexes, this limited the level of multivariate analysis possible. This means that a strong possible protein peak for one gender could be naturalized or reduced by the lack of a protein peak from the other gender. A low protein peak response can than not be interpreted as an absent or low effect response.

In scallops there was a very clear effect of depth (and possibly temperature). The exposed 40 m group was included to show that there really seems to be a depth and/or temperature dependency of these proteins, as the values at 40 m lie between the 20 and 100 m values (figure B.5.10.).

Many of the responses were common for exposure and depth, although a few proteins seem to respond specifically to exposure. The multivariate analysis, using BPS, gave promising results. It is likely that classification trees which could correctly distinguish between exposures could be created. Since the degrees of exposures (and responses) were rather subtle, a larger number of individuals would be needed, preferably with known gender, to effectively distinguish between the groups.

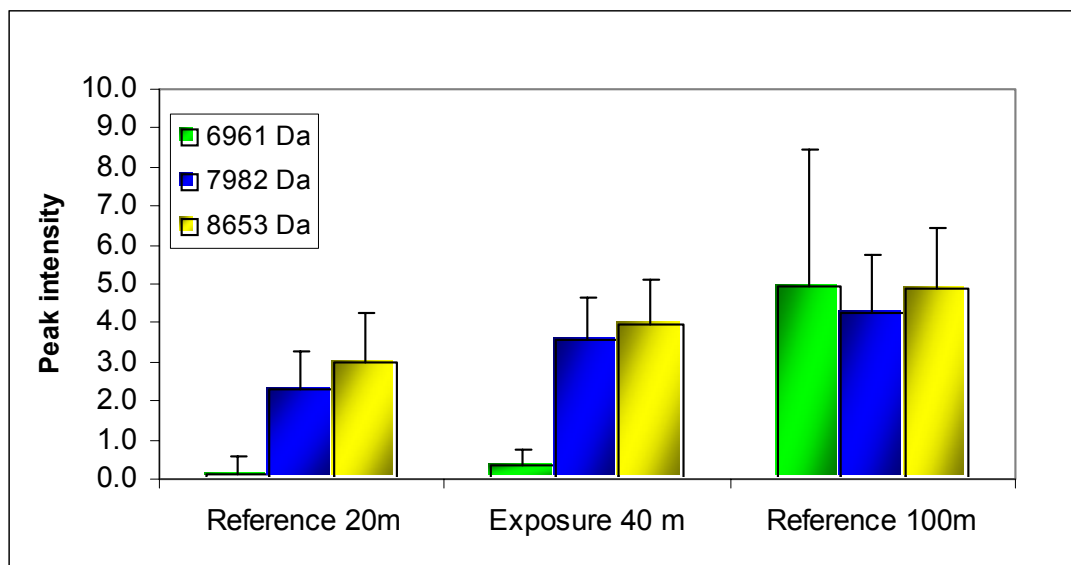


Figure B.5.10. Scallops; Peak intensity of proteins used in classification tree for distinguishing between depths. Mean values with standard deviation lines.

Blue mussels seemed to be less affected by depth compared to scallops, 38 of 58 significantly altered proteins were affected by depth alone, and of these 15 were affected in both the Ref 20 m and Exp 40 m groups. Similarly to scallops, the blue mussels were less affected by exposure than by depth; 16 proteins showed significant response in the Exp 20 m group compared to Ref 20 m, without being affected by depth, 4 of these were common to the Ref 20 m and Exp 40 m changes. 7 proteins were significantly altered in the Exp 40 m group compared to Ref 20 m.

None of these proteins were significantly altered by exposure and the prediction tables also indicate that the effect of depth is a less pronounced compared to scallops, where it was easy to find proteins which could classify the two reference groups. The peak intensities at the different depths are shown for 3 proteins (figure B.5.11.).

Again it can be observed that there seems to be a depth dependency, increased protein expression with increased depth. It should be noted that only the first two proteins (6640 Da and 7062 Da) are significantly changed by depth. The 3021 Da protein is not significantly changed by either depth or exposure, but is nevertheless included by the biomarker pattern software (BPS) to optimize classification. This protein optimizes the statistical probability to classify the proteins (6640 Da and 7062 Da) into groups.

Both scallops and blue mussels were clearly affected by depth and/or temperature and possible other unknown environmental factors. Barite exposure appeared to have less effect than depth, although results indicated that with a larger sample group classification would be possible.

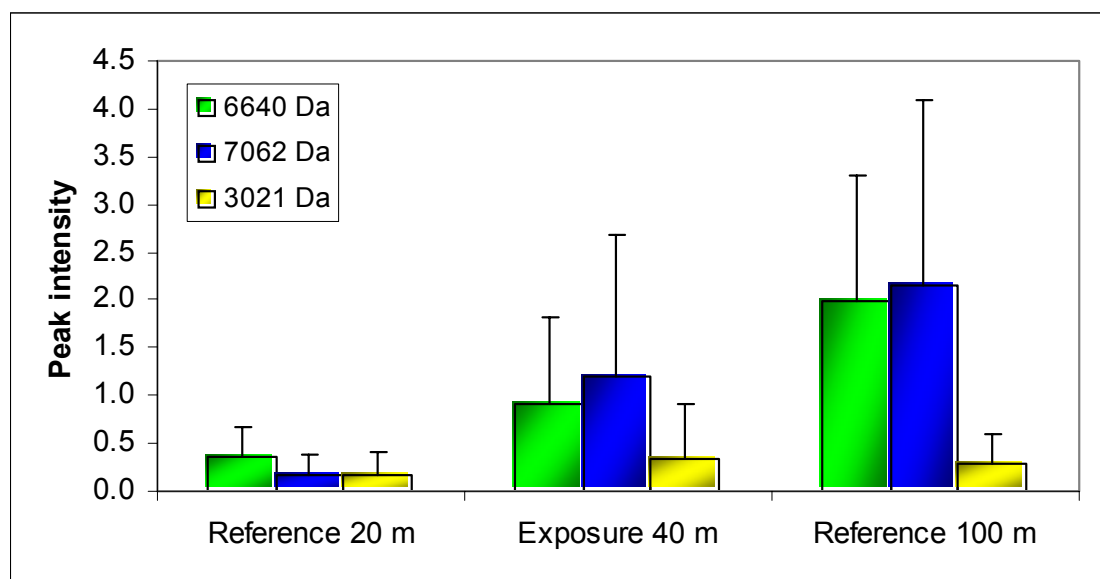


Figure B.5.11. Blue mussels; Peak intensity of proteins used in classification tree for distinguishing between depths. Mean values with standard deviation lines.

B.5.9. Body burden of barite

Small barite particles can enter the digestive system in scallops and mussels since the rejection efficiency is low for non organic particles less than 10 μm . In the intracellular digestion gland organic particles can either be broken down by digestion enzymes or enclosed by movable haemocytes. If barite as inorganic particles is dissolved or enclosed for further break down in the digestive gland is unknown, but metals have been shown to desorb (Weltens, R. et al. 2000), accumulated through feeding or have been admitted from the dissolved phase (Wang and NS. 1999).

Particle size analysis of the discharged drilling wastes revealed a particle distribution from 0.1-200 μm , where particles less than 6 μm constituted the major number of particles and volume in the plume (figure A.5.4). The reduced ability to reject small barite particles would increase the barium uptake in the soft body tissue. The natural distribution of metals in clean reference scallops showed increased concentrations in the pancreas compared to muscle, gills and gonads (figure B.5.12.). An important point is that the natural distribution of barium seems to be located mainly in the pancreas and gills, which could be due to barium particles rather than metabolized barium. Other metals (Zn, As, Sr, Ld) are found in muscle and/or gonad tissue which indicates they have actually been incorporated into the tissue (figure B.5.12.).

The metal values in figure B.5.12. are per tissue and should not be directly compared to values in figure B.5.13, since these values represent the total metal concentration for the whole animal and are diluted from the other tissue components (figure B.5.13).

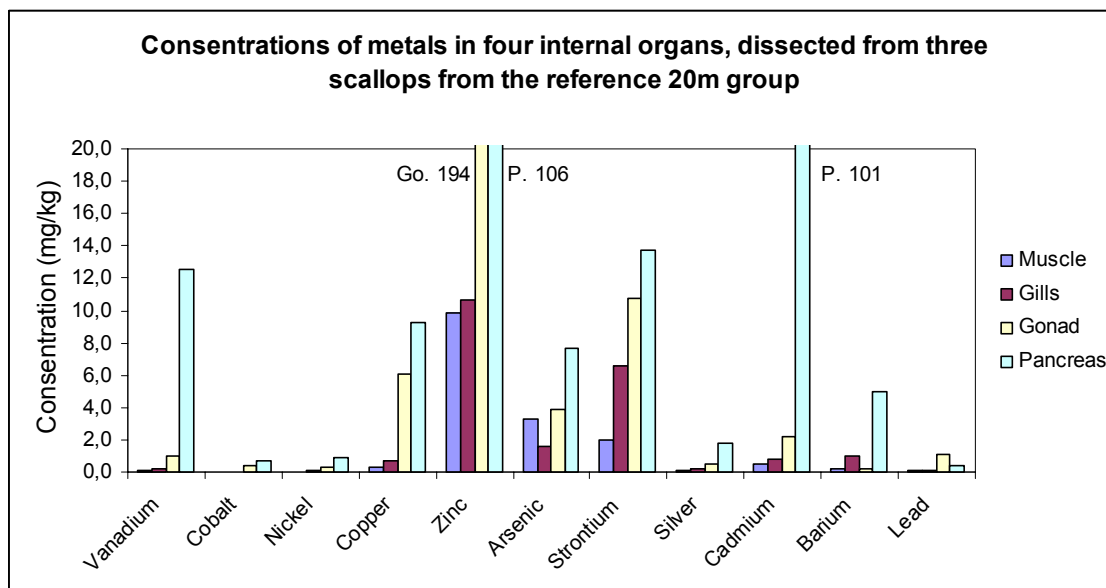


Figure B.5.12. Natural distribution of mean metals values in four scallop organs dissected from the reference group at 20 m.

A trend towards increased barium levels in soft tissue can be seen for all exposed groups, but there were no significant differences between exposed and non exposed mussels or scallops (figure B.5.13). For both species the distribution of barium content in soft tissue relative to depth seems to correlate well with the turbidity measurements of the plume (figure A.6.8.). Although this does not explain the enhanced barium value found in the hard shell part for scallops exposed at 10 and 20 m, which suggest a higher barium exposure at these depths compared to scallops located at 40 m. The concentration of barium and strontium measured in the hard shell fraction was not equal for scallops, which means the hypothesis of similar uptake paths and incorporation of Ba, Ca and Sr must be rejected, leaving adsorbance as the possible reason for barium in this fraction. Significantly different levels of barium were measured in the hard shell part for all exposed scallops groups as compared to the 20 m reference group, but only in the 20 m exposed group when compared to the 100 m reference group. In the mussel groups no significant differences in barium concentration were found in the shell between exposed and non exposed group. A comparison between scallops and mussels shows differences in barium concentrations measured in the shell. A possible explanation based on the adsorbance of tiny particles is that scallops have rough shell surfaces which adsorb particles more easily compared to the smooth shell surfaces on blue mussels.

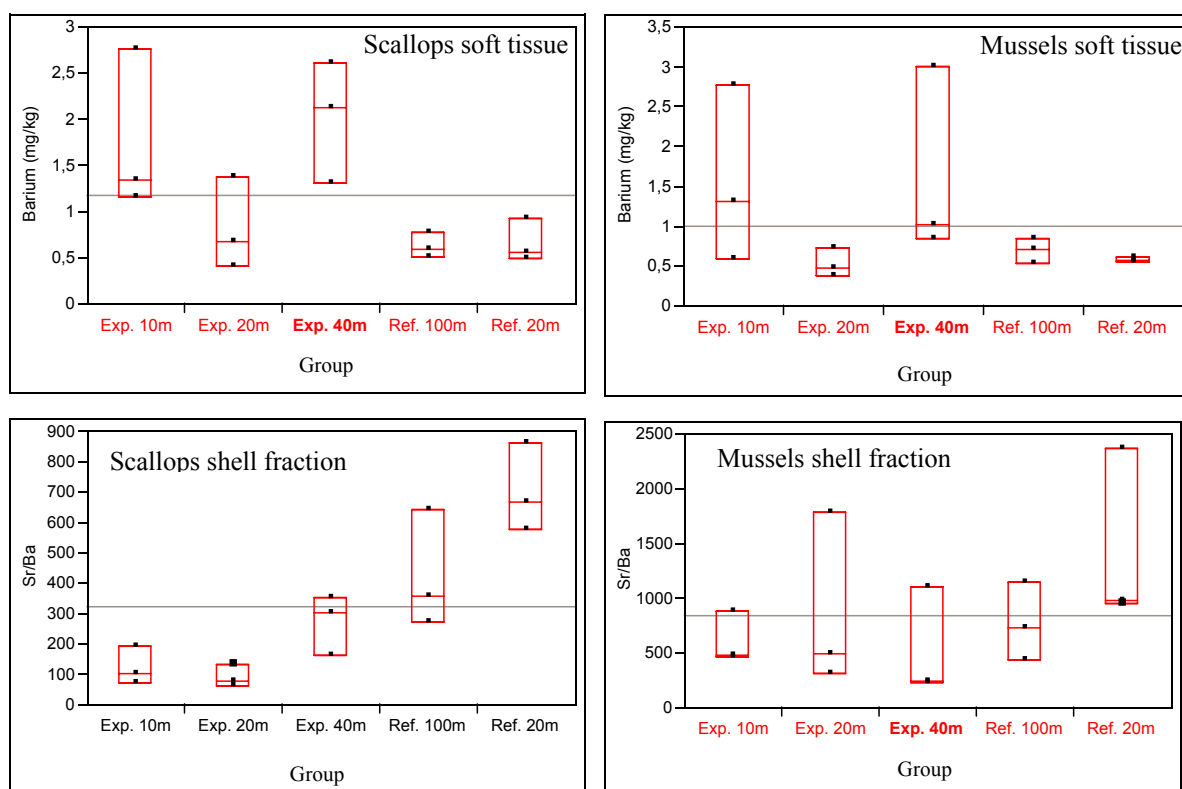


Figure B.5.13. The total concentration of barium in great scallops and blue mussels measured by ICP-MS in samples from soft tissues and the hard shell part. The strontium level was stable; scallops 5.5 ± 0.9 mg Sr/kg and mussels 6.2 ± 0.5 mg Sr/kg). Quantiles boxes with grand mean (grey line).

B.5. 10. Evaluation of the simulated exposure regime.

As seen from part A (figure A.6.13), the discharges of barite particles are patchy and vary a lot between the drilling periods. The tidal current also reduces the exposure time to hours, an exposure regime in which blue mussels may seal and reopen after discharge or could increase uptake as a response to high particle concentrations. In between the drilling periods the transplanted animals also have the opportunity to recover before the next discharge periods. Since there is no knowledge about barite and recovery time during the non exposure periods, this effect remains unsolved.

In the plume the barite concentration at 40 m contains less than 10 % volume of the preferred particle size (2-6 μm) for feeding. As seen from figure A.5.5, the greatest number of particles is less than 0.4 μm in size. These could be passively rejected or actively filtrated with an efficiency of less than 20-30 % (Gosling 1992). The average concentrations shown in table B.5.3 should then be reduced by 70-80 % to find the total body burden. A further reduction could be made due to particles from the feeding range being rejected as pseudofaeces prior to ingestion. In an environment with low organic seston content (8 %), a constant fraction of about 0.93 times the mass of filtered material, measured at "high" seston concentrations ranging from 10 to 90 mg particulate mass/l has been reported (Hawkins, RFM et al. 1996). At lower seston concentrations

(1.4 mg/l) or when particulate organic material is low (10 % POM) the sorting efficiency is reduced (<24 %) and the mussels became non-selective, ingesting both organic and inorganic seston components, probably to meet their nutrient requirements (Arifin Z and LI 1997).

Table B.5.3. Average particle concentrations (essentially barite particles) for the time intervals where discharges have taken place from the drilling rig. The time intervals where the discharges have taken place are defined in Part A, chapter A.5.1. All concentrations are given in ppb (mg/m³).

Station	Average 1. period	Average 2. period	Average 3. period	Average 4. period
Cage Rig A 35 m depth	676.7	392.3	313.4	93.05
20 m	0.47	0.23	0.08	11.17
10 m	0	0	0	2.66
Cage Rig C 100 m	0.184054	0.001667	0	0.013584
20 m	0.100562	0.767123	0	3.278641

Due to the patchy discharges of barite the theoretical approach towards measured barite in soft tissue was difficult. The simulated uptake using measured clearance rate and fixed filtration and rejection rates was not similar to measured body burden values. The results clearly show similar differences in uptake with respect to depth, although calculated tissue concentrations varied between 3 fold lower to 1000 times higher (table B.5.4.). The mismatches are over-represented at high particle concentrations especially for blue mussels. This probably reflects the lack of data in the evaluation related to filtration rate/time/efficiency for each exposure period, closure period and rejection time. This is therefore not sufficient to support any theories regarding the importance of discharge periods, time of exposure or concentration levels.

Table B.5.4. Body burden in mussels and scallops, based on the simulation of the exposure of barite at the SVAN field. Approach m; using measured clearance rate (table B.5.2.) and 0,93 pseudofaeces. Approach t; using 20 % particle uptake and 0,93* pseudofaeces. Boldface data are data based on measured clearance rates for that depth.*

Depth	Approach	Ba in scallops (mg/kg)	Ba in blue mussel (mg/kg)
10 m	m	9,6	57,7
20 m	m	5,9	37,2
35 m	m	407,5	1433,2
10 m	t	0,4	4,3
20 m	t	0,2	2,8
35 m	t	17,2	176,9

As well as active filtration, it is reasonable to believe that barite particles could adsorb to surfaces, which complicates the picture further. As seen from the metal distribution in the scallop reference group (figure B.5.12), the background ratio between gills and pancreas is 1:5. If the barite concentration is increased from the background level to 0.5 mg/l to 20 mg/l, the barium ratio between gills and pancreas change from 1:8 to 1:50 to 1:2 (Bechmann, Westerlund et al. 2006). This could be due to altered incorporation of barium in gills, but the strontium/barium values measured in the shell fraction of exposed scallops and mussels indicate an adsorption of barite (table B.5.12.), though less barite adsorbed to the smooth surface of mussels' shells. Damages found in gills during barite exposure (Bechmann, Westerlund et al. 2006) could be a result of adsorbed particles as well as handling sharp particles or active incorporation of barium.

B.6. Conclusion

The scallops and mussels that were deployed in cages around the Sleipner platform in the North Sea underwent different environmental conditions with rough weather conditions, variation in food supply according to depth and exposure to drill cuttings, mud and chemicals.

The practical approach of using organisms deployed in cages seems useful for screening of drill cutting and mud discharges.

The different conditions of depth and temperature between stations are a challenge and disturb the interpretation of effects.

Based on current knowledge, there is a potential to improve the experimental design by excluding overlapping methods (i.e. GST and TOSC), but to include more measurements (parallels) for each method.

The simulation of the drilling discharge was helpful in; visualizing the progress and the particle concentrations at different depths.

After a month of exposure the biological effects were:

Drill cuttings and mud cause biological effect as demonstrated with the applied methods.

There are species specific responses for clearance rate, but not for GST and TOSC.

Physical disturbance affecting the build up of energy reserves, using energy and reduced gonad weight during exposure to non nutritional inorganic barite particles in scallops.

Repercussion effects on the ability to filtrate particles in mussels and scallops.

A depth and exposure effect, prolonging the death rate and increasing tolerance to extra stress, presumably an effect of unfavourable conditions followed by a reduced metabolic activity, making it less vulnerable to changes.

The increased barium content in the shell and soft tissue of mussels and scallops are good indications of barite exposure. The difference in concentration between these two parts has to be connected to different “uptake” mechanisms. Soft tissue have been exposed through active filtration, further particle handling involving selection and transport directly or through pancreas for discharge as faeces or for further incorporation into tissues. It seems that barium found in the shell part is a function of adsorption only with no or low active incorporation of barium as an addition to calcium.

In scallops and mussels the barium content was higher at 10 and 40 m than animals exposed at 20 m, reflecting a turbidity snapshot particle distribution. The simulation

of the discharge does not explain the “high” barite values found in mussels and scallops located at 10 m depth.

Statistically significant increase of DNA in the comet tail was found for exposed 40 m mussels, but not for the 20 m exposed group, when compared to the reference group at 20 m. These damages arise after the mussels have been exposed to a tidal controlled exposure regime, exposing 40 m caged mussels to pulses (>0-14 mg/L barite) that last not more than hours.

The hepatopancreas seems to contain the majority of the barium in the natural (farmed) scallop population.

Higher levels of ROS (TOSC) and enzymatic responses (GST) relating to non natural materials were found in all exposed groups. The exposed group at 40 m showed the highest oxidative response, which could be connected to the exposure at that depth.

The lysosomal membrane stability was reduced for all mussels groups, compared to what is expected from natural healthy mussels. Exposed 20 m mussels and mussels placed at 100 m suffered the lowest membrane stability.

Proteomics measurements gave a clear protein pattern distinguishing between depths for blue mussels and great scallops. No clear pattern could be found for the exposed groups alone. Low sampling numbers (25 individuals) and lack of gender specifications complicate the proteomic analysis.

PART C

Comparison between risk estimates and biomarker response in general

C.1. Risk calculations for the cage locations

The part C of this report tries to establish a link between the risk method presently developed as a part of the ERMS project and the biomarker responses. First, the risk method used in the ERMS project is briefly outlined in chapter C.1. This chapter also includes calculations of the actual risks for the cages deployed according to the method developed. The chapter C.2 then discusses the link between the biomarker responses and the risks calculated with the revised DREAM model. Due to lack of sufficient data, the chapter C.2 is limited to discuss the possible links between risks calculated and biomarker responses in general, without arriving at specific conclusions.

The present risk method developed during the ERMS project is based on a PEC/PNEC approach, where the PEC is the “*Predicted Environmental Concentration*” and the PNEC is the “*Predicted No Effect Concentration*”.

The principle used is in accordance with the recommendation from the EUs Technical Guidance Document for Risk Assessment (TGD, 2003). The predicted concentration level (the PEC, in this case PEC is produced by modeling the concentration levels) is to be compared with a fixed concentration level (PNEC) below which no or acceptable potential impact on the biota is encountered. The PNEC level is associated with a level of 5 % probability for damage or impact on biota in the recipient.

Two different types of stressors are included for the impacts in the water column caused by drilling discharges. These are:

- Impacts from chemicals with a large oil – water partition coefficient $P_{ow} < 1000$
- Impacts from particle stress caused by weighting material in the mud

The impacts from the chemicals are treated in the same way as for the chemicals in the produced water. Assuming only non-PLONOR chemicals to be included for the risk calculations, the HOCNF scheme (or similar) contains the information necessary (in principle) for characterizing the biodegradability (matter biodegraded over 28 days), the oil-water partition coefficient (P_{ow}) and the NOEC's, EC50's and LC50's for assignment of a proper PNEC value. The risks caused by the chemicals are related to the ratio PEC/PNEC for each chemical. For the PEC values, the model is run in order to determine the PEC values of the chemical in the recipient (for all grid points and at all times). The PEC/PNEC ratio is then determined accordingly.

The PEC/PNEC ratio for the chemical or compound in question is then used to determine the probability of impact on the recipient in terms of probability of risk for damage. The method used is presently according to a method developed by Karman et. al., 1994 (and also published in Karman and Reerink, 1997). When $PEC/PNEC = 1$, this corresponds to a level of probability of damage equal to 5 %. When $PEC/PNEC < 1$, the probability of damage (risk) is lower than 5 %. When $PEC/PNEC > 1$, the risk is correspondingly higher than 5 %.

Figure C.1.1 shows an example of the relation between the PEC/PNEC ratio and the probability of damage (risk). The curve is determined from the formula (based on Karman and Reerink, 1997):

$$\text{Risk} = \int_0^{\ln PEC/PNEC} \left\{ \frac{1}{S_m \sqrt{2\pi}} \exp \frac{-(y - X_m)^2}{2 S_m^2} \right\} dy \quad (\text{C.2.1})$$

Where

Risk = the probability that a species will be affected

X_m = a mean of the logarithmically transformed data

S_m = a standard deviation of the logarithmically transformed data

y = variable to describe the normal probability density function from 0 to $\ln PEC/PNEC$.

The data that are referred to represents data on damage on particular species determined from laboratory experiments.

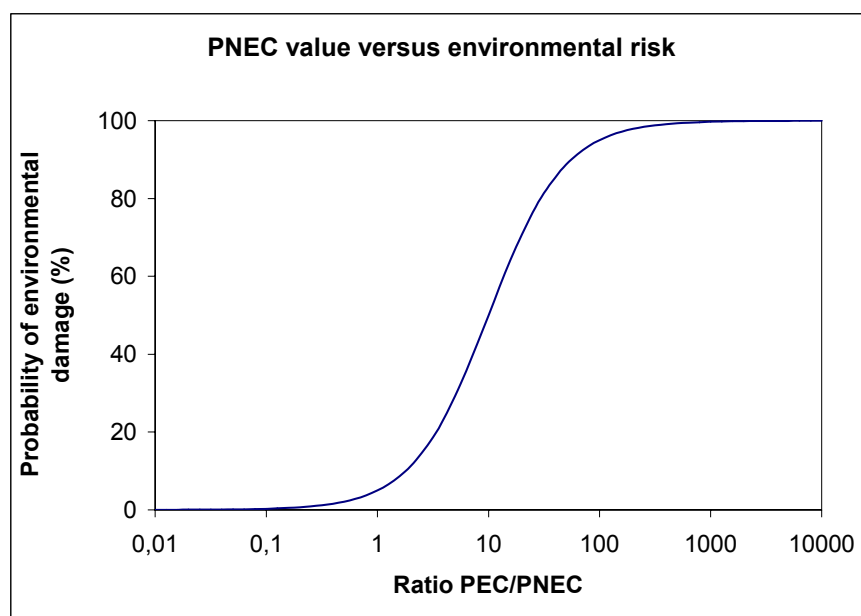


Figure C.1.1. The relation between the PEC/PNEC level and the risk level (in %) for damage on biota. Note that at the level $PEC/PNEC = 1$, the probability of damage is 50%. Based on Karman and Reerink, 1997.

The risk curve shown in the figure above is:

$$S_m = 1.74 \text{ and } X_m = 2.85.$$

These numbers are also presently used for the risk calculations of water soluble chemicals in the water column caused by drilling discharges. The curve shown in Figure C.1.1 relates the calculated PEC/PNEC ratio to the probability of risk in a unique way.

For the water soluble drilling chemicals in the water column, the EIF (*Environmental Impact Factor*) is defined as the water volume where the $PEC/PNEC > 1$, divided by a unit volume equal to $(100\text{m} \times 100\text{m} \times 10\text{m}) = 10^5 \text{ m}^3$ of recipient water. In addition, the EIF water volume is adjusted upwards by a factor of two for those compounds that have a small biodegradation factor combined with a large bioaccumulation factor.

For the actual drilling discharge at the SVAN field, only one non-PLONOR drilling discharge was included in the chemical package, namely the *Glydrill MC* chemical. The EC50 or LC50 value for this chemical was determined to be 310 mg/L from HOCNF testing (HOCNF = *Harmonized Offshore Chemical Notification Format*). Using an assessment factor of 100 (assuming that the duration of the different discharge periods is sufficiently short that the discharge can be categorized as an “acute” discharge), the PNEC for this discharge is determined to be $(310 \text{ mg/L} \text{ divided by the assessment factor } 100 = 3.1 \text{ mg/L})$.

A more general review of the EIF factor and the PEC/PNEC approach for discharges of dissolved components to the sea is found in Johnsen et. al. (2000).

In addition, the ERMS project also includes environmental stresses imposed by (non-spherical) particles in the water column based on Species Sensitive Distributions (SSD's). The ERMS project arrived at (TNO, 2006) PNEC's and risk functions (X_m 's and S_m 's) for barite particles in the water column as follows:

$$\text{PNEC} = 1.47 \text{ ppm}$$

$$X_m = 4.95$$

$$S_m = 3.011$$

Figure C.1.2 shows the risk functions for particle stressor barite in the water column based on SSD's. The risks from the particle stressor barite are added to the risks from the toxic stressors *Glydrill MC* to arrive at the total EIF for the water column.

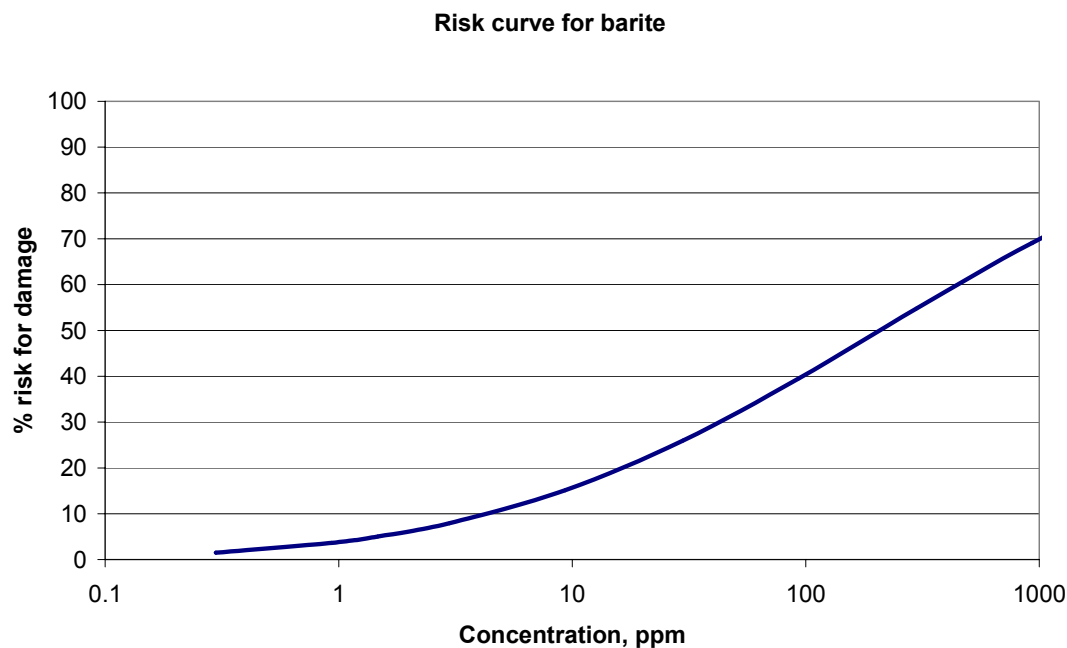


Figure C.1.2. Risk function for the particle stressor barite in the water column based on SSD's. Based on TNO (2006).

The EIF for the discharge at the SVAN field has been calculated by the revised DREAM model as shown in the Figures C.1.3, C.1.4 and C.1.5. The Figure C.1.3 shows the time development of the EIF for the drilling mud discharges at the SVAN field. The Figure C.1.4 shows a pie chart of the different contributors to the EIF. The calculations include both particle (physical) stresses caused by the presence of particles in the water column (barite) and also chemical stress (toxicity) caused by the presence of chemicals in the water column (*Glydrill MC*). It is the barite that dominates the contributions to

the risks for the discharge in question, according to the method developed in the ERMS project. The barite contributes with more than 90 % of the risk. The Figure C.1.5 shows one example (snapshot) of the risks calculated for the discharge at the SVAN field.

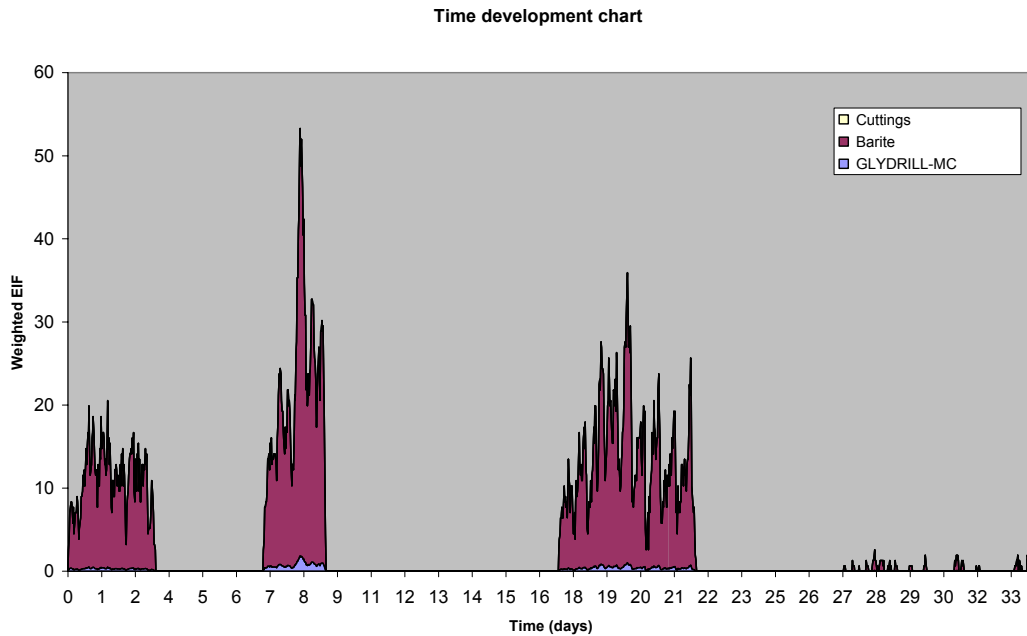


Figure C.1.3. Time series plot of the EIF calculated for the discharge at the SVAN field. Start at 9 September 2003 (Day 0). End at 12 October 2003 (Day 33). PNEC for barite = 1.47 ppm (mg/L). PNEC for Glydrill MC = 3.1 ppm (mg/L). 4 different discharge periods can be identified.

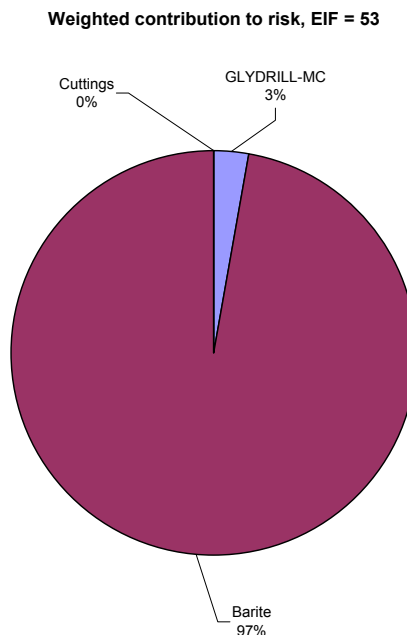


Figure C.1.4. The EIF pie chart for the discharge at the SVAN field, showing the relative contributions from the different stressors (barite and Glydrill MC).

Risk for the water column

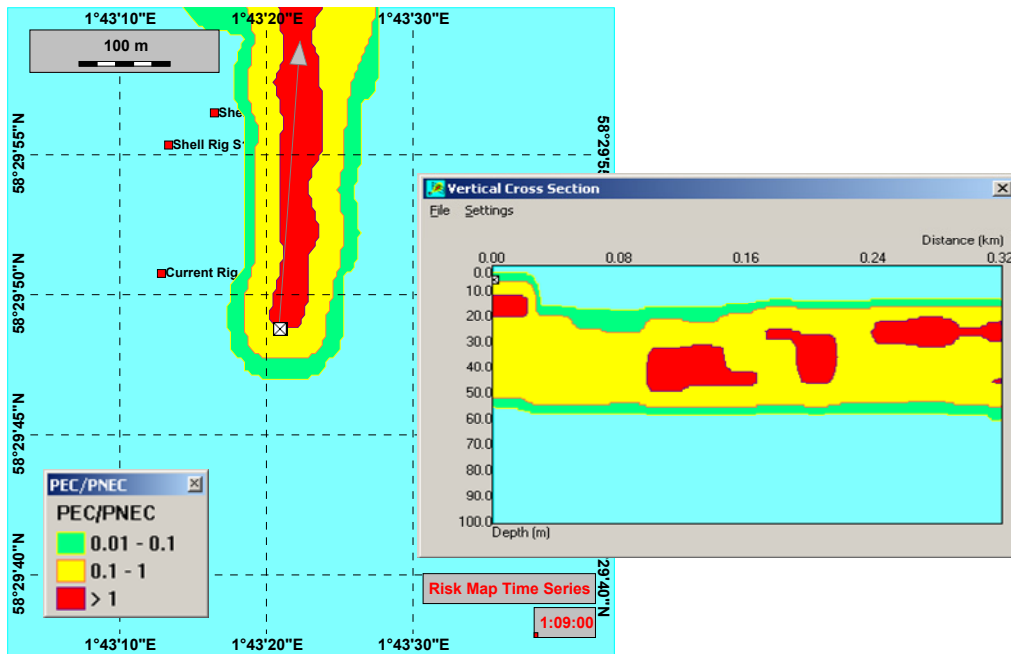


Figure C.1.5. Snapshot of the EIF field (red area indicated with $PEC/PNEC > 1$) calculated for the discharge at the SVAN field. Vertical cross section through the plume area is shown as well.

The results shown in the Figures C.1.3 – C.1.5 are valid for the whole water masses surrounding the discharge point. However, each of the cages is located at one single point in the water, and the risk calculation results for the whole water mass will therefore not be relevant for one single point. Therefore, risks have been calculated for each of the cages retrieved. These calculations will therefore correspond to the calculations of the concentrations at each cage as presented in Chapter A.6.4, see the figures A.6.13 – A.6.17.

The risk results for each of the cages deployed and retrieved consist of:

- Average risks calculated for the whole deployment period (33 days)
- Average risks for the 5 last days of the deployment period
- Time series plots for the risks for the whole deployment period.

Table C.1.1 shows the results for the average risks for the whole deployment period and for the 5 last days of the deployment.

Figures C.1.6 – C.1.10 show the time series plots for the risks calculated for the location of the 5 cages at the shell rigs A and C.

Table C.1.1. Average risks calculated for the cage locations A and C. The risks include potential impacts due to the presence of particles only (essentially barite particles). PNEC for barite particles equal to 1.47 ppm corresponds to a risk level of 5 %. See the risk curve for barite shown in Figure C.1.2.

Risks calculated at the cages (%)		
Station	Average over 33 days	Average over the 5 last days
Cage Rig A 40 m depth	0.21	0.19
20 m	0.005	0.026
10 m	0.001	0.006
Cage Rig C 100 m	0	0
20 m	0.001	0.005

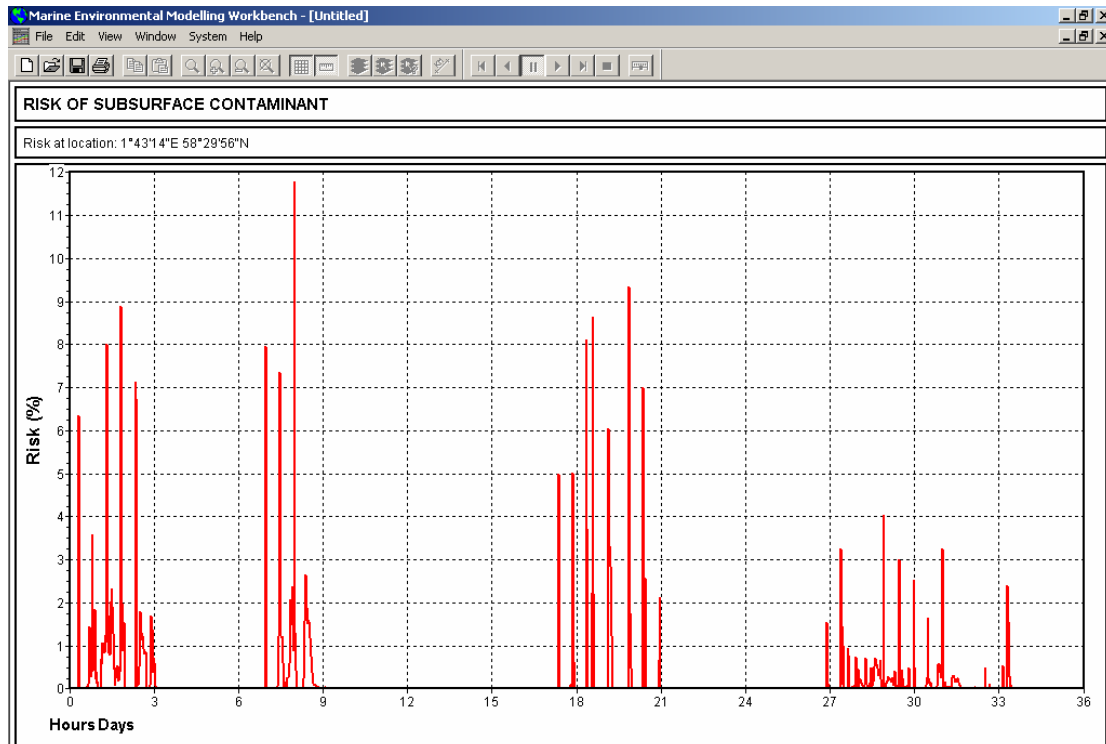


Figure C.1.6. The time series risks due to particle concentrations (essentially barite) calculated for the cage at 40 m depth at shell rig location A.

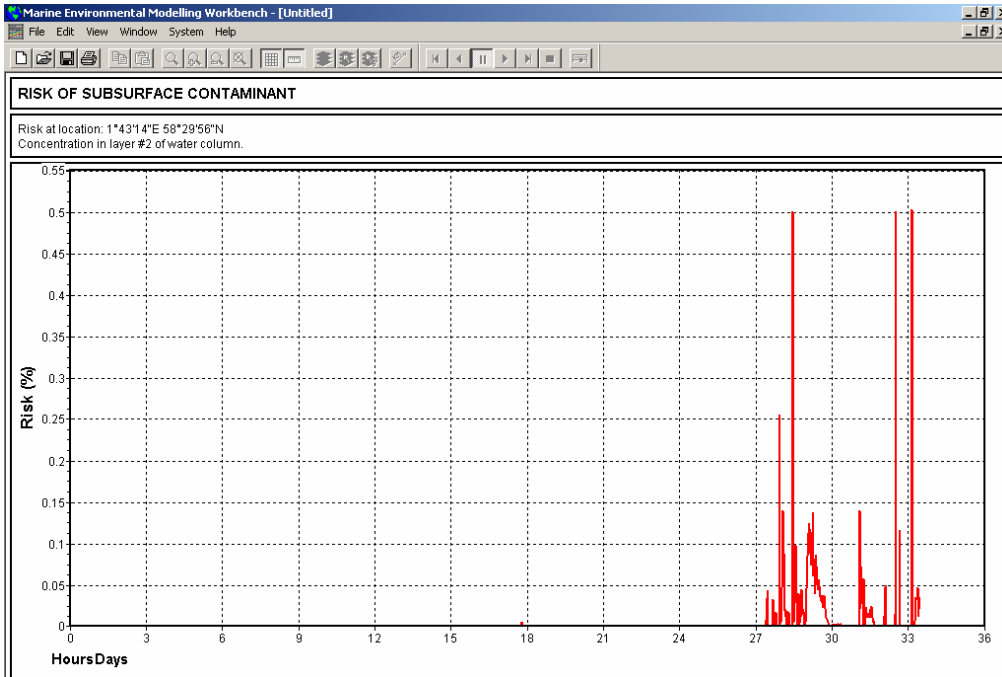


Figure C.1.7. The time series risks due to particle concentrations (essentially barite) calculated for the cage at 20 m depth at shell rig location A.

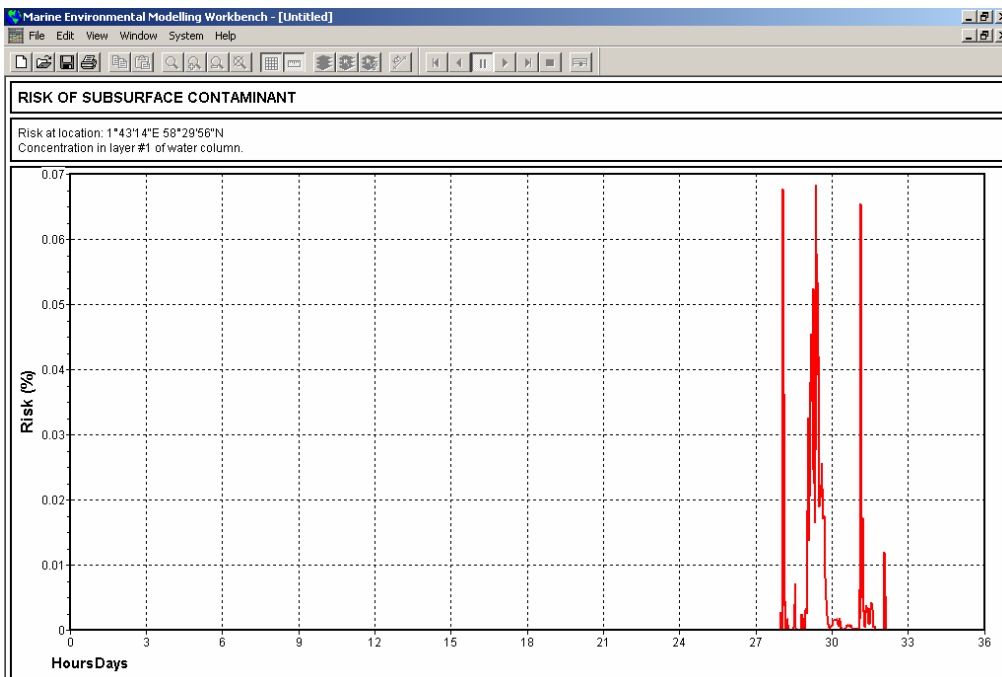


Figure C.1.8. The time series risks due to particle concentrations (essentially barite) calculated for the cage at 10 m depth at shell rig location A.

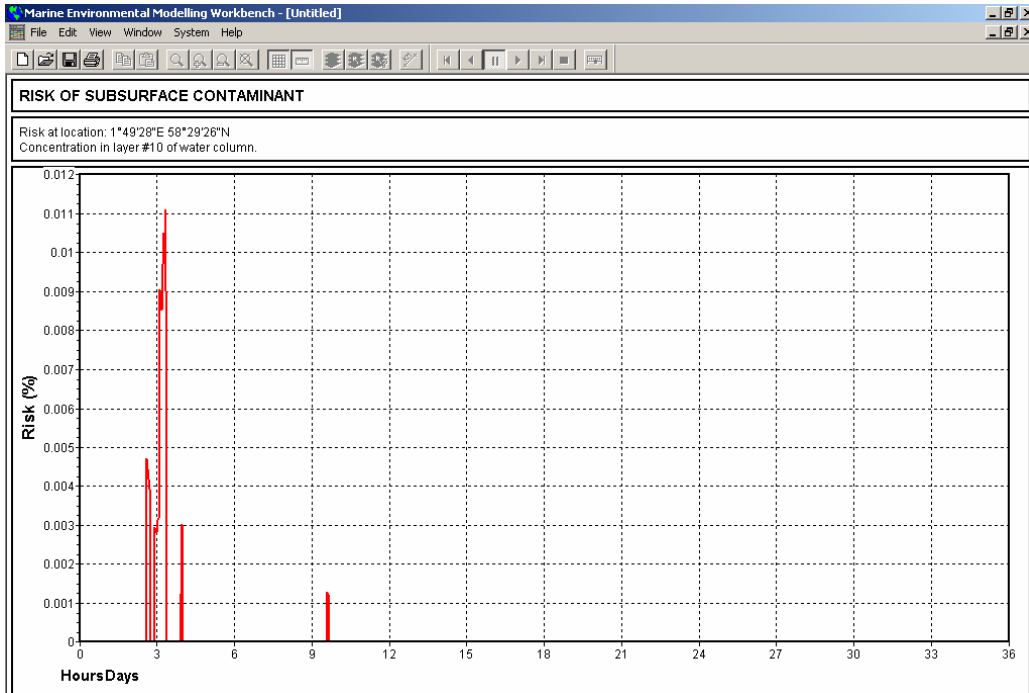


Figure C.1.9. The time series risks due to particle concentrations (essentially barite) calculated for the cage at 100 m depth at shell rig location C.

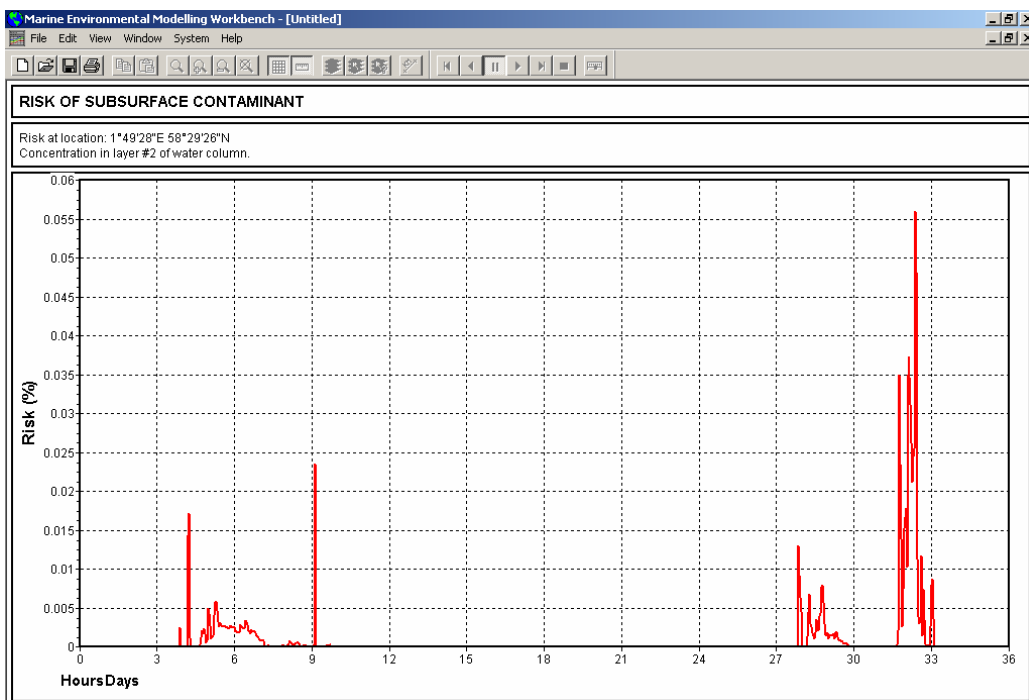


Figure C.1.10. The time series risks due to particle concentrations (essentially barite) calculated for the cage at 20 m depth at shell rig location C.

C.2. Relationship between Risk and Biomarkers

The EIF method produces an expression of impact from simulated drilling discharges. The method is intended to be used to make decisions about drilling operations based on the predicted impact factors. The drilling regime decided upon is represented by a specific discharge set-up and a simulation of risk volume and a calculation of an Environmental Impact Factor (EIF) value. This is an index value which is not directly measurable in the field. Therefore, the EIF value cannot be used directly to control monitor (or validate) that the impacts are within the expected limits.

Therefore, alternative measurement techniques are sought for this purpose. Biological methods such as biomarkers are considered of interest for several reasons:

- Of available methods, they are the closest related to adverse biological effects (often expressed by measures of fitness), which the risk is derived from. The fitness parameters are difficult to measure in the field.
- As compared to chemical concentrations in the water which provide information only of exposure, biomarkers also reveal that biological uptake has taken place, in other words, holds information of bioavailability.
- As compared to chemical body burdens, biomarkers reveal that biotransformation has taken place, which is necessary for biological effects to occur.
- Biomarkers are more economic than chemical measurements because they reduce the number of parameters necessary to measure.
- As compared to biodiversity measurements (which are most feasible for impact assessment on bottom fauna), biomarkers hold the potential for more early warning of possible adverse effects, and they are possible to measure in all compartments.
- Carefully planned suites of biomarkers will give hint of potential type of effects as well as possible source of contamination. This provides good basis for follow-up investigations of signals of possible adverse effects.
- Used correctly, the biomarkers represent a cost effective approach.

The challenge is to be able to link the biomarkers to risk assessment in such a way that it builds a bridge between prognoses made in risk assessment and subsequent diagnosis in field monitoring.

In probabilistic risk assessment the risk is calculated by combining predicted exposure concentrations with a Species Sensitivity Distributions (SSDs) which hold information about probability of adverse effects. In the so-called “Validation” project under the PROOF program a validation link between biomarker signals and risk for produced water discharges has been established (Smit et al. *in prep.*). It seems possible to establish similar validation links related to drilling discharges. This can be judged by the present biomarker based exposures in cages near drilling sites and results from

laboratory studies of biomarker signals in response to simulated drilling discharges (Bechmann, Westerlund et al. 2006).

To give an introduction to how this can be accomplished for drilling discharges, the main features of the validation link and the principles followed is presented in the following:

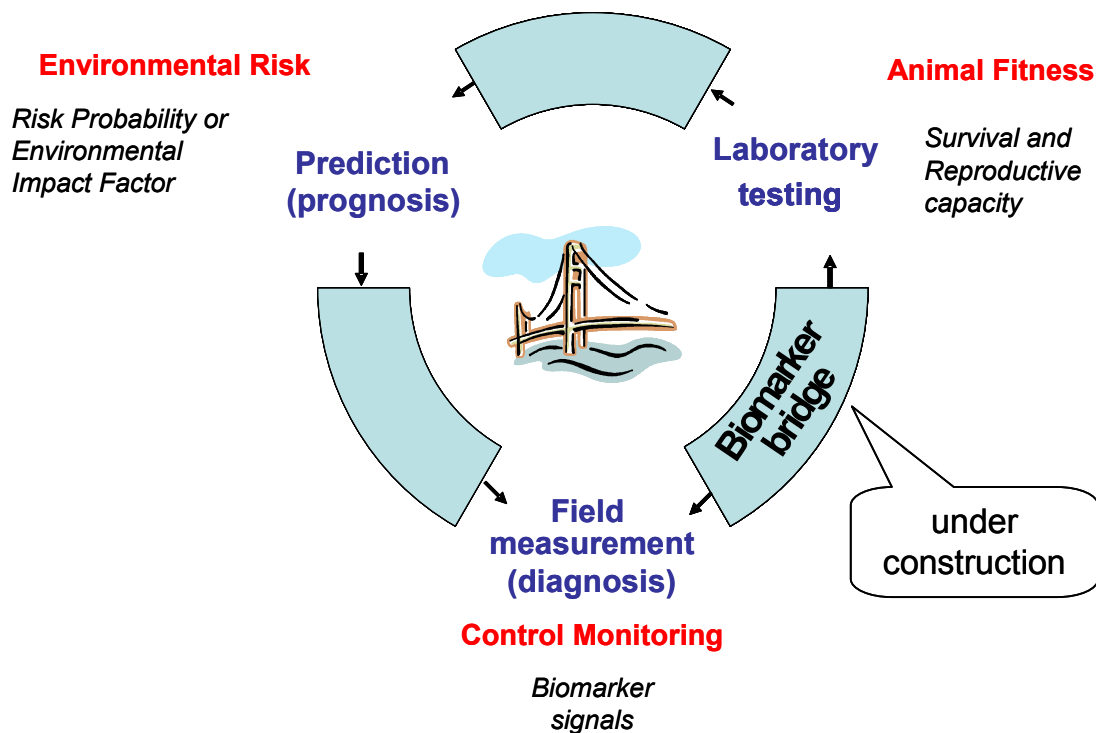


Figure C.2.1: Illustration of a unified concept of Environmental Risk Assessment with Control Monitoring. The Control Monitoring is based on comparison between Field measured Biomarker signals and Predicted Impact in the Risk Assessments. The Predicted Risk Impact is based on Animal Fitness information obtained in Laboratory Tests. The concept is tied together by relationships between Biomarker signals and Survival and Reproductive capacity. This is often referred to as the “Biomarker bridge”.

The approach found most suitable in building the “biomarker bridge” was to establish Biomarker Sensitivity Distributions (BSDs) analogous to the Species Sensitivity Distributions (SSDs) that are used in the present risk calculation procedures. The BSDs may be grouped into different categories according to types of biological effects (genotoxicity, oxidative stress, endocrine disruption etc.). The curves between the Risk curves and the different BSDs represent the actual bridge between the risk and biomarker signals (see Fig. C.2.1.).

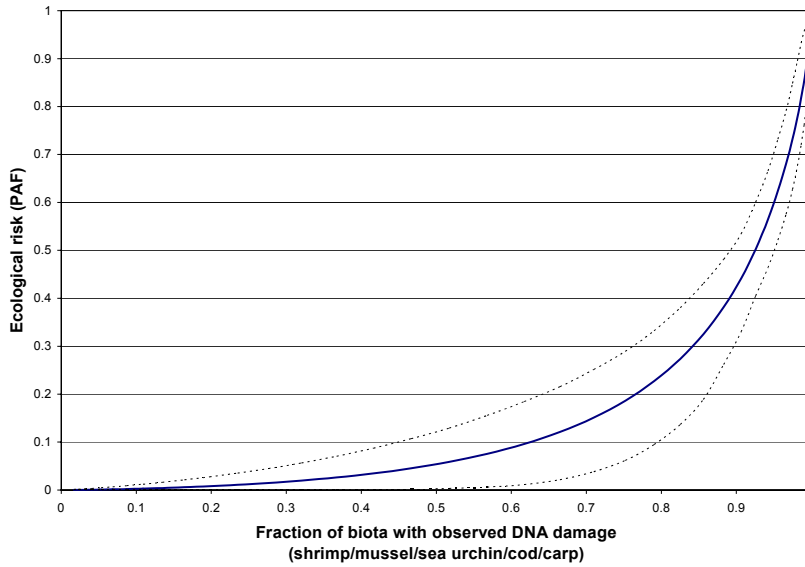


Figure C.2.2: Line with 95% confidence limits showing the relationship between a Risk curve and a Biomarker Sensitivity Distribution curve, representing the bridge (validation link) between the risk and biomarker signals. PAF = “Potentially Affected Fraction” of species.

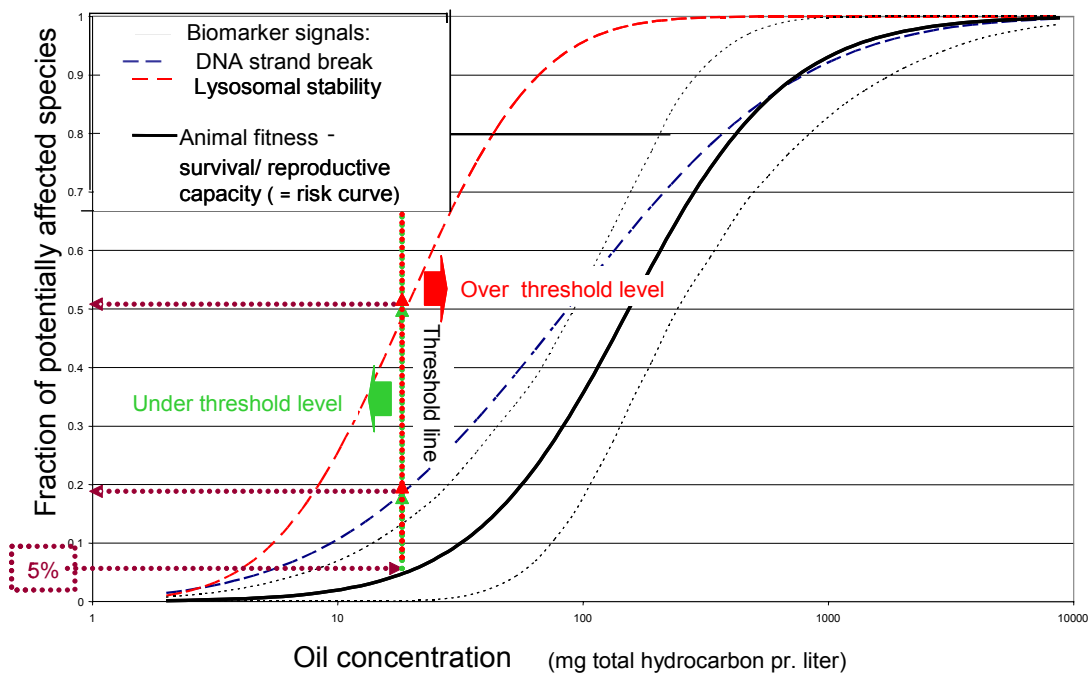


Figure C.2.3: Sensitivity Distributions in relation to different concentrations of oil with respect to fitness (SSD = risk curve) and two types of biomarker responses (BSDs; i.e. DNA strand break base don Alkaline Unwinding Assay and Lysosomal Membrane Stability). 95% confidence limits for fitness are shown by black dotted lines.

Figure C.2.3. shows how sensitivity for two biomarkers was distributed in relation to the corresponding sensitivity for fitness distribution for dispersed crude oil (which was used to approximate produced water). How this can be used in practical field monitoring is illustrated in Fig. C.2.3. If we choose that less than 5% of the species in an area shall be influenced by a discharge, we may establish a limit line which crosses the risk curve in the 5% level (red/green vertical line in Fig. C.2.3). The points to the right of this line will be over the threshold level and signal unacceptable effects in the recipient, while the points to the left will be below and indicate that the effects are within the acceptable level.

In the points where the limit line crosses the two BSD curves we can read which signal levels this corresponds to for the biomarkers (see Fig. C.2.4). In the current studies the biomarker responses are expressed as deviance from negative control values. The conditions in the field will be based on a suite of biomarkers in representative species for the actual environmental compartment or ecosystem.

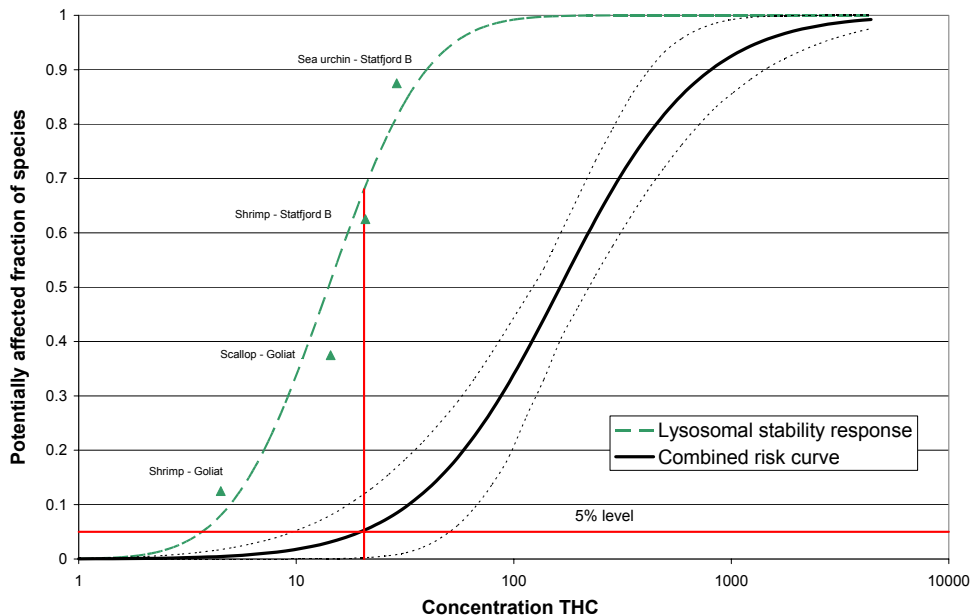


Figure C.2.4: SSD fitness and BSD lysosomal stability curves fitted against exposure concentrations of THC. Vertical red line through the horizontal red line that marks 5% level of fitness crosses the BSD line at the 0,7 fraction of affected species. This means that when 5% of the species are adversely affected it corresponds to lysosomal stability different from control in 70% of the species.

The above represents the main features of the concept, which will be developed in further detail in the last phase of the “Validation” project. This is expected to be completed by September 2006. It is recommended that a similar work be done for drilling discharges. Preliminary results from the laboratory effect studies of drilling discharges (Bechmann et al. 2006) and the biological measurements carried out in the present study indicate that there is correspondence between laboratory and field data. This is a prerequisite to be able to develop a unified concept of risk assessment and monitoring for drilling discharges.

This can then both be used as a tool to validate the ERMS model and for further control monitoring of predicted impacts and environmental risk in the field. It should be noted that biomarkers in this system also could be supplemented by biosensor signals to serve in real time applications.

APPENDIX

Appendix A. Solutions

The physiological saline solution was made by dissolving into distilled water to give a 1 L solution:

4.77 g	Hepes (99%)
1.47 g	CaCl ₂ (Calcium Chloride 99.5 %)
13.06 g	MgSO ₄ (99.0-102 %)
25.48 g	NaCl (Sodium chloride 99,8 %)
0.75g	KCl (Potassium chloride 99,5%)

The solution was adjusted to pH 7.36 with 1 M NaOH.

A stock solution of Neutral Red (C.I. 50040 Sigma) was prepared by dissolving 28.8 mg of dye in 1 ml of Dimethyl sulfoxide (DMSO), and a working solution was made of 10 µl stock solution into 5 ml physiological saline.

Akvamiljø, IRIS and SINTEF Experimental validation of drilling effects in the field

MIZ	Ref1 ref2	p	ratio	Ref1 exp1	p	ratio	Ref1 exp2	p	Ratio	Ref2 exp1	p	Ratio	Ref2 exp2	p	Ratio	Exp1 exp2	p	Ratio
23841	d	0.1713	0.8	d	0.5032	0.6	d	0.0388	0.2	d	0.2563	0.7	d	0.6766	0.3	d	0.1327	0.4
24576	u	0.0000	7.6	u	0.6484	1.7	u	0.1838	4.9	d	0.0000	0.2	d	0.0076	0.6	u	0.4669	2.9
25200	d	0.6484	0.8	d	0.3368	0.8	d	0.5411	0.9	n	0.8084	1.0	u	0.8538	1.1	u	0.7052	1.1
25810	n	0.7636	1.0	n	0.8538	1.0	u	0.5540	1.1	d	0.7196	0.9	u	0.6908	1.1	u	0.4320	1.1
25953	n	0.8538	1.0	n	0.7784	1.0	u	0.7636	1.1	n	0.9768	1.0	u	0.6766	1.1	u	0.6071	1.1
26534	n	0.9613	1.0	u	0.7636	1.1	u	0.7196	1.1	u	0.8084	1.1	u	0.8538	1.1	n	0.9923	1.0
26706	n	0.7489	1.0	n	0.7784	1.0	n	0.8084	1.0	u	0.6484	1.1	u	0.6766	1.1	n	0.9150	1.0
27282	n	0.6624	1.0	u	0.0825	1.1	u	0.0971	1.1	u	0.3084	1.1	u	0.3368	1.1	n	0.9768	1.0
27888	n	0.5157	1.0	u	0.0068	1.1	u	0.0336	1.1	u	0.1229	1.1	u	0.3773	1.1	n	0.4096	1.0
29536	n	0.5671	1.0	d	0.3272	0.8	u	0.2815	1.4	d	0.1713	0.9	u	0.3879	1.4	u	0.0215	1.6
30815	d	0.0388	0.6	d	0.3773	0.9	d	0.3177	0.7	u	0.0045	1.6	u	0.0933	1.1	d	0.0512	0.7
31540	d	0.0006	0.5	n	0.4788	1.0	d	0.0585	0.7	u	0.0000	2.1	u	0.0667	1.4	d	0.0054	0.7
32381	d	0.0045	0.7	d	0.8084	0.9	d	0.0204	0.7	u	0.0096	1.5	u	0.4909	1.1	d	0.0512	0.8
35370	d	0.1138	0.5	n	0.7934	1.0	d	0.1429	0.6	u	0.0896	1.9	u	0.8690	1.1	d	0.1229	0.6
36443	d	0.2563	0.8	d	0.3567	0.7	d	0.1277	0.7	d	0.7636	0.9	d	0.5803	0.8	d	0.4669	0.9
38528	d	0.0005	0.7	d	0.0407	0.9	d	0.1229	0.9	u	0.0141	1.3	u	0.0353	1.2	n	0.8234	1.0
39265	d	0.5671	0.9	d	0.6345	0.9	u	0.5936	1.1	n	0.9304	1.0	u	0.3368	1.2	u	0.2563	1.1
43275	u	0.8843	1.1	d	0.0489	0.7	d	0.1377	0.9	d	0.0860	0.6	d	0.2992	0.8	u	0.6208	1.4
44761	n	0.9768	1.0	n	0.8996	1.0	d	0.5936	0.8	n	0.9923	1.0	d	0.6484	0.9	d	0.7052	0.9
48819	d	0.1903	0.9	d	0.5283	0.9	d	0.0305	0.7	n	0.2903	1.0	d	0.1483	0.8	d	0.0370	0.8
49533	n	0.6208	1.0	d	0.7052	0.9	d	0.1138	0.8	d	0.8690	0.9	d	0.1775	0.8	d	0.1483	0.9
53472	u	0.2646	1.1	u	0.2328	1.2	u	0.4320	1.1	n	0.9613	1.0	n	0.3773	1.0	n	0.3177	1.0
62935	d	0.2483	0.9	u	0.5936	1.1	d	0.4669	0.9	u	0.5032	1.2	n	0.5936	1.0	d	0.9768	0.8
63820	d	0.6766	0.9	u	0.9768	1.1	n	0.8538	1.0	u	0.6071	1.2	u	0.5283	1.1	d	0.8538	0.9
74218	d	0.0426	0.8	d	0.7784	0.9	d	0.2992	0.9	u	0.0825	1.2	u	0.2328	1.1	d	0.5283	0.9
76236	d	0.2730	0.9	n	0.9768	1.0	n	0.8996	1.0	u	0.2108	1.2	u	0.2992	1.1	n	0.9459	1.0
94209	n	0.8690	1.0	n	0.8084	1.0	d	0.9613	0.9	n	0.7342	1.0	n	0.8996	1.0	d	0.5803	0.9
96816	d	0.9768	0.9	n	0.4909	1.0	d	0.2992	0.9	n	0.5803	1.0	n	0.5283	1.0	n	0.3773	1.0
102377	u	0.2992	1.1	u	0.6624	1.1	u	0.4669	1.1	n	0.5936	1.0	u	0.8084	1.1	u	0.8996	1.1
104009	u	0.2646	1.1	u	0.5157	1.1	u	0.3669	1.2	n	0.6484	1.0	n	0.8386	1.0	u	0.8538	1.1
112876	d	0.4096	0.9	u	0.9613	1.1	d	0.0758	0.7	u	0.7636	1.2	d	0.3987	0.7	d	0.1713	0.6
114296	d	0.6208	0.9	u	0.4096	1.2	d	0.2483	0.8	u	0.3084	1.3	d	0.4669	0.8	d	0.0535	0.6
115417	n	0.7784	1.0	u	0.3368	1.3	d	0.2730	0.8	u	0.1775	1.3	d	0.6908	0.9	d	0.0585	0.7
117273	u	0.2903	1.3	u	0.3084	1.3	n	0.8234	1.0	n	0.8690	1.0	d	0.4551	0.8	d	0.3177	0.8
119792	u	0.0076	2.3	u	0.4320	1.3	u	0.6908	1.2	d	0.0407	0.6	d	0.0033	0.5	n	0.8690	1.0
131858	u	0.8538	1.1	u	0.1775	1.3	u	0.8690	1.1	u	0.3773	1.2	u	0.8234	1.1	d	0.1429	0.8
133771	u	0.7636	1.1	u	0.5671	1.3	n	0.6624	1.0	u	0.8084	1.2	d	0.5283	0.9	d	0.3272	0.8
153380	n	0.9768	1.0	u	0.0860	1.4	u	0.6071	1.1	u	0.1052	1.4	u	0.7784	1.1	d	0.1775	0.8
171055	u	0.8234	1.2	u	0.0489	1.5	d	0.9150	0.9	u	0.0791	1.2	d	0.6484	0.8	d	0.0263	0.6
175888	u	0.4320	1.2	u	0.0585	1.6	n	0.7784	1.0	u	0.2903	1.3	d	0.4909	0.8	d	0.0276	0.6

Akvamiljø, IRIS and SINTEF Experimental validation of drilling effects in the field

M/Z	Ref1	ref2	p	ratio	Ref1	exp1	p	ratio	Ref1	exp2	p	Ratio	Ref2	exp1	p	Ratio	Ref2	exp2	p	Ratio	Exp1	exp2	p	Ratio
18554	n		0.8843	1.0	n		0.8386	1.0	n		0.9768	1.0	d		0.8538	0.9	n		0.7784	1.0	u		0.7636	1.1
18678	n		0.8843	1.0	d		0.5283	0.9	d		0.6345	0.9	d		0.8538	0.9	n		0.7489	1.0	n		0.6484	1.0
19058	u		0.5803	1.1	n		0.8538	1.0	n		0.9150	1.0	d		0.7784	0.9	d		0.5157	0.9	n		0.7784	1.0
19569	u		0.0697	1.3	u		0.5411	1.1	u		0.4788	1.1	d		0.1713	0.8	d		0.2038	0.9	n		0.7636	1.0
20845	u		0.0060	2.1	u		0.0825	2.0	u		0.9304	1.2	n		0.4788	1.0	d		0.0127	0.6	d		0.1052	0.6
21473	u		0.0000	2.8	u		0.0697	1.5	u		0.0353	1.8	d		0.0022	0.5	d		0.0238	0.6	u		0.5803	1.2
21846	u		0.0064	1.7	u		0.0585	2.2	u		0.0896	1.5	u		0.3084	1.3	d		0.3084	0.9	d		0.9150	0.7
22385	u		0.3272	1.6	u		0.9768	1.7	u		0.2483	1.9	n		0.5283	1.0	u		0.8234	1.2	u		0.3567	1.1
22883	u		0.2404	1.1	u		0.1653	1.5	u		0.0353	1.6	u		0.7784	1.3	u		0.3272	1.4	u		0.6345	1.1
23504	u		0.0194	1.5	u		0.0166	1.5	u		0.1327	1.3	n		0.8996	1.0	d		0.4909	0.9	d		0.3467	0.9
24265	u		0.2646	1.2	u		0.0068	1.3	u		0.0184	1.3	u		0.5411	1.1	u		0.4096	1.1	n		0.9613	1.0
24655	u		0.0157	1.4	u		0.0933	1.2	u		0.0012	1.4	d		0.2038	0.9	n		0.8996	1.0	u		0.0791	1.2
25111	n		0.4669	1.0	u		0.2730	1.3	u		0.0612	1.4	u		0.0727	1.3	u		0.0305	1.5	u		0.6208	1.1
27605	u		0.0489	1.4	n		0.8690	1.0	u		0.1229	1.3	d		0.0107	0.7	n		0.6908	1.0	u		0.0612	1.4
29023	u		0.0002	1.3	d		0.5671	0.7	u		0.1138	1.1	d		0.0000	0.5	d		0.0407	0.8	u		0.0353	1.6
31537	d		0.0045	0.7	d		0.1653	0.8	d		0.5540	0.9	u		0.2903	1.1	u		0.0896	1.3	u		0.4434	1.1
32473	d		0.0336	0.7	d		0.2108	0.8	d		0.2038	0.8	u		0.2815	1.2	u		0.2253	1.2	u		0.6345	1.1
33912	d		0.0226	0.4	d		0.2563	0.6	d		0.1277	0.5	u		0.1052	1.5	u		0.3368	1.4	d		0.5936	0.9
35797	d		0.0007	0.3	d		0.4207	0.7	d		0.1903	0.6	u		0.0175	2.7	u		0.0388	2.4	d		0.6908	0.9
36119	d		0.0037	0.3	d		0.4320	0.7	d		0.2038	0.6	u		0.0226	2.1	u		0.0612	2.0	d		0.7052	0.9
36417	d		0.0015	0.3	d		0.7784	0.8	d		0.2108	0.7	u		0.0054	2.5	u		0.0896	2.0	d		0.3773	0.8
38078	u		0.0388	1.5	u		0.2815	1.2	u		0.4669	1.1	d		0.2815	0.9	d		0.1595	0.8	d		0.6345	0.9
39032	d		0.0238	0.3	d		0.9304	0.9	d		0.2404	0.6	u		0.0194	3.2	u		0.3272	2.2	d		0.2903	0.7
40185	d		0.0215	0.6	d		0.5157	0.9	d		0.3879	0.8	u		0.2253	1.6	u		0.1903	1.4	d		0.8690	0.9
41695	u		0.0226	3.1	d		0.4909	0.7	u		0.6624	1.3	d		0.0033	0.2	d		0.0667	0.4	u		0.2253	1.8
46891	u		0.0175	1.5	u		0.1277	1.3	u		0.3467	1.2	d		0.4320	0.9	d		0.1229	0.8	d		0.4909	0.9
52374	d		0.6908	0.8	d		0.0081	0.5	d		0.0068	0.5	d		0.0149	0.7	d		0.0166	0.7	n		0.6766	1.0
54300	d		0.3987	0.5	d		0.5032	0.5	d		0.1483	0.4	u		0.8843	1.1	d		0.4788	0.8	d		0.4788	0.8
57265	d		0.8538	0.8	d		0.9459	0.9	d		0.5157	0.7	u		0.7784	1.1	d		0.4669	0.9	d		0.2992	0.8
63830	n		0.0091	1.0	d		0.7196	0.9	n		0.1094	1.0	n		0.1483	1.0	u		0.7052	1.1	u		0.4096	1.1
65235	n		0.3773	1.0	d		0.4551	0.9	n		0.3773	1.0	d		0.7934	0.9	n		0.9459	1.0	u		0.7489	1.1
76933	n		0.6484	1.0	d		0.2903	0.9	d		0.1229	0.9	d		0.4788	0.9	d		0.5032	0.9	n		0.6345	1.0
77918	n		0.8386	1.0	d		0.3084	0.9	d		0.1327	0.9	d		0.3879	0.9	d		0.3272	0.9	n		0.6766	1.0
87442	u		0.1483	1.4	n		0.9613	1.0	u		0.7636	1.3	d		0.0612	0.7	d		0.0290	0.9	u		0.8690	1.3
93488	n		0.7196	1.0	u		0.4788	1.2	u		0.4551	1.1	u		0.3177	1.2	u		0.4669	1.2	n		0.9150	1.0
99640	d		0.5032	0.9	u		0.8843	1.3	u		0.5936	1.6	u		0.8234	1.5	u		0.8386	1.8	u		0.6908	1.2
103601	d		0.5157	0.9	u		0.7636	1.2	u		0.4788	1.4	u		0.8843	1.4	u		0.5803	1.6	u		0.7342	1.1
153003	n		0.6208	1.0	d		0.3669	0.9	d		0.0825	0.9	n		0.7342	1.0	d		0.2903	0.9	d		0.2404	0.9

REFERENCES

- Akvaplan-niva (2006). "Field Trial at Sleipner Vest Alfa Nord: Effects on drilling activities on benthic communities". ERMS Report No. 16, Akvaplan-niva Report APN-411.3041.2 dated 6 July 2006.
- Arifin Z and B.-Y. Li (1997). "Feeding response and carbon assimilation by the blue mussel *Mytilus trossulus* exposed to environmentally relevant seston matrices" MARINE ECOLOGY-PROGRESS SERIES 160: 241-253
- Barlow, M. J. and P. F. Kingston (2001). "Observations on the effects of barite on the gill tissues of the suspension feeder *Cerastoderma edule* (Linne) and the deposit feeder *Macoma balthica* (Linne)." Marine Pollution Bulletin 42(1): 71-76.
- Bechmann, R. K., S. Westerlund, et al. (2006). Impacts of drilling mud discharges on water column organism and filter feeding bivalves, IRIS-Akvamiljø report 2006/038. .
- Beyer, J. B. S. (2003). Handbook: Biomarkers for assessing biological effects of discharges from the offshore oil and gas industry.
- Bjørnstad, A., L. B.K., et al. (2003). Use of proteomics (SELDI-TOF) in assesment of endocrine distrupction in molloscs and crustaceans. PRIMO 12, Tampa, Florida ; US, May 2003.
- Black, M. C., J. R. Ferrell, et al. (1996). "DNA strand breakage in freshwater mussels (*Anodonta grandis*) exposed to lead in the laboratory and field." Environmental Toxicology and Chemistry 15(5): 802-808.
- Bolognesi, C., R. Rabboni, et al. (1996). "Genotoxicity biomarkers in *M-galloprovincialis* as indicators of marine pollutants." COMPARATIVE BIOCHEMISTRY AND PHYSIOLOGY C-PHARMACOLOGY TOXICOLOGY & ENDOCRI 113(2): 319-323.
- Bradford, M. M. (1976). "A rapid and sensitive method for the quantitation of microgram quantities of protein utilizing the principle of protein-dye binding." Analytical Biochemistry 72: 248-254.
- Camus, L., M. B. Jones, et al. (2002). "Total oxyradical scavenging capacity and cell membrane stability of haemocytes of the Artic scallop, *Chlamys islandicus*, following benzo(a)pyrene exposure." Marine Environmental Research 54: 425-430.
- Cranford, P. J. and D. C. Gordon (1991). "Chronic Sublethal Impact of Mineral Oil-based Drilling Mud Cuttings on Adult Sea Scallops." Marine Pollution Bulletin 22(7): 339 - 344.
- Cranford, P. J. and D. C. Gordon (1999). "Chronic toxicity and physical disturbance effects of water- and oil-based drilling fluids and some major constituents on adult sea scallops (*Placopecten magellanicus*)." Marine Environmental Research 48(3): 225-256.
- Depledge, M., A. Aagaard, et al. (1995). "Assessment of Trace Metal Toxicity Using Molecular, Physiological and Behavioural Biomarkers." Marine Pollution Bulletin 31(1-3): 19-27.
- Depledge, M. H. and Z. Billinghamurst (1999). Ecological significance of endocrine disruption in marine invertebrates.

- Dixon, D. R., A. M. Pruski, et al. (2004). "The effects of hydrostatic pressure change on DNA integrity in the hydrothermal-vent mussel *Bathymodiolus azoricus*; implications for future deep-sea mutagenicity studies." Mutation Research **552**: 235-246.
- ERMS (2006a): Implementation of the near-field module in the ERMS model - draft report. ERMS report No. 23. SINTEF report under preparation.
- ERMS (2006b): Documentation report for the revised DREAM model. ERMS report No. 18. SINTEF report dated 31 August 2006.
- Gosling, E. (1992). THE MUSSEL MYTILUS: ECOLOGY, PHYSIOLOGY, GENETICS AND CULTURE. AMSTERDAM, ELSEVIER.
- Hardy, D. (1991). Scallop farming. Fishing new books. Oxford, England, Osney Mead: 69-128.
- Hawkins, A., S. RFM, et al. (1996). "Novel observations underlying the fast growth of suspension-feeding shellfish in turbid environments: *Mytilus edulis* " MARINE ECOLOGY-PROGRESS SERIES **131**(1-3): 179-190.
- Hovgaard, P. (1984). Blåskjell i Ryfylkefjordene, Ryfylkeprosjektet - Rådgivende utvalg for fjordundersøkelser.
- Johnsen, S., T.K. Frost, M. Hjelsvold and T.R. Utvik, 2000: "The Environmental Impact Factor – a proposed tool for produced water impact reduction, management and regulation". SPE paper 61178 presented at the SPE International Conference on Health, Safety and Environment in Oil and Gas Exploration and Production held in Stavanger, Norway, 26 – 28 June 2000.
- Karman, C.C. and Reerink, H.G., 1997: "Dynamic Assessment of the Ecological Risk of the Discharge of produced Water from Oil and Gas producing Platforms". Paper presented at the SPE conference in 1997, Dallas, USA. SPE paper No. SPE 37905.
- Karman, C.C. et. al., 1994: "Ecotoxicological Risk of Produced Water from Oil Production Platforms in the Statfjord and Gullfax Fields". TNO Environmental Sciences. Laboratory for Applied Marine Research, den Helder, The Netherlands. Report TNO-ES, February 1994.
- Larsen, B. K., B. A., et al. (2003). Application of protomics (SELDI-TOF) for study of the integrated responses to nonylphenol, oil and alkylated phenols in juvenile turbot. PRIMO 12. (Tampa, Florida ; US, May 2003).
- Lowe, D. M., V. U. Fossato, et al. (1995). "Contaminant-induced lysosomal membrane damage in blood cells of mussels *Mytilus galloprovincialis* from the Venice Lagoon: an *in vitro* study." Marine Ecology Progress Series **129**: 189-196.
- Lowe, D. M., M. N. Moore, et al. (1992). "Contaminant impact on interactions of molecular probes with lysosomes in living hepatocytes from dab *Limanda limanda*." Mar. Ecol. Progr. Ser. **91**: 135-140.
- Lowe, D. M. and R. K. Pipe (1994). "Contaminant-induced lysosomal membrane damage in marine mussel digestive cells: an *in vitro* study." 30.
- Rank, J. (1999). "Use of comet assay on the blue mussel, *Mytilus edulis*, from coastal waters in Denmark." NEOPLASMA **46**: 9-10.
- Regoli, F., S. Gorbi, et al. (2002). "Oxidative stress in ecotoxicology: from the analysis of individual antioxidants to a more integrated approach." Marine Environmental Research **54**(3-5): 419-423.
- Regoli, F., M. Nigro, et al. (2000). "Total oxidant scavenging capacity (TOSC) of microsomal and cytosolic fractions from Antarctic, Arctic and Mediterranean

- scallops: differentiation between three potent oxidants." Aquatic Toxicology **49**(1-2): 13-25.
- Regoli, F., M. Nigro, et al. (2000). "Total oxidant scavenging capacity of Antarctic, Arctic, and Mediterranean scallops." Italian Journal of Zoology **67**: 85-94.
- Regoli, F. and G. W. Winston (1998). "Applications of a new method for measuring the total oxyradical scavenging capacity in marine invertebrates." Marine Environmental Research **46**(1-5): 439-442.
- Regoli, F. and G. W. Winston (1999). "Quantification of total oxidant scavenging capacity of antioxidants for peroxydinitrite, peroxy radicals, and hydroxyl radicals." Toxicology and applied Pharmacology **156**: 96-105.
- Regoli, F., G. W. Winston, et al. (2003). "Integrating enzymatic responses to organic chemical exposure with total oxyradical absorbing capacity and DNA damage in the European eel *Anguilla anguilla*." Environmental Toxicology and Chemistry **22**(9): 2120-2129.
- RF (2003). Grunnlagsundersøkelser av miljøforholdene ved Alfa Nord 2002". RF - Rogalandforskning Report RF – 2003/085 carried out for Statoil dated 31 March 2003. Written in Norwegian. .
- Risso-de Faverney, C., A. Devaux, et al. (2001). "Cadmium induces apoptosis and genotoxicity in rainbow trout hepatocytes through generation of reactive oxygen species." Aquatic Toxicology **53**(1): 65-76.
- Singh, N. P., M. T. McCoy, et al. (1988). "A simple technique for quantification of low levels of DNA damage in individual cells." Exp. Cell Res. **175**: 184-191.
- SINTEF (2004). ERMS Field Trials during production drilling at Sleipner Vest Alfa Nord (SVAN), September 2003. ERMS Report No. 2 dated 5 February 2004, SINTEF report STF66 F04012.
- SINTEF (2006). Documentation Report for the revised DREAM model. DRAFT No. 5, June 2006. ERMS Report No. 18. .
- Steinert, S. A. (1996). "Contribution of apoptosis to observed DNA damage in mussel cells." MARINE ENVIRONMENTAL RESEARCH **42**(1-4): 253-259.
- Steinert, S. A., R. S. Montee, et al. (1998). "Influence of sunlight on DNA damage in mussels exposed to polycyclic aromatic hydrocarbons." MARINE ENVIRONMENTAL RESEARCH **46**(1-5): 355-358.
- Steinert, S. A., R. StreibMontee, et al. (1998). "DNA damage in mussels at sites in San Diego Bay." MUTATION RESEARCH-FUNDAMENTAL AND MOLECULAR MECHANISMS OF MUTAGENESIS **399**(1): 65-85.
- TGD (2003): Technical Guidance Document on Risk Assessment", part II". European Commission, Joint Research Centre. European Communities, 2003.
- TNO (2006): THE SUSPENDED MATTER REPORT. Smit, M.G.D., K.I.E, Holthaus, N.B.H.M. Kaag and R.G. Jak (2006): The derivation of a PNECwater for weighting agents in drilling mud. TNO-report. R2006-DH-R-0044. ERMS report no 6.
- Turkey, J. W. (1977). "Exploratory Data Analysis, Reading, Mass.:" Addison-Westley.
- Van den Belt, K., V. P. S., et al. (2000). "Toxicity of cadmium-contaminated clay to the zebrafish *Danio rerio* " ARCHIVES OF ENVIRONMENTAL CONTAMINATION AND TOXICOLOGY **38** (2): 191-196.
- Walne, P. R. (1974). Culture of bivalve molluscs. 50 years experience at Conwy. Farnham-Surrey-England, Fishing news books Ltd.
- Wang, W. and F. NS. (1999). "Delineating metal accumulation pathways for marine invertebrates " SCIENCE OF THE TOTAL ENVIRONMENT **238**: 459-472.

Weltens, R., G. R., et al. (2000). "Ecotoxicity of contaminated suspended solids for filter feeders (*Daphnia magna*)."
ARCHIVES OF ENVIRONMENTAL CONTAMINATION AND TOXICOLOGY **39**(3): 315-323.